Sensor and Simulation Notes

Note 214

May 1976

Analysis and Synthesis of an Impedance-Loaded Loop Antenna Using the Singularity Expansion Method

Ronald Fred Blackburn
University of Mississippi

ABSTRACT

Although many electromagnetic problems can be treated satisfactorily by means of a static or steady-state approximation, there are an increasing number of problems in which the transient behavior is of paramount importance. A continuing need exists to handle these problems efficiently and in such a way that a wide range of responses to differing inputs may be considered or that the desired response may be synthesized. The purpose of this work is to show how the singularity expansion method (SEM) may be used to significantly simplify the calculation and synthesis of the response of a transmitting loop antenna excited by an electromagnetic pulse.

Paralleling the well-known description of lumped circuits in terms of their poles and zeros, a compact representation of the loop antenna in terms of its poles and zeros is derived.

214

SKL

Sensor and Simulation Notes

Note 214

May 1976

Analysis and Synthesis of an Impedance-Loaded Loop Antenna Using the Singularity Expansion Method

Ronald Fred Blackburn
University of Mississippi

ABSTRACT

Although many electromagnetic problems can be treated satisfactorily by means of a static or steady-state approximation, there are an increasing number of problems in which the transient behavior is of paramount importance. A continuing need exists to handle these problems efficiently and in such a way that a wide range of responses to differing inputs may be considered or that the desired response may be synthesized. The purpose of this work is to show how the singularity expansion method (SEM) may be used to significantly simplify the calculation and synthesis of the response of a transmitting loop antenna excited by an electromagnetic pulse.

Paralleling the well-known description of lumped circuits in terms of their poles and zeros, a compact representation of the loop antenna in terms of its poles and zeros is derived.

The resulting time domain description of the loop response is simply a sum of terms involving the residues, the excitation, and the exponentially damped sinusoids whose complex frequencies are the pole frequencies. These poles or natural frequencies are the frequencies at which radiation from a scatterer or antenna can take place without an applied excitation.

One objective of this research is to investigate the possible use of the singularity expansion method to synthesize radiated time domain waveforms by uniformly loading a loop antenna. In particular, one wishes to choose the loading so as to realize some desired pole-zero configuration on the structure. It is shown that the effect of the loading can be interpreted as introducing a feedback loop into a block diagram representation of the impedance transfer function. This observation permits one to use the root-locus techniques well-known in the area of feedback control theory to predict certain features of the pole trajectories as the loading is continuously varied. Furthermore, the pole positions for a given impedance loading can be found with the aid of contour plots of the magnitude and phase of the impedance transfer function.

Combining the use of the above techniques for the analysis of loading together with the singularity expansion repre-

sentation, we extend to electromagnetic problems a capability to possibly synthesize the desired response when the input or excitation waveform is given.

ACKNOWLEDGMENTS

The completion of a dissertation requires the time, effort and guidance and help of many people. I wish to express my gratitude to those who assisted me in this endeavor.

I wish to express my sincere appreciation to Dr. Donald R. Wilton for his valuable assistance and expert counsel as my advisor for his generous devotion of time and effort to this study.

To the members of my Doctoral Committee, Dr. William Causey, Dr. Darko Kajfez, Dr. Ronald J. Pogorzelski and Dr. Charles Smith, I wish to express my sincere appreciation for the guidance and counsel provided.

I am also indebted to Dr. Chalmers M. Butler without whose support and advice a doctoral degree could never be attained.

For their advice in computer applications and technical programming, I am most grateful to Mr. Terry Brown and Mr. Joe Martinez of The Dikewood Corporation.

To Lt. Col. Larry W. Wood and Dr. Carl E. Baum of the Air Force Weapons Laboratory, Lt. Col. Gordon Wepfer of the Office of Scientific Research, Dr. Fred Tesche of Science Applications, Inc., Mr. Dusty Rhodes and Mrs. Dorothy Atkinson, I offer my special thanks for the variety of ways

that they have helped me in my pursuit of this degree. In this regard, I would like to express my gratitude to Dr. K. R. Umashankar of the University of Mississippi, Dr. Clayborne D. Taylor of Mississippi State University, and Dr. J. Phillip Castillo of the Air Force Weapons Laboratory for their encouragement and assistance. I am especially grateful to Mrs. Joanne Wilton whose cooperation greatly helped to make this study possible. And for her proficient clerical services, I thank Mrs. Betty Shannon for reviewing and typing the manuscript.

TABLE OF CONTENTS

LIST OF TABLES

LIST OF FIGURES

CHAPTER I

INTRODUCTION

Although there are many electromagnetic problems which can be treated satisfactorily by means of a static or steady-state approximation, there are an increasing number of problems in which the transient behavior is of paramount importance. These problems are usually difficult because they pose the problem of solving the field equations as functions of both time and space.

A few electromagnetic scattering and radiation problems can be analytically solved directly in the time domain. However, for most problems a direct time domain solution generally must be obtained by numerical methods. These methods are, at best, tedious to apply and are often plagued by stability problems.

A commonly more fruitful approach to obtaining transient field solutions is to first transform the time out of the field equations. Most engineers are familiar with this transform technique. In this method the time dependence is transformed out of the field equations by either a Fourier or Laplace transform. The transformed equations are functions of space, with frequency appearing merely as a parameter of the problem. The problem

is then solved in the frequency domain either analytically or numerically using, for example, a moment method technique. Once this steady-state solution of a problem has been obtained, it is then relatively simple to obtain the more general solution representing the response of the object to an impressed field varying arbitrarily with time. This is done by Fourier inversion of the spectrum of the solution quantity weighted by the spectrum of the excitation.

For solutions obtained either by time harmonic analysis coupled with Fourier inversion or by direct time domain techniques, a change in the spatial or temporal behavior of the excitation requires that considerable effort be spent in recalculating the response of the structure. One is lead to ask whether or not the long-established description of lumped circuits in terms of their poles and zeros might also be used to provide a more compact representation of electromagnetic field problems. In the case of electrical networks, specifying the finite number of pole and zero frequencies of a network quantity (impedance, transfer function, etc.) completely determines the quantity at all frequencies. Furthermore, the time domain response of a linear circuit excited by an arbitrary waveform may be determined from

knowledge of the location of these pole singularities of the response function in the complex frequency plane, as well as their corresponding residues. The resulting time domain description of the circuit response is simply a sum of terms involving the residues, the excitation, and the exponentially damped sinusoids whose complex frequencies are the pole frequencies.

The techniques of circuit theory are based on the assumptions that path lengths in the circuit are neglible and that all electric and magnetic fields are essentially confined to the circuit elements. Field theory, on the other hand, must deal with fluxes in two or three space dimensions. Given that circuit theory actually has its foundations in field theory, one might suspect that circuit theory techniques should have analogs in the field theory.

That the pole-zero techniques of lumped circuit theory can indeed be extended to electromagnetic scattering was recognized by C. E. Baum [1] who formalized the singularity expansion method (SEM) as applied to general scattering problems. In his approach a conducting scatterer is described in terms of an integral equation for the induced surface current density. The inverse of the integral operator is then expanded in terms of its

poles and their operator-valued residues. The circuit equivalent of this approach is the expansion of the inverse of the impedance matrix of an n-port network into a partial fraction representation in terms of the poles of the network and their matrix-valued residues. Thus in SEM, field theory is no longer considered to be something apart from circuit and transmission line theories, but rather as extensions of these concepts. Quantities which must be known for the expansion of the scattering operator (i.e., the inverse of the integral operator relating induced currents to scattered fields) in terms of its singularities are the natural frequencies, modes, and coupling coefficients.

The natural frequencies are the frequencies at which radiation from a scatterer or antenna can take place without an applied excitation. In other words, the natural frequencies are the poles of the structure. We see immediately that the poles must be either in the left half of the s plane or on the imaginary axis in order to exclude fields which grow exponentially with time. Poles on the imaginary axis, however, correspond to undamped sinusoids which therefore cannot lose energy by radiation. Hence, poles on the imaginary axis of the s plane must correspond to interior cavity resonances which do not radiate

exterior fields. The usual sinusoidal steady-state resonant frequencies of the structure are approximately the imaginary parts of the complex pole frequencies. For certain response quantities, it is possible for pole-zero cancellation to occur. In these cases, the natural frequencies do not appear explicitly in the response functions of the antenna.

At each pole frequency there is an associated modal current distribution. Generally speaking, as a complex excitation frequency approaches a natural resonance frequency, the current distribution approaches that of the modal current distribution associated with the pole. One is familiar with this behavior in, say, dipole antennas where at resonance the current distribution is approximately a sinusoidal standing wave with the number of nodes appropriate to the electrical length of the antenna. The amplitude of the current depends on the difference in the pole and excitation frequencies as well as on a coupling coefficient which relates the excitation to the proportion of a given mode which is excited.

The objective of this research is to investigate the possible use of the singularity expansion method to synthesize radiated time domain waveforms by uniformly loading a loop antenna. In particular, we wish to choose

the loading so as to realize some desired pole-zero configuration on the structure. Since synthesis design is usually carried out in practice by iterated analyses, we approach the synthesis problem by first building up an array of tools for analysis. These include a rather extensive set of tables for the poles and residues of unloaded loops. The data in these tables permit one to calculate either the time domain or the frequency domain response of a loop over a large frequency range for an arbitrary excitation. A product expansion representation of the loop "transfer admittance" function is then derived which permits the rapid calculation of magnitude and phase contours for the transfer admittance. Plots of these contours, in turn, yield information on the shifting of poles that is possible by impedance loading. Adding further insight into the problem of determining the pole shifts are extensions of the root locus techniques commonly used in control theory. The extensions permit the techniques to be used in the present problem in which there are a countably infinite number of poles.

With the combined use of the above techniques, some progress is made toward the development of an approach to the synthesis problem. As in circuit theory, the synthesis procedure may begin with either of two different starting

points. In the first, the synthesis problem is considered solved when the transfer function relating the response quantity to the excitation has specified poles and possibly specified residues. In the case of the loaded loop, this becomes a problem of requiring the loading impedance function to interpolate the unloaded loop transfer impedance function at the pole frequencies. If the residues are left unspecified, it is also possible to determine whether or not the synthesized loading function is positive real.

The other starting point sets out to solve a more difficult but more practical problem. Here one is given the time domain response and excitation waveforms and asked to synthesize the loading function required to approximately achieve the desired time domain response. In this case, the poles of the resulting structure may not even be needed, depending on the synthesis algorithm. It is emphasized that the electromagnetic synthesis problem has an additional complication which does not have an analog in lumped circuit synthesis. This is, of course, the time delay associated with the geometry of the structure. This problem is beyond the scope of this work and it is anticipated that further development along these lines will require some approximation of an infinite

number of poles by time delay factors in the transfer function.

CHAPTER II

SINGULARITY EXPANSION METHOD ANALYSIS OF THE UNLOADED LOOP

There exists a continuing need to handle electromagnetic transient problems efficiently and in such a way that a wide range of responses to differing inputs may be considered or that the desired response may be synthesized. The purpose of this discussion is to show how the singularity expansion method (SEM) may be used to significantly simplify the calculation and synthesis of the response of a transmitting loop antenna excited by an electromagnetic pulse. The frequency domain response of a loop has been extensively treated in the literature [2], [3], [4], and good summaries of these treatments, with some extensions, are given by King and Harrison [5] and King [6].

In the following, we merely summarize the theory of Wu [4] as given by King and Harrison [5]. Referral is made to the latter for details of the derivations, and their notation is generally followed. We have appropriately extended the theory of Wu [4] into the complex frequency or, equivalently, the Laplace transform domain. Although these results may be obtained merely by the substitution $s = j\omega$ in Wu's equations, we present below

the derivation for reference purposes.

The usual method of approaching the problem is to write an integral equation for the current induced in the loop which involves the driving voltage waveform. Because of the rotational symmetry of the loop, Fourier analysis of both the excitation and the current permits us to derive a "transfer impedance" relating these Fourier components. The modal transfer impedance is just the ratio of the corresponding Fourier components of excitation (voltage) and current. These transfer impedances contain both the frequency and geometrical dependences of the loop.

2.1 Summary of Wu's Theory for an Unloaded Loop Extended to Complex Frequencies

In the following, the derivation of the solution for the current on a conducting loop antenna is summarized following closely the presentation of King and Harrison [5]. As shown in Figure 1, the center of the loop coincides with the origin of a cylindrical coordinate system denoted ρ, ϕ, and z, with the plane of the loop lying in the plane $z = 0$. The radius of the loop b is assumed much larger than the wire radius a. Furthermore, the value of a is small compared with the wavelength, i.e.,

$$a^2 << b^2, \quad |ka|^2 << 1 \qquad (2.1)$$

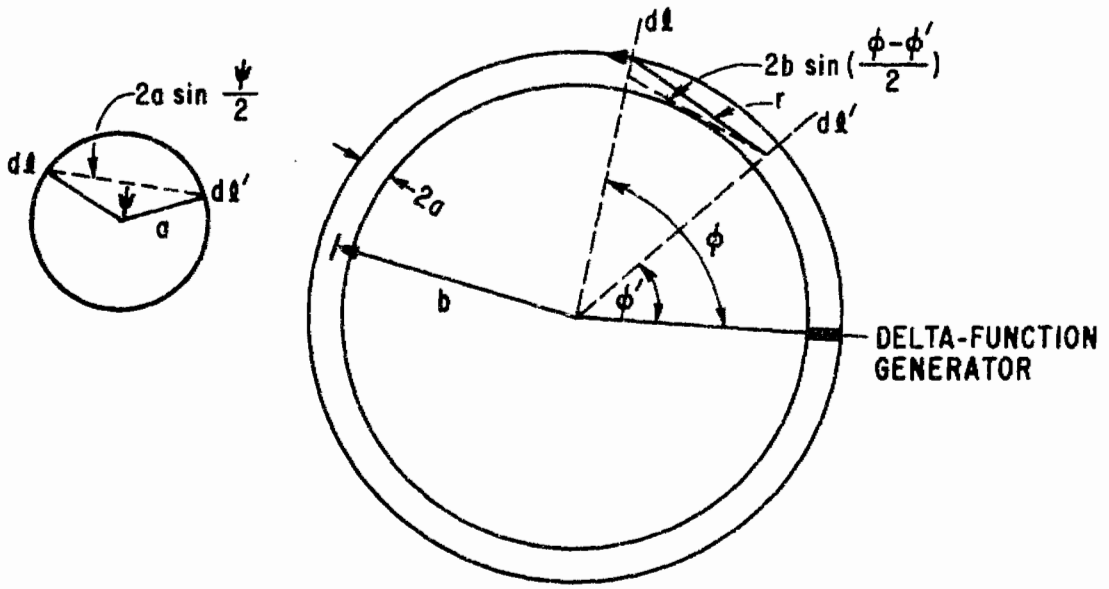

Figure 1. Schematic of loop antenna

The value of $I(\phi')$ is obtained from an integral equation obtained by invoking the boundary conditions. The appropriate boundary condition is that the tangential electric field must vanish at the surface of the loop. The value of the electric field impressed across a delta gap generator located at $\phi = 0$ is $V_o^e(s)$. If the structure is impedance loaded, the sum of the voltage drops across the impedance must also be included. For a uniformly loaded structure this is easily accomplished, since the voltage drop per unit length (i.e., the electric field) is merely proportional to the current at the same point. Considering only the unloaded case here, we have

$$E_\phi(s) = - \frac{V_o^e(s)\delta(\phi)}{b} = - \left(\frac{1}{\rho} \frac{\partial \Phi}{\partial \phi} + sA_\phi \right), \quad \rho = b \tag{2.2}$$

on the surface of the wire at ϕ, where the scalar and vector potentials at the element $d\ell = b d\phi$ are given by

$$\Phi = \frac{1}{4\pi\varepsilon} \int_{-\pi}^{\pi} q(\phi')\, W(\phi - \phi')\, d\phi' \tag{2.3}$$

$$A_\phi = \frac{\mu}{4\pi} \int_{-\pi}^{\pi} I(\phi')\, W(\phi - \phi') \cos(\phi - \phi')\, d\phi' \tag{2.4}$$

Denoting the speed of light by c, the kernel is defined by

$$W(\phi - \phi') = \frac{b}{2\pi} \int_{-\pi}^{\pi} \frac{e^{-s/c\ r}}{r}\, d\Psi \qquad (2.5)$$

where

$$r \approx \sqrt{4b^2 \sin^2 (\phi - \phi')/2 + A^2} \qquad (2.6)$$

and

$$A \approx 2a \sin (\Psi/2) \qquad (2.7)$$

In (2.4) and (2.5) the ϕ component of the surface density current $J_\phi(\phi)$ is assumed to be uniform around the wire. $I(\phi)$ is the total current,

$$I(\phi) = 2\pi a\ J_\phi(\phi) \qquad (2.8)$$

where, because of (2.1), the Ψ-directed component of surface current J_Ψ is assumed to be negligible. Note that the voltage excitation is given by

$$\int_{-\pi}^{\pi} bE_\phi(s)\, d\phi = V_o^e(s) \qquad (2.9)$$

By the equation of continuity,

$$\left(\frac{1}{b}\right) \frac{dI(\phi')}{d\phi'} + sq(\phi') = 0 \qquad (2.10)$$

and it follows from (2.10) and (2.3) that

$$\frac{\partial \Phi}{\partial \phi} = \frac{1}{4\pi\epsilon sb} \int_{-\pi}^{\pi} \frac{\partial I(\phi')}{\partial \phi'} \frac{\partial}{\partial \phi'} W(\phi - \phi')\, d\phi' \qquad (2.11)$$

Integrating Equation (2.11) by parts,

$$\frac{\partial \Psi}{\partial \phi} = \frac{-1}{4\pi\varepsilon sb} \frac{\partial^2}{\partial \phi^2} \int_{-\pi}^{\pi} I(\phi')\, W(\phi - \phi')\, d\phi' \qquad (2.12)$$

and substituting (2.12) and (2.4) into (2.2), one obtains

$$V_o^e(s)\delta(\phi) = \frac{jn_o}{4\pi} \int_{-\pi}^{\pi} K(\phi - \phi')\, I(\phi')\, d\phi' \qquad (2.13)$$

where a new kernel $K(\phi - \phi')$ is defined as

$$K(\phi - \phi') = -j \left[\frac{sb}{c} \cos(\phi - \phi') - \frac{c}{sb} \frac{\partial^2}{\partial \phi^2} \right] W(\phi - \phi') \qquad (2.14)$$

$W(\phi - \phi')$, defined by (2.5), may be expanded in a Fourier series

$$W(\phi - \phi') = \sum_{-\infty}^{\infty} K_m(s)\, e^{-jm(\phi - \phi')} \qquad (2.15)$$

The K_m may be evaluated in terms of $W(\phi - \phi')$, yielding

$$K_n(s) = \frac{1}{2\pi} \int_{-\pi}^{\pi} W(\phi - \phi')\, e^{jn(\phi - \phi')}\, d\phi = K_{-n}(s) \qquad (2.16)$$

Using the results of (2.15) and rewriting (2.14), a simple expression is obtained for $K(\phi - \phi')$ where

$$K(\phi - \phi') = \sum_{-\infty}^{\infty} a_n(s)\, e^{-jn(\phi-\phi')} \qquad (2.17)$$

and

$$a_n(s) = \frac{-jsb}{2c}\left(K_{n+1}(s) + K_{n-1}(s)\right) - \frac{jn^2c}{sb} K_n(s) = a_{-n}(s) \qquad (2.18)$$

If we let $\theta = \phi - \phi'$ and $A = 2a \sin(\Psi/2)$, the determination of the a_n depends upon the evaluation of the coefficients in Equation (2.16), which, with the definition $R(\theta) = r/b$, may be rewritten in the form

$$K_n(s) = \frac{1}{4\pi^2} \int_{-\pi}^{\pi} d\Psi \int_{-\pi}^{\pi} \frac{e^{jn\theta}\, e^{-sb/c\, R(\theta)}}{R(\theta)}\, d\theta \qquad (2.19)$$

As shown by Wu, Equation (2.19) may be approximately written in terms of integrals of Anger-Weber functions for unrestricted n, as

$$K_o(s) = \frac{1}{\pi} \ln \frac{8b}{a} - \frac{1}{2}\left[\int_o^{\xi} \Omega_o(X)\, dX + j \int_o^{\xi} J_o(X)\, dX\right] \qquad (2.20)$$

$$K_{-n}(s) = K_n(s) = \frac{1}{\pi}\left[K_0\left(\frac{na}{b}\right) I_0\left(\frac{na}{b}\right) + C_n\right]$$

$$- \frac{1}{2}\int_0^{\xi}\left[\Omega_{2n}(X) + jJ_{2n}(X)\right] dX$$

where $\xi = -j2sb/c$ and I_0 and K_0 are modified Bessel functions of the first and second kind, respectively, and γ is Euler's constant. The constant C_n is defined as

$$C_n = \ln 4n + \gamma - 2\sum_{m=0}^{n-1}\frac{1}{(2m+1)} \qquad (2.21)$$

Using the above results, (2.13) reduces to

$$V_0^e(s)\delta(\phi) = \frac{j\eta_0}{4\pi}\sum_{-\infty}^{\infty} a_n(s)\int_{-\pi}^{\pi} e^{-jn(\phi-\phi')} I(\phi')\, d\phi' \qquad (2.22)$$

Expanding the above current in a Fourier series, one has

$$I_s(\phi) = \sum_{-\infty}^{\infty} I_n(s)\, e^{-jn\phi} \qquad (2.23)$$

where the $I_n(s)$ coefficients are given by

$$I_n(s) = \frac{1}{2\pi}\int_{-\pi}^{\pi} I(\phi')\, e^{jn\phi'}\, d\phi' \qquad (2.24)$$

Combining the results of (2.22) and (2.24), we obtain

$$V_o^e(s)\delta(\phi) = \frac{jn_o}{2} \sum_{-\infty}^{\infty} a_n(s)\, I_n(s)\, e^{-jn\phi} \qquad (2.25)$$

This is a Fourier series with the coefficients $(jn_o/2)$ $a_n(s)\, I_n(s)$. The coefficients are obtained by using the properties of the delta function,

$$\frac{jn_o a_n(s) I_n(s)}{2} = \frac{1}{2\pi} \int_{-\pi}^{\pi} V_o^e(s)\, \delta(\phi)\, e^{jn\phi}\, d\phi = \frac{V_o^e(s)}{2\pi} \qquad (2.26)$$

Finally,

$$I_n(s) = \frac{-jV_o^e(s)}{n_o \pi a_n(s)} \qquad (2.27)$$

where the coefficient $-j/[n_o \pi a_n(s)]$ of $V_o^e(s)$ may be identified as the transfer admittance of the n^{th} Fourier component of current. In the following we repeatedly refer to this quantity as the "transfer function" or transfer admittance. Its reciprocal is called the "transfer impedance."

2.2 Expansion of the Transfer Admittance in Terms of Its Singularities

To calculate the current, or equivalently, the transfer impedance of a loop antenna, we have had to solve the corresponding field problem--that is, we have solved Maxwell's equations subject to the boundary conditions at the surface of the antenna. Having thus obtained the transfer admittance for the loop antenna, we next study its properties to determine the corresponding basic properties of the loop antenna. However, some of the most important general properties of the antenna transfer admittance may be obtained from much more basic considerations. These properties are common to all dynamical systems--mechanical and acoustical as well as electrical systems, and they are independent of the particular form of the equations as long as these equations are linear.

Such properties were considered by Brune [7] with special reference to electric networks, but these results are easily extended to all linear dynamical systems including systems with an infinite number of degrees of freedom.

The natural oscillation constants of any passive physical system, that is, a system without concealed sources of power, must lie either in the left half of

the complex s plane or on the imaginary axis; otherwise, the real part of the complex frequencies of oscillation would be positive, and the oscillations would grow in amplitude without any contribution of power by the system. An antenna in free space loses power by radiation, whether its terminals are short circuited or left floating; hence, the poles of its transfer admittance are in the left half of the s plane. The only exception is the point at the origin. This point corresponds to a static field.

Recognizing that the solutions of electromagnetic problems are analytic functions of the complex frequency s except at these pole singularities (complex natural frequencies of oscillation) is the basis of the singularity expansion method (SEM) introduced by Baum [1]. By expanding the transfer admittance in a partial fraction series, one needs only the poles and their residues to completely determine the transfer function either in the time or the frequency domain.

One of the advantages of the singularity expansion method as compared to other more conventional methods is that it provides a means of characterizing the electromagnetic properties of a body with a discrete set of complex numbers together with a set of modal current distributions. These quantities are uniquely determined

by the body itself and do not depend, for example, on the driving source. Once these quantities are known, a wide variety of antenna problems can be solved without having to re-solve the boundary value problem. The singularity expansion method is therefore useful for two reasons: (1) it provides physical insight into the problem and (2) it reduces an electromagnetics problem to the minimum number of quantities necessary to completely represent it.

The analytic property of $1/a_n(s)$ with respect to s allows the use of various theorems of complex variables in obtaining information about its properties. The basic idea involved in this technique is to expand the transfer function of $1/a_n(s)$ in terms of its singularities in the complex frequency plane. Such singularities can take various forms such as poles, branch points (and associated branch cuts), essential singularities, and singularities at infinity. For a restricted class of objects, which includes the loop antenna, these s-plane singularities are limited to poles and possible singularities at infinity.

Once one has found the complex natural frequencies of oscillation and their corresponding current distributions, it then remains only to determine to what extent each modal current is excited by a given Fourier component

of the input waveform. For the loop antenna the excitation of each modal current is proportional to the product of the residue of the transfer admittance and the Laplace transform of the corresponding Fourier component of the excitation. To determine the natural frequencies of the loop, it is necessary to find the poles s_{ni} of the transfer admittance factor $1/a_n(s)$.

To do this, one observes in (2.18) and (2.20) that $a_n(s)$ is analytic for all s for $n = 0$, and for all s except $s = 0$ when $n \neq 0$. This implies that $1/a_n(s)$ is analytic for all s except possibly for poles at the zeros of $a_n(s)$. Therefore, since $a_n(s)$ vanishes at these zeros, say s_{ni}, $I_n(s_{ni})$ may be nonzero with $V_n(s_{ni}) = 0$, i.e., no excitation is required at the natural frequencies in order to have a current. Thus, at the pole frequencies, we have source free solutions of the integral equation. Umashankar [8] has shown that

$$\frac{1}{a_n(s)} = \sum_i \frac{R_{ni}}{s - s_{ni}} \qquad (2.28)$$

i.e., the transfer admittance can be written entirely as a residue series involving its poles s_{ni} and residues R_{ni}. This is the desired expansion of the transfer admittance in terms of its singularities.

By our definition of the pole frequencies, we have

$$a_n(s_{ni}) = \lim_{s \to s_{ni}} a_n(s) = 0 \tag{2.29}$$

and the corresponding residues R_{ni} are given by

$$R_{ni} = \lim_{s \to s_{ni}} \frac{(s - s_{ni})}{a_n(s)} = \left[\frac{da_n}{ds}\right]^{-1}\Bigg|_{s = s_{ni}} \tag{2.30}$$

From (2.30) the R_{ni} can be written as

$$R_{ni} = 1/a'_{ni}(s_{ni}) \tag{2.31}$$

where

$$a'_n(s_{ni}) = \frac{da_n}{ds}\Bigg|_{s = s_{ni}} \tag{2.32}$$

Using (2.28) in (2.27), we may write the n^{th} Fourier component of the current as

$$I_n(s) = \frac{1}{jn\eta_o\pi} \sum_i \frac{R_{ni}}{s - s_{ni}} V_o^e(s) \tag{2.33}$$

The equivalent expression in the time domain is

$$i_n(t) = \left(\sum_i R'_{ni}\, e^{s_{ni}t}\right) \bigstar v_o^e(t) \tag{2.34}$$

where

$$R'_{ni} = \frac{1}{jn_o\pi} R_{ni} \tag{2.35}$$

and R'_{ni} and s_{ni} must appear in complex conjugate pairs in order for the time domain response to be real. The star in (2.34) denotes convolution.

Expression (2.34) implies that poles must be in the left half plane to avoid an exponentially increasing current as a function of time. This is explained physically by the fact that source free currents must eventually radiate away all their energy; hence

$$i_n(t) \xrightarrow[t\to\infty]{} 0, \; n \neq 0 \; , \; i_o(t) \xrightarrow[t\to\infty]{} \text{constant} \tag{2.36}$$

Making use of (2.23) and 2.27),

$$I(\phi) = \sum_{-\infty}^{\infty} I_n(s)^{-jn\phi}$$

$$= \frac{-jV_o^e(s)}{n_o\pi} \left[\frac{1}{a_o(s)} + 2 \sum_{i}^{n} \frac{\cos n\phi}{a_n(s)} \right] \tag{2.37}$$

Expanding $a_n(s)$ in its partial fraction representation, we have finally

$$I(\phi) = \frac{-jV_o^e(s)}{\eta_o \pi} \left[\sum_{i=1}^{\infty} \frac{R_{oi}}{s - s_{oi}} + 2 \sum_{n=1}^{\infty} \left(\cos n\phi \sum_{i=1}^{\infty} \frac{R_{ni}}{s - s_{ni}} \right) \right] \qquad (2.38)$$

Equation (2.38) is for the case of an antenna excited at $\phi = 0$ by a delta gap. In the more general case, the excitation can be represented by an arbitrary incident field $E_\phi^{inc}(\phi,s)$. Fourier expansion of $E_\phi^{inc}(\phi,s)$ allows the derivation to proceed as for the case of an antenna and the result is

$$I(\phi,s) = \sum_{n,i} \frac{R'_{ni} \, e^{jn\phi} \int_0^{2\pi} E_\phi^{inc}(\phi',s) \, e^{-jn\phi'} \, b d\phi'}{s - s_{ni}} \qquad (2.39)$$

The terms $e^{jn\phi}$ are called by Baum [1] the modal current distributions, and the terms $e^{-jn\phi'}$ are the coupling vectors. The quantity

$$V_n(s) = \int_0^{2\pi} E_\phi^{inc}(\phi',s) \, e^{-jn\phi'} \, b d\phi' \qquad (2.40)$$

is called the coupling coefficient and indicates how much of each mode the incident field excites. The s_{ni} are the

poles or complex natural resonant frequencies.

If V_o^e is equal to unit for frequencies $s = j\omega$ in (2.37), then $I(\phi,j\omega)$ is the current response due to a unit voltage source in the real frequency domain. Hence $I(0,j\omega)$ is the input admittance and $1/I(0,j\omega)$ is the input impedance of the antenna. Hence, if a particular pole is close to the imaginary axis, the impedance at real frequencies in the vicinity of this zero is small, and we have the phenomenon known as resonance. If several poles are near the imaginary axis, the impedance will fluctuate between small and large values as the frequency passes these points. As the poles recede from the imaginary axis, the fluctuations become less pronounced, and the "resonance curves" become flatter.

An equivalent circuit can be developed representing the field equations of Maxwell for an electromagnetic field containing conductors and bound charges. Both transient and sinusoidal field phenomena may thus be studied by numerical and analytical circuit methods; such a circuit model applies, of course, to radiation from a loop antenna [9]. The circuit models can in principle be developed for all curvilinear-orthogonal reference frames to allow the solution, to any desired degree of accuracy, of any two- or three-dimensional

problem. The models correspond to the approximation of a transmission line in one dimension by a cascaded series of sections containing ordinary lumped circuit elements R, L, C, and G's. Since the field equations of Maxwell may thus be represented by a stationary network (within any desired degree of accuracy), it may be stated that [9]:

> Any theorem, formula, concept, or law that is valid for stationary networks (such as reciprocity theorems, Thevenin's theorem, concepts of dualism, reduction formulas, generalization postulates, etc.) can be translated into a corresponding theorem, formula, concept, or law relating to the electromagnetic field.

As the number of elements in the circuit increases, the number of poles also increases. As a consequence of the above circuit model of Maxwell's equations, continuous structures, including all of free space, are limits of networks with an increasingly larger number of increasingly smaller meshes. The number of their zeros and poles will be infinite. (In fact, this must be true of any physical circuit since all physical circuits are continuous and cannot be wholly disassociated from the surrounding space.)

Thus, there are an infinite number of complex resonant frequencies whose locations are in the left half of the complex frequency plane, and which occur in complex conjugate pairs, as a consequence of the above theorem.

In order to generate a real-time-domain response, poles of the transfer impedance function must appear in complex conjugate pairs and their residues must be in complex conjugate pairs for poles not on the negative real axis.

It is then recognized that the transient response of an object can be viewed as a superposition of a series of damped sinusoidal oscillations at the so-called natural frequencies of the object. It has been observed in many electromagnetic pulse (EMP) scattering and interaction problems that the time dependence of various quantities, such as the current induced on an object in an EMP simulator, seems to be described by only a few of these exponentially damped sinusoidal oscillations[1].

2.3 Numerical Techniques and Results

The expression for $a_n(s)$, (2.18) to (2.21), involves integrals of Anger-Weber functions of complex arguments. These functions have been computed using an extension to complex arguments of the methods described in [10]. A parametric study of the roots of $a_n(s)$ as a function of the ratio b/a has been carried out using a numerical search procedure. The roots, of course, satisfy the requirement that they should appear only in the left half of the s plane and in complex conjugate pairs.

The so-called Muller's Method has been used to

numerically determine the roots of $a_n(s)$. In this method three values of $a_n(s)$ are computed from three estimates of the root, say at s_{n-2}, s_{n-1}, and s_n. Using these values, a quadratic interpolation formula [11] is used to approximate $a_n(s)$ in the vicinity of the given points. The root of the quadratic nearest the best estimate, say s_n, is designated s_{n+1} and the procedure is repeated using s_{n-1}, s_n, s_{n+1} until $|s_{n+1} - s_n|/|s_n|$ is less than a preassigned number. For more details, the reader is referred to reference [11].

Approximate pole locations to initialize the procedure are not necessary, though in practice having good initial estimates of pole locations will considerably reduce the number of iterations required to find the various roots. This searching procedure is in general found to be quite efficient, but it has been found to be rather difficult to find all of the poles in certain regions when good initial estimates are unavailable. One method which has been employed to overcome this difficulty is to actually plot magnitude contours of the function in the complex s plane. The regions near zeros of $a_n(s)$ show up clearly on the contour plot and provide more accurate initializing data for Muller's Method. Furthermore, the contour plots themselves are useful in determining the poles of the loaded structure, as we shall

see in Chapter III.

The residue for $1/a_n(s)$ may be easily calculated by the residue theorem using a circular contour about the pole as shown in Figure 2.

By the residue theorem, we have

$$R_{ni} = \frac{1}{2\pi j} \oint_{C_{ni}} \frac{ds}{a_n(s)} \tag{2.41}$$

In Figure 2, let

$$s - s_i = \varepsilon e^{j\phi}, \qquad s = s_i + \varepsilon e^{j\phi}$$
$$ds = j\varepsilon e^{j\phi}\, d\phi \tag{2.42}$$

and substituting (2.42) into (2.41), we have

$$R_{ni} = \frac{1}{2\pi j} \oint_{C_{ni}} \frac{j\varepsilon e^{j\phi}\, d\phi}{a_n(s)\left(s_{ni} + \varepsilon e^{j\phi}\right)} \tag{2.43}$$

For a numerical approximation, we may divide the contour, C_{ni} into m equal subdivisions and apply the simple rectangular rule for integration:

$$R_{ni} \simeq \frac{\varepsilon}{2\pi} \sum_{n=1}^{m} \frac{e^{j\, 2(n-1)\pi/m}\, (2\pi/m)}{a_n(s)\left[s_{ni} + \varepsilon e^{j\, 2(n-1)\pi/m}\right]} \tag{2.44}$$

Thus the residue at the pole s_{ni} for $a_n(s)$ is

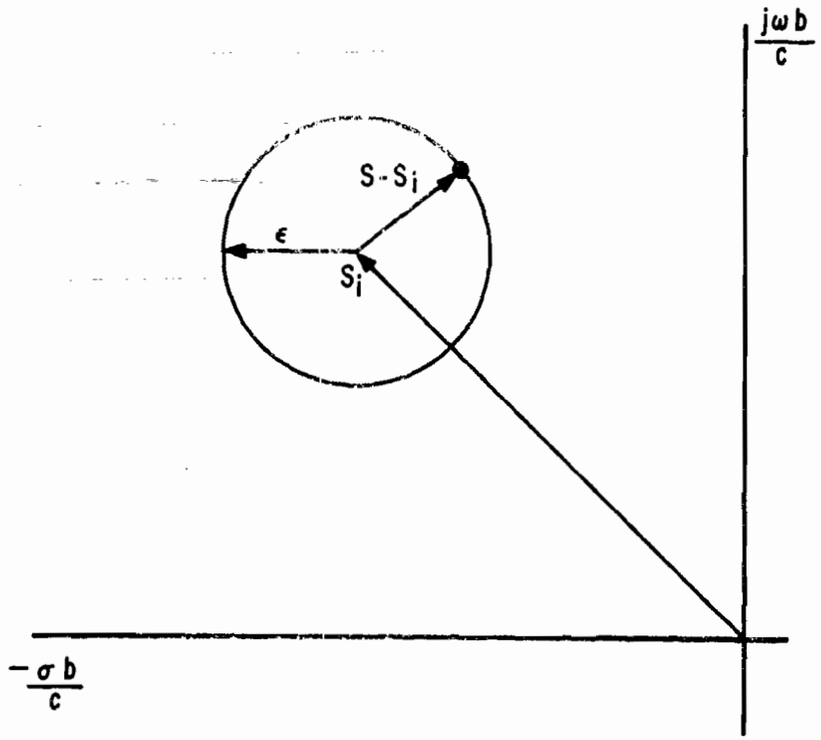

Figure 2. Contour in s-plane for calculating residues

$$R_{ni} = \frac{\varepsilon}{m} \sum_{n=1}^{m} \frac{e^{j\,2(n-1)\pi/m}}{a_n(s)\left[s_i + \varepsilon e^{j\,2(n-1)\pi/m}\right]} \qquad (2.45)$$

In equation (2.28) an important feature is that the function $1/a_n(s)$ may be represented by its poles and residues with no additional entire function required, as shown by Umashankar [8].

Several checks were made to determine the rate of convergence of (2.45). The value of ε was varied from 10^{-1} to 10^{-5} while simultaneously the value of m was varied from 3 to 24. It was found that for the combination of $\varepsilon = 10^{-3}$ and $m = 3$, accurate answers with a relative error of the order of 10^{-7} were obtained. A large number of these pole locations $s = s_{ni}$ and corresponding residues R_{ni} have been calculated and tabulated for a wide range of the loop parameter $\Omega = 2\ell n(2\pi b/a)$. These results permit one to use (2.34) to calculate time domain loop currents for arbitrary excitation without resorting to the comparatively inefficient process of Fourier transformation.

By direct calculation we find in the complex frequency plane an infinite number of complex resonant frequencies whose locations suggest three separate categories of resonant frequency or pole types for each mode

number n:

Type I

There is a single pole very near the $s = j\omega$ axis at approximately $\omega = n$. This pole gives the principal contribution to the time domain response of the loop at late times and the imaginary part of the pole location corresponds closely to the resonant frequency of the loop for an excitation of the form $e^{jn\phi}$.

Type II

There are n+1 of these poles (including conjugate pairs) which lie roughly on the left-hand side of an ellipse centered at $s = 0$ and with a semimajor axis somewhat larger than n.

Type III

There is a layer of poles lying almost parallel to the $s = j\omega$ axis. The layer contains an infinite number of poles and they are spaced approximately $\Delta\omega = \pi c/b$ units apart, where b is the loop radius.

As with thin cylindrical wires, increasing the wire radius has the effect of shifting the Type I poles near the $j\omega$ axis away from the axis, or equivalently, increasing the damping constants of those modes in the time domain [12]. Types II and III poles located further away from the imaginary axis, however, move away from the

imaginary axis as the radius approaches zero.

Pole and residue data for the three loop sizes $\Omega = 2\ell n 2\pi b/a = 10$, 15, and 20 are presented in Figures 3 through 8 and Tables 1 through 8 for modes n = 0 through 20. For a particular mode, Type II poles fall on an elliptically shaped curve with n + 1 poles (including conjugate pairs). There will be one more pole (Type I) at approximately $\omega = n$. Displayed in Figures 4, 6, and 8, corresponding to $\Omega = 10$, 15, and 20, respectively, are the layers of Type III poles parallel to the $s = j\omega$ axis. These poles are shown for each mode 0 through 20 for values of $\omega b/c = 0$ to $\omega b/c = 30$.

The residue corresponding to each of the poles plotted in Figures 3 through 8 are tabulated in Tables 1 through 8. These are tabulated in three columns for the three loop sizes $\Omega = 10$, 15, and 20. The first number in each column represents the real value of the residue, and the second is its imaginary value. The index is a unique four-digit number that identifies a particular pole. The first two digits are the mode number for modes 0 through 20. The last two digits can be grouped into three different categories corresponding to the three different types of poles. A double zero (00) in the last two digits of the index corresponds to the single Type I pole very near

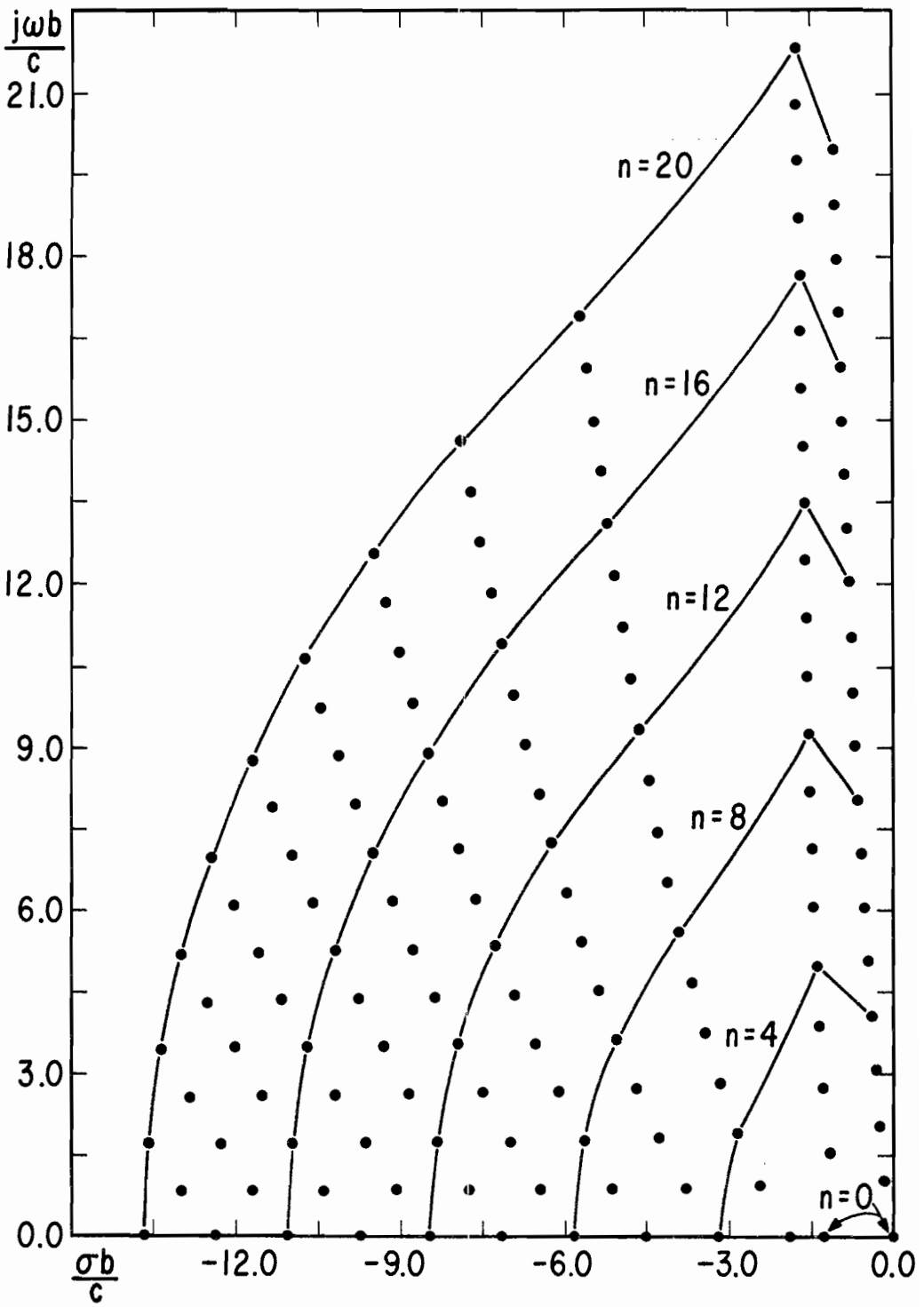

Figure 3. Natural frequencies of circular loop, Types I and II, Ω = 10.0

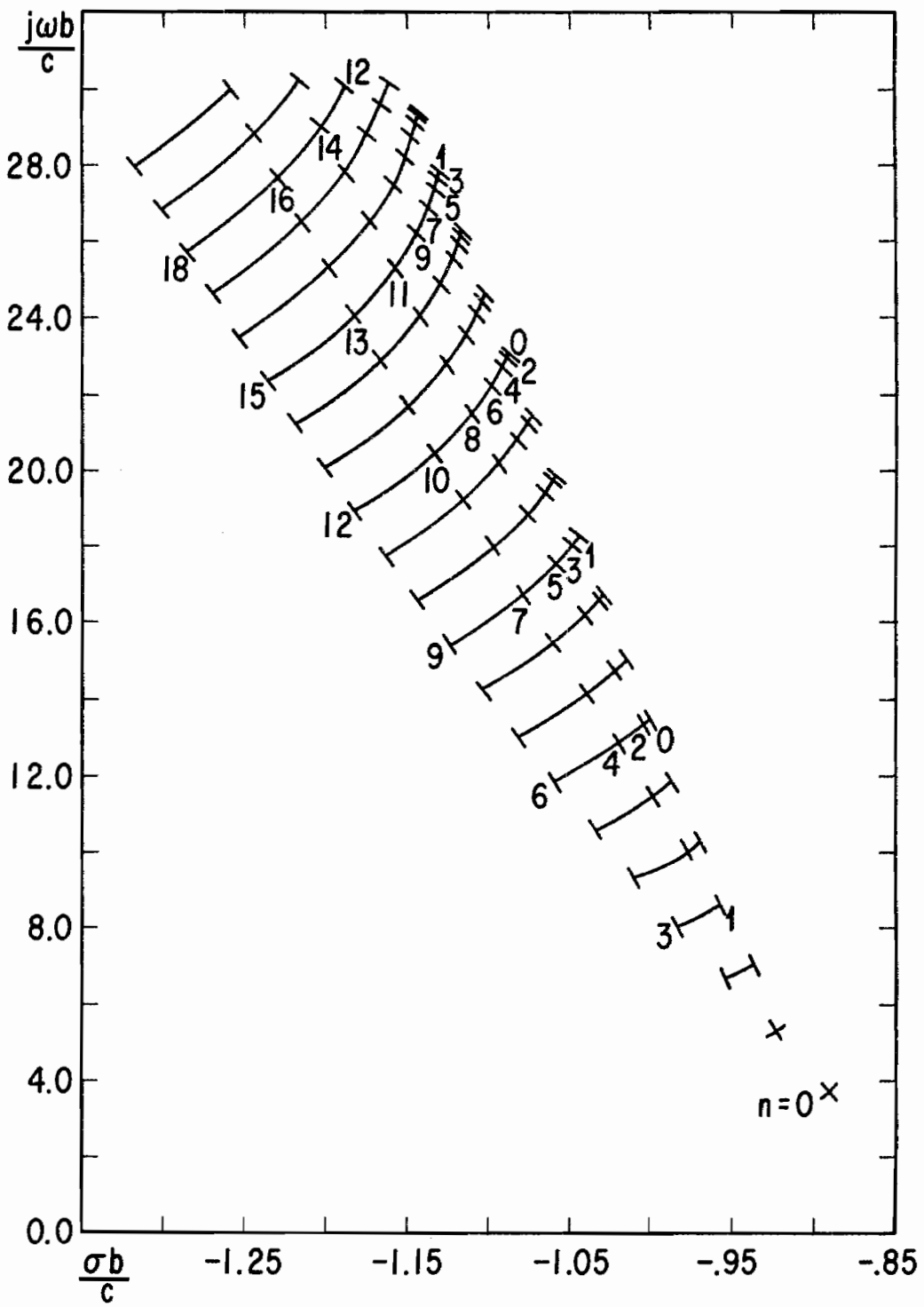

Figure 4. Natural frequencies of circular loop, Type III, Ω = 10.0

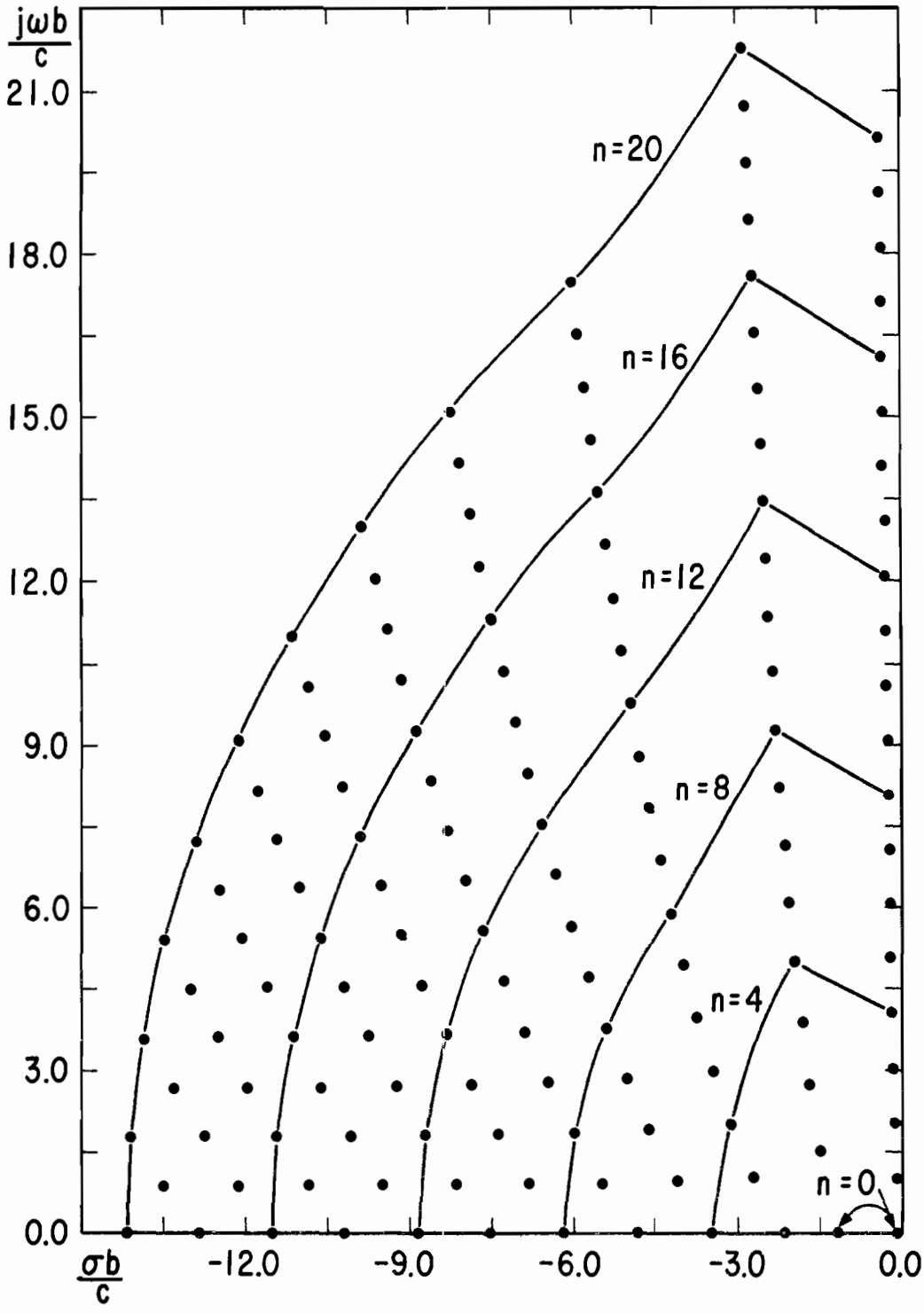

Figure 5. Natural frequencies of circular loop, Types I and II, Ω = 15.0

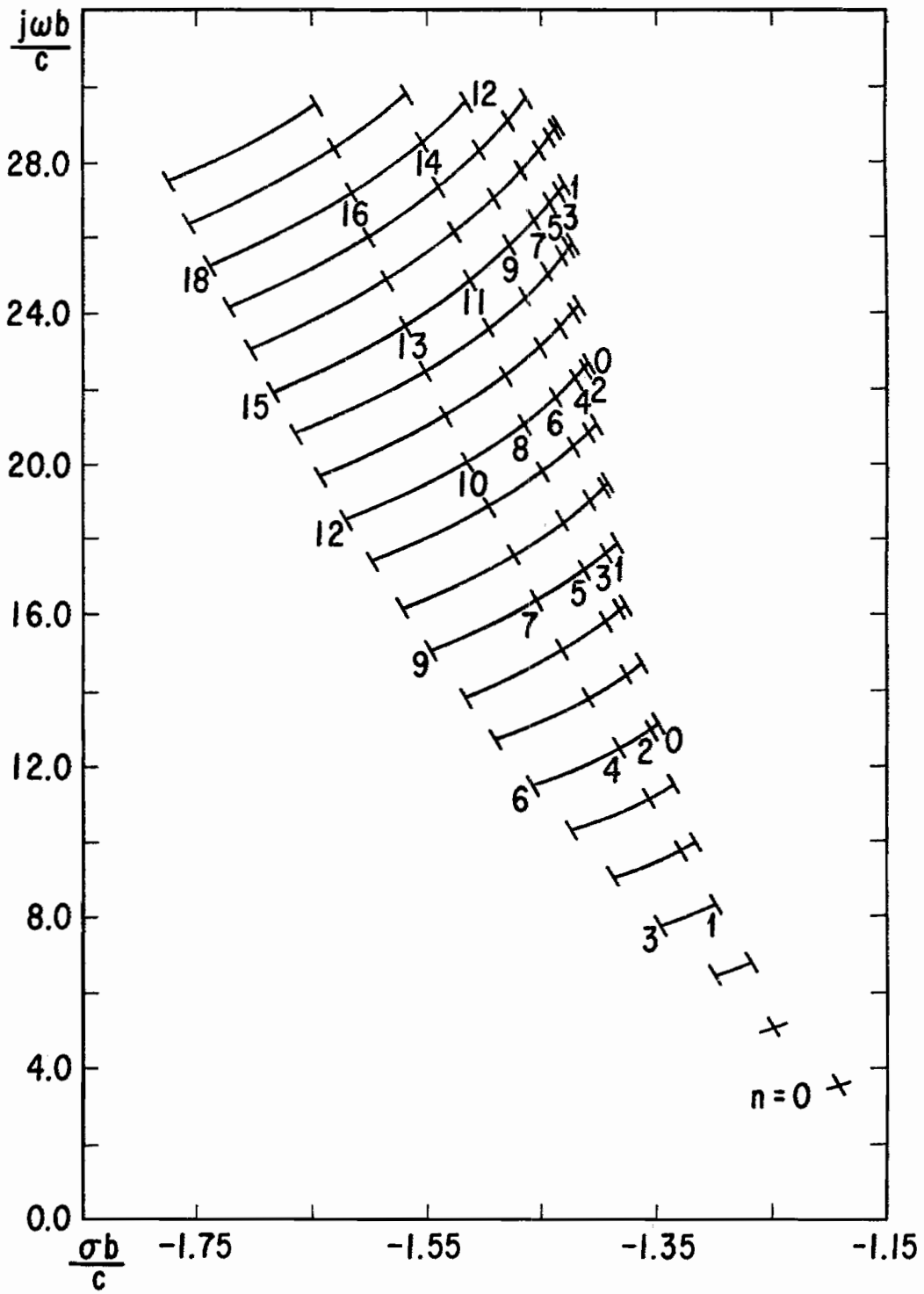

Figure 6. Natural frequencies of circular loop, Type III, Ω = 15.0

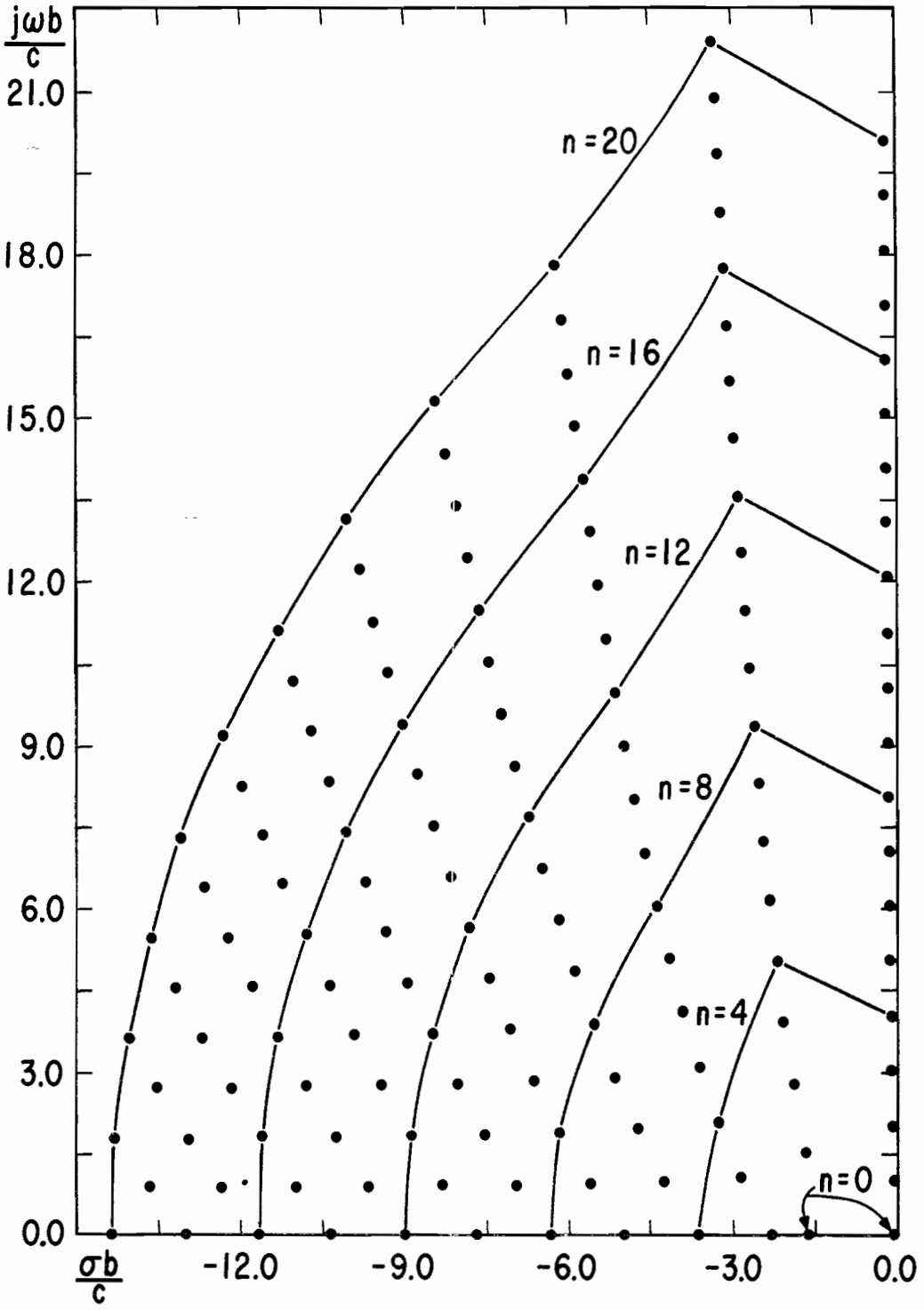

Figure 7. Natural frequencies of circular loop, Types I and II, $\Omega = 20.0$

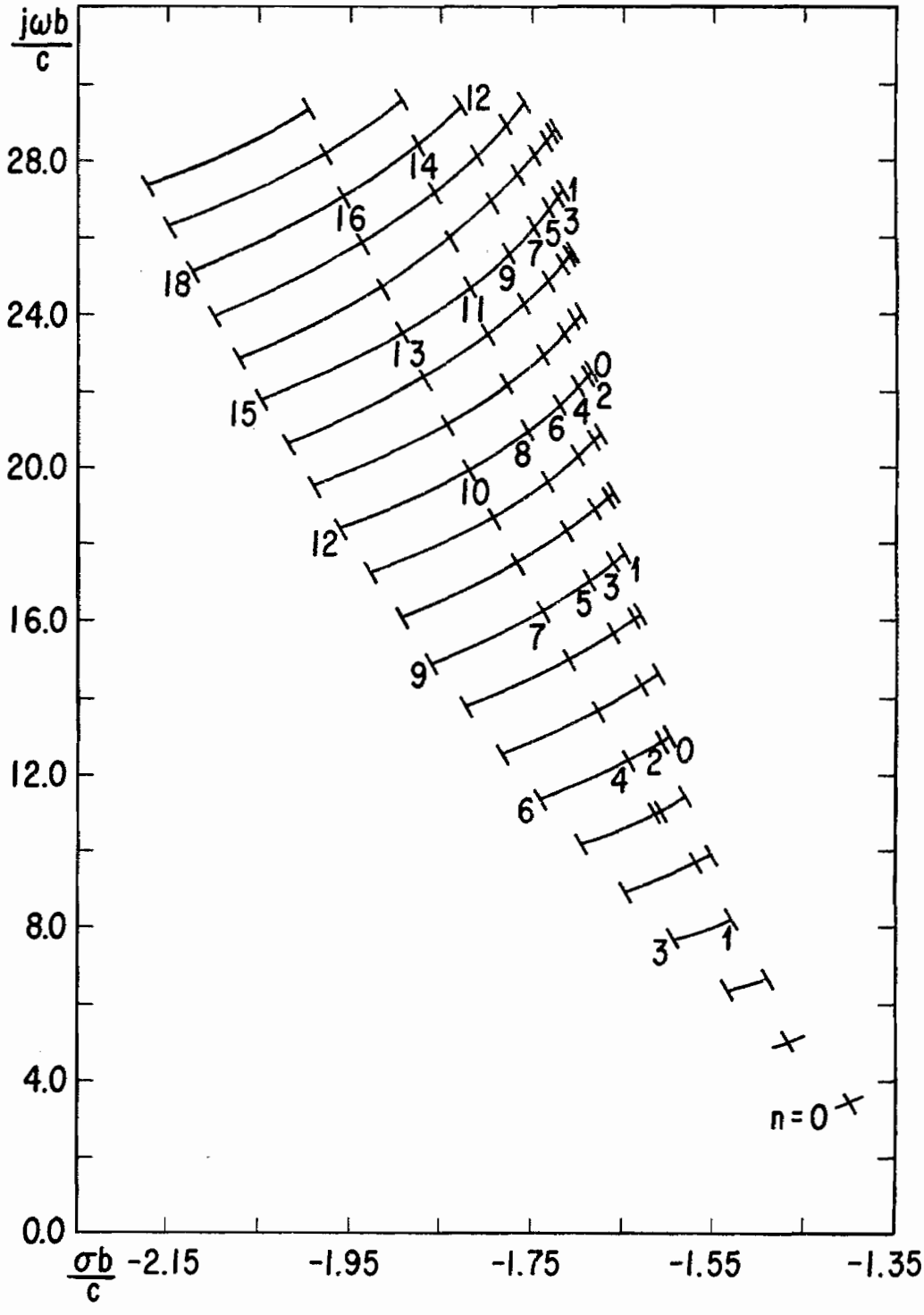

Figure 8. Natural frequencies of circular loop, Type III, $\Omega = 20.0$

Table 1. Residues of the Poles for Pole Indices 0000 to 0801

Pole Index	Ω = 10.0		Ω = 15.0		Ω = 20.0	
	Real	Imaginary	Real	Imaginary	Real	Imaginary
0000	9.6815E-01	0.0	5.4716E-01	0.0	3.8119E-01	0.0
0001	-2.9470E-01	0.0	-1.5274E-01	0.0	-1.0051E-01	0.0
0100	5.9642E-01	2.2783E-01	3.1394E-01	5.2905E-02	2.1011E-01	2.2899E-02
0101	-2.2305E-01	-2.5019E-01	-1.1240E-01	-8.2087E-02	-7.2183E-02	-4.5932E-02
0200	6.8334E-01	2.8602E-01	3.3907E-01	5.5632E-02	2.2112E-01	2.2788E-02
0201	-2.2568E-01	-2.5470E-01	-1.0174E-01	-6.6389E-02	-6.1741E-02	-3.5420E-02
0202	-1.1205E-01	0.0	-5.9709E-02	0.0	-4.0706E-02	0.0
0300	7.4769E-01	3.4247E-01	3.5724E-01	5.8464E-02	2.2872E-01	2.3055E-02
0301	-2.3759E-01	-2.7773E-01	-1.0105E-01	-5.9250E-02	-5.9145E-02	-3.0076E-02
0302	-8.5631E-02	3.4770E-02	-4.3284E-02	1.2467E-02	-2.9036E-02	6.8028E-03
0400	7.9708E-01	3.9755E-01	3.7184E-01	6.1174E-02	2.3465E-01	2.3413E-02
0401	-2.4677E-01	-3.0735E-01	-1.0231E-01	-5.5331E-02	-5.8299E-02	-2.6869E-02
0402	-7.2780E-02	5.3439E-02	-3.6693E-02	1.8668E-02	-2.4528E-02	1.0300E-02
0403	-6.8024E-02	0.0	-3.0160E-02	0.0	-1.9486E-02	0.0
0500	8.3480E-01	4.5073E-01	3.8424E-01	6.3744E-02	2.3954E-01	2.3794E-02
0501	-2.5137E-01	-3.3948E-01	-1.0415E-01	-5.2955E-02	-5.8080E-02	-2.4713E-02
0502	-6.3657E-02	6.6648E-02	-3.2820E-02	2.2656E-02	-2.1974E-02	1.2496E-02
0503	-6.0045E-02	1.7067E-02	-2.5133E-02	5.5337E-03	-1.5958E-02	3.1224E-03
0600	8.6287E-01	5.0120E-01	3.9512E-01	6.6188E-02	2.4375E-01	2.4174E-02
0601	-2.5121E-01	-3.7187E-01	-1.0617E-01	-5.1445E-02	-5.8140E-02	-2.3156E-02
0602	-5.6169E-02	7.7061E-02	-3.0156E-02	2.5580E-02	-2.0272E-02	1.4057E-02
0603	-5.4423E-02	2.8663E-02	-2.2211E-02	8.8515E-03	-1.3978E-02	4.9584E-03
0604	-5.4773E-02	0.0	-2.0890E-02	0.0	-1.2924E-02	0.0
0700	8.8293E-01	5.4817E-01	4.0489E-01	6.8522E-02	2.4746E-01	2.4546E-02
0701	-2.4673E-01	-4.0299E-01	-1.0823E-01	-5.0473E-02	-5.8339E-02	-2.1976E-02
0702	-4.9577E-02	8.5709E-02	-2.8158E-02	2.7889E-02	-1.9033E-02	1.5254E-02
0703	-4.9716E-02	3.7647E-02	-2.0204E-02	1.1163E-02	-1.2658E-02	6.2035E-03
0704	-5.1116E-02	1.1338E-02	-1.8461E-02	3.1974E-03	-1.1248E-02	1.7734E-03
0800	8.9649E-01	5.9105E-01	4.1378E-01	7.0761E-02	2.5078E-01	2.4906E-02
0801	-2.3867E-01	-4.3179E-01	-1.1028E-01	-4.9858E-02	-5.8613E-02	-2.1048E-02

Table 2. Residues of the Poles for Pole Indices 0802 to 1205

Pole Index	Ω = 10.0		Ω = 15.0		Ω = 20.0	
	Real	Imaginary	Real	Imaginary	Real	Imaginary
0802	-4.3558E-02	9.3095E-02	-2.6574E-02	2.9805E-02	-1.8079E-02	1.6218E-02
0803	-4.5440E-02	4.5068E-02	-1.8696E-02	1.2921E-02	-1.1691E-02	7.1242E-03
0804	-4.7987E-02	2.0048E-02	-1.6801E-02	5.3596E-03	-1.0136E-02	2.9433E-03
0805	-4.8913E-02	0.0	-1.6347E-02	0.0	-9.7631E-03	0.0
0900	9.0495E-01	6.2952E-01	4.2199E-01	7.2918E-02	2.5380E-01	2.5255E-02
0901	-2.2795E-01	-4.5768E-01	-1.1229E-01	-4.9494E-02	-5.8928E-02	-2.0301E-02
0902	-3.7949E-02	9.9501E-02	-2.5271E-02	3.1447E-02	-1.7313E-02	1.7023E-02
0903	-4.1392E-02	5.1407E-02	-1.7497E-02	1.4336E-02	-1.0942E-02	7.8455E-03
0904	-4.5033E-02	2.7242E-02	-1.5556E-02	6.9643E-03	-9.3233E-03	3.7889E-03
0905	-4.6974E-02	8.6710E-03	-1.4911E-02	2.1226E-03	-8.7854E-03	1.1504E-03
1000	9.0956E-01	6.6353E-01	4.2963E-01	7.5001E-02	2.5658E-01	2.5591E-02
1001	-2.1544E-01	-4.8039E-01	-1.1425E-01	-4.9313E-02	-5.9264E-02	-1.9686E-02
1002	-3.2666E-02	1.0511E-01	-2.4168E-02	3.2889E-02	-1.6682E-02	1.7713E-02
1003	-3.7483E-02	5.6920E-02	-1.6508E-02	1.5521E-02	-1.0337E-02	8.4338E-03
1004	-4.2114E-02	3.3414E-02	-1.4566E-02	8.2299E-03	-8.6924E-03	4.4386E-03
1005	-4.5036E-02	1.5851E-02	-1.3836E-02	3.6725E-03	-8.0726E-03	1.9697E-03
1006	-4.6033E-02	0.0	-1.3636E-02	0.0	-7.9024E-03	0.0
1100	9.1141E-01	6.9323E-01	4.3679E-01	7.7021E-02	2.5915E-01	2.5917E-02
1101	-2.0193E-01	-4.9993E-01	-1.1616E-01	-4.9270E-02	-5.9612E-02	-1.9171E-02
1102	-2.7663E-02	1.1004E-01	-2.3213E-02	3.4178E-02	-1.6149E-02	1.8315E-02
1103	-3.3671E-02	6.1760E-02	-1.5668E-02	1.6542E-02	-9.8347E-03	8.9283E-03
1104	-3.9172E-02	3.8819E-02	-1.3748E-02	9.2715E-03	-8.1824E-03	4.9599E-03
1105	-4.2998E-02	2.2055E-02	-1.2983E-02	4.8778E-03	-7.5199E-03	2.5911E-03
1106	-4.4970E-02	7.2036E-03	-1.2684E-02	1.5327E-03	-7.2612E-03	8.1128E-04
1200	9.1136E-01	7.1895E-01	4.4355E-01	7.8983E-02	2.6155E-01	2.6231E-02
1201	-1.8809E-01	-5.1649E-01	-1.1802E-01	-4.9333E-02	-5.9964E-02	-1.8735E-02
1202	-2.2915E-02	1.1439E-01	-2.2374E-02	3.5346E-02	-1.5692E-02	1.8850E-02
1203	-2.9945E-02	6.6028E-02	-1.4941E-02	1.7440E-02	-9.4084E-03	9.3536E-03
1204	-3.6190E-02	4.3600E-02	-1.3053E-02	1.0156E-02	-7.7580E-03	5.3918E-03
1205	-4.0821E-02	2.7539E-02	-1.2278E-02	5.8574E-03	-7.0730E-03	3.0839E-03

Table 3. Residues of the Poles for Pole Indices 1206 to 1601

Pole Index	Ω = 10.0		Ω = 15.0		Ω = 20.0	
	Real	Imaginary	Real	Imaginary	Real	Imaginary
1206	-4.3708E-02	1.3477E-02	-1.1929E-02	2.7126E-03	-6.7647E-03	1.4210E-03
1207	-4.4695E-02	0.0	-1.1827E-02	0.0	-6.6741E-03	0.0
1300	9.1009E-01	7.4107E-01	4.4996E-01	8.0894E-02	2.6380E-01	2.6536E-02
1301	-1.7439E-01	-5.3035E-01	-1.1983E-01	-4.9480E-02	-6.0317E-02	-1.8361E-02
1302	-1.8404E-02	1.1823E-01	-2.1625E-02	3.6417E-02	-1.5293E-02	1.9331E-02
1303	-2.6304E-02	6.9796E-02	-1.4299E-02	1.8244E-02	-9.0402E-03	9.7259E-03
1304	-3.3169E-02	4.7846E-02	-1.2450E-02	1.0924E-02	-7.3969E-03	5.7586E-03
1305	-3.8496E-02	3.2440E-02	-1.1678E-02	6.6800E-03	-6.7008E-03	3.4880E-03
1306	-4.2219E-02	1.9082E-02	-1.1306E-02	3.6627E-03	-6.3634E-03	1.9005E-03
1307	-4.4153E-02	6.3224E-03	-1.1148E-02	1.1710E-03	-6.2205E-03	6.0569E-04
1400	9.0811E-01	7.6003E-01	4.5607E-01	8.2758E-02	2.6592E-01	2.6831E-02
1401	-1.6120E-01	-5.4186E-01	-1.2159E-01	-4.9694E-02	-6.0667E-02	-1.8037E-02
1402	-1.4123E-02	1.2162E-01	-2.0949E-02	3.7407E-02	-1.4942E-02	1.9768E-02
1403	-2.2754E-02	7.3119E-02	-1.3726E-02	1.8973E-02	-8.7179E-03	1.0057E-02
1404	-3.0123E-02	5.1618E-02	-1.1918E-02	1.1605E-02	-7.0843E-03	6.0763E-03
1405	-3.6033E-02	3.6839E-02	-1.1158E-02	7.3881E-03	-6.3838E-03	3.8280E-03
1406	-4.0497E-02	2.4153E-02	-1.0776E-02	4.4540E-03	-6.0292E-03	2.2907E-03
1407	-4.3320E-02	1.2033E-02	-1.0588E-02	2.1075E-03	-5.8542E-03	1.0791E-03
1408	-4.4291E-02	0.0	-1.0531E-02	0.0	-5.8008E-03	0.0
1500	9.0577E-01	7.7623E-01	4.6190E-01	8.4580E-02	2.6793E-01	2.7117E-02
1501	-1.4875E-01	-5.5134E-01	-1.2331E-01	-4.9962E-02	-6.1014E-02	-1.7755E-02
1502	-1.0065E-02	1.2460E-01	-2.0333E-02	3.8330E-02	-1.4630E-02	2.0168E-02
1503	-1.9305E-02	7.6043E-02	-1.3209E-02	1.9642E-02	-8.4323E-03	1.0354E-02
1504	-2.7070E-02	5.4960E-02	-1.1442E-02	1.2216E-02	-6.8099E-03	6.3558E-03
1505	-3.3453E-02	4.0785E-02	-1.0698E-02	8.0097E-03	-6.1090E-03	4.1200E-03
1506	-3.8553E-02	2.8761E-02	-1.0315E-02	5.1300E-03	-5.7444E-03	2.6167E-03
1507	-4.2189E-02	1.7267E-02	-1.0111E-02	2.8824E-03	-5.5491E-03	1.4622E-03
1508	-4.4097E-02	5.7722E-03	-1.0021E-02	9.3144E-04	-5.4624E-03	4.7123E-04
1600	9.0331E-01	7.9006E-01	4.6748E-01	8.6363E-02	2.6984E-01	2.7395E-02
1601	-1.3716E-01	-5.5911E-01	-1.2498E-01	-5.0275E-02	-6.1356E-02	-1.7508E-02

Table 4. Residues of the Poles for Pole Indices 1602 to 1900

Pole Index	Ω = 10.0		Ω = 15.0		Ω = 20.0	
	Real	Imaginary	Real	Imaginary	Real	Imaginary
1602	-6.2230E-03	1.2723E-01	-1.9768E-02	3.9195E-02	-1.4350E-02	2.0537E-02
1603	-1.5966E-02	7.8609E-02	-1.2737E-02	2.0259E-02	-8.1769E-03	1.0624E-02
1604	-2.4032E-02	5.7912E-02	-1.1012E-02	1.2772E-02	-6.5664E-03	6.6048E-03
1605	-3.0780E-02	4.4314E-02	-1.0287E-02	8.5639E-03	-5.8675E-03	4.3749E-03
1606	-3.6407E-02	3.2946E-02	-9.9084E-03	5.7195E-03	-5.4974E-03	2.8948E-03
1607	-4.0764E-02	2.2090E-02	-9.6972E-03	3.5405E-03	-5.2892E-03	1.7804E-03
1608	-4.3559E-02	1.1133E-02	-9.5875E-03	1.6982E-03	-5.1806E-03	8.5077E-04
1609	-4.4525E-02	0.0	-9.5533E-03	0.0	-5.1468E-03	0.0
1700	9.0092E-01	8.0186E-01	4.7286E-01	8.8111E-02	2.7166E-01	2.7665E-02
1701	-1.2652E-01	-5.6545E-01	-1.2662E-01	-5.0626E-02	-6.1693E-02	-1.7290E-02
1702	-2.5935E-03	1.2955E-01	-1.9245E-02	4.0011E-02	-1.4096E-02	2.0880E-02
1703	-1.2746E-02	8.0850E-02	-1.2304E-02	2.0835E-02	-7.9466E-03	1.0871E-02
1704	-2.1028E-02	6.0504E-02	-1.0620E-02	1.3282E-02	-6.3481E-03	6.8292E-03
1705	-2.8044E-02	4.7453E-02	-9.9145E-03	9.0643E-03	-5.6529E-03	4.6005E-03
1706	-3.4090E-02	3.6732E-02	-9.5441E-03	6.2418E-03	-5.2801E-03	3.1361E-03
1707	-3.9066E-02	2.6531E-02	-9.3313E-03	4.1113E-03	-5.0636E-03	2.0506E-03
1708	-4.2673E-02	1.6145E-02	-9.2109E-03	2.3465E-03	-4.9406E-03	1.1648E-03
1709	-4.4584E-02	5.4302E-03	-9.1559E-03	7.6368E-04	-4.8842E-03	3.7821E-04
1800	8.9867E-01	8.1194E-01	4.7803E-01	8.9826E-02	2.7341E-01	2.7929E-02
1801	-1.1684E-01	-5.7061E-01	-1.2821E-01	-5.1008E-02	-6.2024E-02	-1.7097E-02
1802	8.2954E-04	1.3157E-01	-1.8758E-02	4.0783E-02	-1.3865E-02	2.1200E-02
1803	-9.6537E-03	8.2800E-02	-1.1903E-02	2.1374E-02	-7.7375E-03	1.1098E-02
1804	-1.8079E-02	6.2767E-02	-1.0259E-02	1.3754E-02	-6.1508E-03	7.0331E-03
1805	-2.5274E-02	5.0226E-02	-9.5746E-03	9.5211E-03	-5.4602E-03	4.8025E-03
1806	-3.1633E-02	4.0135E-02	-9.2143E-03	6.7109E-03	-5.0868E-03	3.3486E-03
1807	-3.7118E-02	3.0604E-02	-9.0034E-03	4.6146E-03	-4.8651E-03	2.2840E-03
1808	-4.1451E-02	2.0831E-02	-8.8779E-03	2.9062E-03	-4.7322E-03	1.4303E-03
1809	-4.4260E-02	1.0584E-02	-8.8104E-03	1.4068E-03	-4.6605E-03	6.9011E-04
1810	-4.5237E-02	0.0	-8.7890E-03	0.0	-4.6378E-03	0.0
1900	8.9665E-01	8.2055E-01	4.8302E-01	9.1511E-02	2.7508E-01	2.8186E-02

Table 5. Residues of the Poles for Pole Indices 1901 to 0038

Pole Index	Ω = 10.0		Ω = 15.0		Ω = 20.0	
	Real	Imaginary	Real	Imaginary	Real	Imaginary
1901	-1.0810E-01	-5.7480E-01	-1.2977E-01	-5.1416E-02	-6.2350E-02	-1.6925E-02
1902	4.0521E-03	1.3335E-01	-1.8302E-02	4.1517E-02	-1.3654E-02	2.1500E-02
1903	-6.6944E-03	8.4487E-02	-1.1529E-02	2.1881E-02	-7.5464E-03	1.1310E-02
1904	-1.5201E-02	6.4729E-02	-9.9245E-03	1.4194E-02	-5.9713E-03	7.2199E-03
1905	-2.2499E-02	5.2658E-02	-9.2619E-03	9.9415E-03	-5.2859E-03	4.9850E-03
1906	-2.9073E-02	4.3170E-02	-8.9130E-03	7.1369E-03	-4.9132E-03	3.5378E-03
1907	-3.4956E-02	3.4313E-02	-8.7064E-03	5.0645E-03	-4.6884E-03	2.4884E-03
1908	-3.9910E-02	2.5195E-02	-8.5794E-03	3.3977E-03	-4.5488E-03	1.6588E-03
1909	-4.3552E-02	1.5482E-02	-8.5048E-03	1.9601E-03	-4.4664E-03	9.5296E-04
1910	-4.5494E-02	5.2313E-03	-8.4701E-03	6.4108E-04	-4.4279E-03	3.1105E-04
2000	8.9486E-01	8.2790E-01	4.8785E-01	9.3167E-02	2.7669E-01	2.8436E-02
2001	-1.0027E-01	-5.7820E-01	-1.3130E-01	-5.1848E-02	-6.2669E-02	-1.6771E-02
2002	7.0805E-03	1.3489E-01	-1.7874E-02	4.2216E-02	-1.3459E-02	2.1783E-02
2003	-3.8722E-03	8.5940E-02	-1.1180E-02	2.2362E-02	-7.3708E-03	1.1507E-02
2004	-1.2410E-02	6.6419E-02	-9.6133E-03	1.4607E-02	-5.8070E-03	7.3923E-03
2005	-1.9743E-02	5.4772E-02	-8.9721E-03	1.0332E-02	-5.1271E-03	5.1513E-03
2006	-2.6443E-02	4.5853E-02	-8.6355E-03	7.5273E-03	-4.7559E-03	3.7080E-03
2007	-3.2617E-02	3.7659E-02	-8.4349E-03	5.4714E-03	-4.5296E-03	2.6698E-03
2008	-3.8080E-02	2.9226E-02	-8.3090E-03	3.8354E-03	-4.3855E-03	1.8583E-03
2009	-4.2465E-02	2.0117E-02	-8.2309E-03	2.4443E-03	-4.2955E-03	1.1784E-03
2010	-4.5337E-02	1.0286E-02	-8.1879E-03	1.1909E-03	-4.2457E-03	5.7248E-04
2011	-4.6340E-02	0.0	-8.1741E-03	0.0	-4.2298E-03	0.0
0031	8.2815E-02	-1.3988E-01	9.9561E-03	-8.9579E-02	-4.2350E-03	-6.0370E-02
0032	7.5120E-02	-7.4634E-02	1.4131E-02	-5.2785E-02	2.7842E-03	-3.5035E-02
0033	6.7087E-02	-4.6155E-02	1.3484E-02	-3.8494E-02	3.5937E-03	-2.5179E-02
0034	5.9855E-02	-2.9319E-02	1.2575E-02	-3.0702E-02	3.5961E-03	-1.9868E-02
0035	5.3293E-02	-1.8238E-02	1.1780E-02	-2.5729E-02	3.4365E-03	-1.6522E-02
0036	4.7375E-02	-1.0622E-02	1.1120E-02	-2.2246E-02	3.2503E-03	-1.4208E-02
0037	4.2101E-02	-5.2913E-03	1.0571E-02	-1.9652E-02	3.0722E-03	-1.2506E-02
0038	3.7452E-02	-1.5370E-03	1.0110E-02	-1.7634E-02	2.9107E-03	-1.1198E-02

Table 6. Residues of the Poles for Pole Indices 0039 to 0436.

Pole Index	Ω = 10.0		Ω = 15.0		Ω = 20.0	
	Real	Imaginary	Real	Imaginary	Real	Imaginary
0039	3.3736E-02	1.0506E-03	9.6986E-03	-1.5993E-02	2.7846E-03	-1.0159E-02
0131	8.1333E-02	-1.0730E-01	1.2415E-02	-7.0875E-02	-4.9828E-04	-4.7243E-02
0132	7.1975E-02	-6.0344E-02	1.3909E-02	-4.5625E-02	3.2179E-03	-3.0038E-02
0133	6.3909E-02	-3.7634E-02	1.3079E-02	-3.4600E-02	3.6058E-03	-2.2502E-02
0134	5.6814E-02	-2.3673E-02	1.2206E-02	-2.8219E-02	3.5220E-03	-1.8186E-02
0135	5.0469E-02	-1.4340E-02	1.1468E-02	-2.3990E-02	3.3469E-03	-1.5360E-02
0136	4.4814E-02	-7.8875E-03	1.0859E-02	-2.0951E-02	3.1636E-03	-1.3354E-02
0137	3.9819E-02	-3.3646E-03	1.0350E-02	-1.8644E-02	2.9932E-03	-1.1850E-02
0138	3.5455E-02	-1.7655E-04	9.9221E-03	-1.6823E-02	2.8406E-03	-1.0678E-02
0231	8.1152E-02	-9.3077E-02	1.2577E-02	-6.3606E-02	8.3704E-05	-4.1919E-02
0232	7.0030E-02	-5.1664E-02	1.3646E-02	-4.1733E-02	3.2650E-03	-2.7288E-02
0233	6.1505E-02	-3.1785E-02	1.2785E-02	-3.2125E-02	3.5476E-03	-2.0792E-02
0234	5.4339E-02	-1.9592E-02	1.1942E-02	-2.6487E-02	3.4415E-03	-1.7011E-02
0235	4.8102E-02	-1.1463E-02	1.1239E-02	-2.2700E-02	3.2660E-03	-1.4499E-02
0236	4.2640E-02	-5.8585E-03	1.0661E-02	-1.9947E-02	3.0886E-03	-1.2694E-02
0237	3.7872E-02	-1.9402E-03	1.0179E-02	-1.7838E-02	2.9254E-03	-1.1327E-02
0238	3.3855E-02	7.4036E-04	9.8279E-03	-1.6189E-02	2.7796E-03	-1.0258E-02
0331	8.1522E-02	-8.4337E-02	1.2595E-02	-5.9743E-02	2.1186E-04	-3.9019E-02
0332	6.8627E-02	-4.5584E-02	1.3467E-02	-3.9274E-02	3.2321E-03	-2.5536E-02
0333	5.9556E-02	-2.7463E-02	1.2584E-02	-3.0404E-02	3.4796E-03	-1.9600E-02
0334	5.2261E-02	-1.6506E-02	1.1752E-02	-2.5204E-02	3.3682E-03	-1.6142E-02
0335	4.6087E-02	-9.2698E-03	1.1069E-02	-2.1702E-02	3.1960E-03	-1.3835E-02
0336	4.0779E-02	-4.3128E-03	1.0509E-02	-1.9144E-02	3.0243E-03	-1.2168E-02
0337	3.6201E-02	-8.8434E-04	1.0044E-02	-1.7175E-02	2.8670E-03	-1.0900E-02
0431	8.2030E-02	-7.8092E-02	1.2648E-02	-5.7364E-02	2.3376E-04	-3.7193E-02
0432	6.7504E-02	-4.0992E-02	1.3363E-02	-3.7577E-02	3.1843E-03	-2.4317E-02
0433	5.7908E-02	-2.4123E-02	1.2449E-02	-2.9133E-02	3.4169E-03	-1.8718E-02
0434	5.0479E-02	-1.4101E-02	1.1617E-02	-2.4213E-02	3.3046E-03	-1.5470E-02
0435	4.4350E-02	-7.5591E-03	1.0942E-02	-2.0903E-02	3.1361E-03	-1.3304E-02
0436	3.9172E-02	-3.1130E-03	1.0392E-02	-1.8484E-02	2.9693E-03	-1.1738E-02

Table 7. Residues of the Poles for Pole Indices 0437 to 0935

Pole Index	Ω = 10.0		Ω = 15.0		Ω = 20.0	
	Real	Imaginary	Real	Imaginary	Real	Imaginary
0437	3.4751E-02	-1.5451E-04	9.9332E-03	-1.6608E-02	2.8234E-03	-1.0545E-02
0531	8.2516E-02	-7.3258E-02	1.2747E-02	-5.5771E-02	2.2764E-04	-3.5942E-02
0532	6.6539E-02	-3.7363E-02	1.3315E-02	-3.6336E-02	3.1385E-03	-2.3420E-02
0533	5.6474E-02	-2.1466E-02	1.2363E-02	-2.8155E-02	3.3626E-03	-1.8039E-02
0534	4.8926E-02	-1.2188E-02	1.1522E-02	-2.3422E-02	3.2505E-03	-1.4935E-02
0535	4.2837E-02	-6.2031E-03	1.0848E-02	-2.0249E-02	3.0850E-03	-1.2871E-02
0536	3.7771E-02	-2.1722E-03	1.0302E-02	-1.7932E-02	2.9218E-03	-1.1379E-02
0631	8.2922E-02	-6.9338E-02	1.2882E-02	-5.4642E-02	2.1594E-04	-3.5035E-02
0632	6.5674E-02	-3.4414E-02	1.3307E-02	-3.5389E-02	3.0990E-03	-2.2732E-02
0633	5.5204E-02	-1.9310E-02	1.2313E-02	-2.7379E-02	3.3167E-03	-1.7498E-02
0634	4.7557E-02	-1.0642E-02	1.1457E-02	-2.2775E-02	3.2046E-03	-1.4499E-02
0635	4.1508E-02	-5.1156E-03	1.0778E-02	-1.9701E-02	3.0413E-03	-1.2510E-02
0636	3.6507E-02	-1.4137E-03	1.0234E-02	-1.7462E-02	2.8808E-03	-1.1076E-02
0731	8.3231E-02	-6.6066E-02	1.3043E-02	-5.3812E-02	2.0568E-04	-3.4351E-02
0732	6.4878E-02	-3.1971E-02	1.3329E-02	-3.4645E-02	3.0664E-03	-2.2187E-02
0733	5.4064E-02	-1.7536E-02	1.2290E-02	-2.6746E-02	3.2782E-03	-1.7058E-02
0734	4.6341E-02	-9.3799E-03	1.1415E-02	-2.2236E-02	3.1657E-03	-1.4135E-02
0735	4.0329E-02	-4.2358E-03	1.0729E-02	-1.9235E-02	3.0038E-03	-1.2205E-02
0736	3.5746E-02	-9.1274E-04	1.0217E-02	-1.7020E-02	2.8598E-03	-1.0811E-02
0831	8.3446E-02	-6.3284E-02	1.3222E-02	-5.3185E-02	1.9896E-04	-3.3821E-02
0832	6.4136E-02	-2.9920E-02	1.3373E-02	-3.4045E-02	3.0401E-03	-2.1746E-02
0833	5.3034E-02	-1.6060E-02	1.2287E-02	-2.6221E-02	3.2463E-03	-1.6693E-02
0834	4.5251E-02	-8.3398E-03	1.1391E-02	-2.1778E-02	3.1327E-03	-1.3828E-02
0835	3.9281E-02	-3.5204E-03	1.0695E-02	-1.8833E-02	2.9716E-03	-1.1942E-02
0931	8.3575E-02	-6.0889E-02	1.3415E-02	-5.2701E-02	1.9617E-04	-3.3400E-02
0932	6.3439E-02	-2.8180E-02	1.3434E-02	-3.3552E-02	3.0193E-03	-2.1383E-02
0933	5.2095E-02	-1.4823E-02	1.2299E-02	-2.5777E-02	3.2197E-03	-1.6385E-02
0934	4.4271E-02	-7.4774E-03	1.1381E-02	-2.1384E-02	3.1047E-03	-1.3565E-02
0935	3.8348E-02	-2.8843E-03	1.0676E-02	-1.8484E-02	2.9441E-03	-1.1713E-02

Table 8. Residues of the Poles for Pole Indices 1031 to 2031

Pole Index	Ω = 10.0		Ω = 15.0		Ω = 20.0	
	Real	Imaginary	Real	Imaginary	Real	Imaginary
1031	8.3629E-02	-5.8808E-02	1.3616E-02	-5.2323E-02	1.9706E-04	-3.3061E-02
1032	6.2779E-02	-2.6694E-02	1.3506E-02	-3.3141E-02	3.0033E-03	-2.1078E-02
1033	5.1236E-02	-1.3779E-02	1.2324E-02	-2.5397E-02	3.1977E-03	-1.6122E-02
1034	4.3383E-02	-6.7584E-03	1.1383E-02	-2.1041E-02	3.0808E-03	-1.3337E-02
1131	8.3619E-02	-5.6990E-02	1.3823E-02	-5.2023E-02	2.0122E-04	-3.2784E-02
1132	6.2154E-02	-2.5418E-02	1.3589E-02	-3.2793E-02	2.9913E-03	-2.0820E-02
1133	5.0447E-02	-1.2894E-02	1.2358E-02	-2.5069E-02	3.1796E-03	-1.5895E-02
1134	4.2575E-02	-6.1552E-03	1.1393E-02	-2.0740E-02	3.0605E-03	-1.3138E-02
1231	8.3555E-02	-5.5393E-02	1.4034E-02	-5.1784E-02	2.0820E-04	-3.2555E-02
1232	6.1560E-02	-2.4317E-02	1.3678E-02	-3.2496E-02	2.9826E-03	-2.0598E-02
1233	4.9719E-02	-1.2142E-02	1.2400E-02	-2.4781E-02	3.1648E-03	-1.5698E-02
1234	4.1816E-02	-5.6757E-03	1.1411E-02	-2.0475E-02	3.0427E-03	-1.2962E-02
1331	8.3447E-02	-5.3986E-02	1.4248E-02	-5.1592E-02	2.1760E-04	-3.2364E-02
1332	6.0996E-02	-2.3363E-02	1.3773E-02	-3.2239E-02	2.9768E-03	-2.0407E-02
1333	4.9046E-02	-1.1500E-02	1.2448E-02	-2.4528E-02	3.1528E-03	-1.5524E-02
1431	8.3301E-02	-5.2743E-02	1.4463E-02	-5.1438E-02	2.2905E-04	-3.2205E-02
1432	6.0458E-02	-2.2536E-02	1.3873E-02	-3.2016E-02	2.9734E-03	-2.0240E-02
1433	4.8421E-02	-1.0951E-02	1.2502E-02	-2.4302E-02	3.1432E-03	-1.5370E-02
1531	8.3124E-02	-5.1642E-02	1.4679E-02	-5.1314E-02	2.4224E-04	-3.2070E-02
1532	5.9946E-02	-2.1816E-02	1.3975E-02	-3.1820E-02	2.9721E-03	-2.0094E-02
1533	4.7840E-02	-1.0479E-02	1.2559E-02	-2.4101E-02	3.1357E-03	-1.5234E-02
1631	8.2923E-02	-5.0667E-02	1.4894E-02	-5.1214E-02	2.5690E-04	-3.1956E-02
1632	5.9457E-02	-2.1190E-02	1.4080E-02	-3.1647E-02	2.9726E-03	-1.9965E-02
1731	8.2701E-02	-4.9801E-02	1.5108E-02	-5.1135E-02	2.7281E-04	-3.1860E-02
1732	5.8990E-02	-2.0645E-02	1.4187E-02	-3.1493E-02	2.9746E-03	-1.9851E-02
1831	8.2463E-02	-4.9032E-02	1.5322E-02	-5.1073E-02	2.8978E-04	-3.1778E-02
1832	5.8544E-02	-2.0169E-02	1.4295E-02	-3.1356E-02	2.9779E-03	-1.9749E-02
1931	8.2212E-02	-4.8349E-02	1.5534E-02	-5.1024E-02	3.0764E-04	-3.1709E-02
2031	8.1950E-02	-4.7743E-02	1.5744E-02	-5.0986E-02	3.2627E-04	-3.1650E-02

the $\omega b/c$ axis at approximately $\omega = n$. Type II poles, which vary in number according to the mode number n, have indices, the last two digits of which range from 01 to as high as 11.

For example, for $\Omega = 10$ mode 20 (Figure 3), the index number 2000 represents the pole at (-1.08, 19.96); 2001 represents the pole at (-1.77, 21.82); 2002 the pole at (-5.70, 16.90); and finally, 2011 the pole at (-13.66, 0.0). For a given mode, an increasing number in the last two index digits moves along the elliptical arc from near the $\omega b/c$ axis toward the negative real axis in a counter-clockwise manner. These first two types of poles have been plotted in Figures 3, 5, and 7. The third category of poles, Type III, contains an infinite number of poles lying almost parallel to the $\omega b/c$ axis. Only the poles such that $\omega b/c < 30$ are tabulated. Again, the first two digits of the index number represent the mode number; however, here the last two digits all begin with 3, denoting poles of the third type. These range from 31 up to as high as 39. For example, for $\Omega = 10$ mode 0 (Figure 4), the index number 0031 represents a pole at (-0.89, 3.76); 0032 represents a pole at (-0.93, 7.05); and 0039 a pole at (-1.15, 29.46). Poles in this layer are numbered sequentially beginning with the pole having

the smallest imaginary part and proceeding away from the σ axis. These Type III poles are plotted in Figures 4, 6, and 8.

Umashankar [8] notes that asymptotically for Type III poles there are only two sets of roots, one set for even modes and another set for odd modes. The convergence to these two sets of values for the lower orders can be readily seen in Figures 4, 6, and 8, where for increasing values of s along the $\omega b/c$ axis all Type III poles converge, regardless of mode, to one distinct set of values for even modes and one for odd modes. In Tables 1 through 8 it can be seen that for relatively large values of s the residues follow the same pattern. For large s all even modes tend to the same residues regardless of mode; similarly for all odd modes.

These tables of pairs of complex numbers representing the poles and residues of the admittance transfer function are uniquely determined by the loop geometry, independent of excitation. They provide, through the partial fraction expansion of the admittance transfer functions, a means of accurately characterizing the electromagnetic properties of loop antennas for three relatively different sized antennas through mode 20. The representation of the time domain response in terms of the poles s_{ni} and residues R_{ni}

yields time domain results which compare well with the Fourier transform of frequency domain data. However, a comparison in the frequency domain of the integral representation and the partial fraction representation of the transfer admittance function at the same frequency indicates that the latter representation does not appear to converge to the correct result. This is illustrated in Figure 9 where the partial fraction and integral representation of $1/a_0(j\omega)$ are compared. One notes the apparently constant offset in the imaginary part, which should be zero at $\omega = 0$. Since a constant would represent an additional entire function added to the partial fraction expansion, this problem was studied in some detail.

An obvious possible source of error would be that the s_{ni} and R_{ni} were not being computed to sufficient accuracy. The early results were computed using standard precision arithmetic on the CDC 6600 with 14 significant digits of accuracy. The Anger-Weber function calculation was evaluated by using an alternating series expansion. To check for roundoff errors, the entire routine was rewritten for double precision which carries 28 significant digits. The new routine was checked against the original, but the troublesome imaginary value at the origin

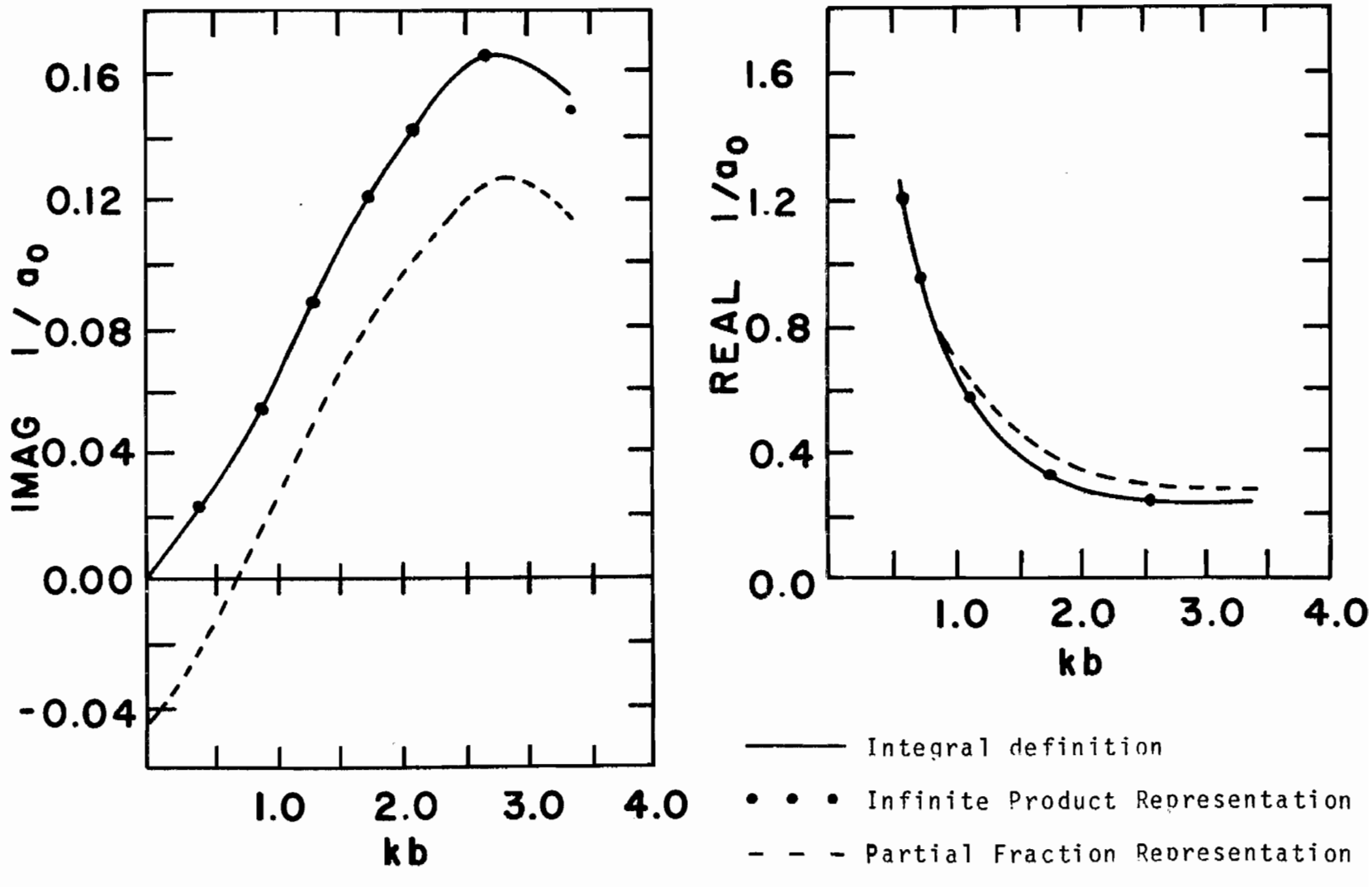

Figure 9. Real and imaginary part of $1/a_0(j\omega)$

remained virtually unchanged.

One result of the conversion to double precision was the extension of the range of the argument for which the Anger-Weber function could be accurately calculated. This permitted poles s_{ni} and residues R_{ni} to be calculated in the region $|\omega b/c| \leq 30.0$ in the s plane. Using the result of [8], the asymptotic formula was also used to compute s_{ni} and R_{ni} for values near $\omega b/c = 30.0$. In the regions where the two calculations could be compared, some small differences were noted between the accurate value of s_{ni} and R_{ni} calculated using the series expansion method and that computed using the asymptotic formula. It is certainly true, then, that for values of s_{ni} and R_{ni} in the range of $\omega b/c$ from 30 up to possibly several hundred, small errors are introduced by the asymptotic formula.

At $s = 0$, the partial fraction series becomes

$$1/a_n(o) = - \sum_i R_{ni}/s_{ni} \qquad (2.46)$$

where the series must sum to zero to have the correct value. It is easily seen that errors in the poles and residues will give $1/a_n(s)$ the wrong behavior near $s = 0$. Furthermore, dividing the partial fraction series into those terms whose poles and residues are computed from

the series representation of the Anger-Weber function and those computed from the asymptotic formula, we have

$$1/a_n(s) = \sum_{\substack{i \\ \mathrm{Im}\left(\frac{s_{ni}b}{c}\right) \leq 30}} \frac{R_{ni}}{s - s_{ni}} + \sum_{\substack{i \\ \mathrm{Im}\left(\frac{s_{ni}b}{c}\right) > 30}} \frac{R_{ni}}{s - s_{ni}} \qquad (2.47)$$

The last series for the range of $s = j\omega$, considered in Figure 9, can be approximately replaced by

$$\sum_{\substack{i \\ \mathrm{Im}\left(\frac{s_{ni}b}{c}\right) > 30}} \frac{R_{ni}}{s_{ni}} \qquad (2.48)$$

since s is small compared to s_{ni}. Errors in these terms would explain the constant offset shown in Figure 9. Adding further weight to this argument is the fact that similar plots of $1/a_n(s)$ for other values of n in the same range of s show the same nearly constant offset, the value of the constant being independent of n. This is not surprising, however, when one recalls that the asymptotic

formula predicts the same set of poles and residues for all even n and another set for all odd n.

In order to alleviate the convergence difficulty in the s domain, an infinite product representation was used. The product representation has the advantage that both the poles and zeros of the function are automatically included in the representation. A further advantage of this formulation is that the residues R_{ni} are not required. These expansions for $1/a_n(s)$ are derived in Appendix A and are given by (2.49) and (2.50):

$$\frac{1}{a_n(s)} = \frac{jsb}{n^2 c\, K_n(o) \prod_{i=1}^{\infty} \left[\left(i - s/s_i\right) e^{\left(s/s_i\right)}\right]} \qquad (2.49)$$

for $n \neq 0$ where the s_i are singularities of the n^{th} mode and K_n is evaluated at s equals zero;

$$\frac{1}{a_o(s)} = \frac{jc}{sb\, K_1(o) \prod_{i=1}^{\infty} \left[\left(1 - s/s_i\right) e^{\left(s/s_i\right)}\right]} \qquad (2.50)$$

when $n = 0$ or where s_i are the singularities of mode zero and K_1 is evaluated at s equals zero.

Another calculation of $1/a_o(s)$ using (2.50) appears in Figure 9. The offset in the imaginary part is completely eliminated. By reformualting the problem, the constant offset has disappeared, and the agreement of the series and product representations tend to validate the accuracy of the calculated s_{ni}. It is therefore concluded that the poor convergence of (2.28) in the frequency domain is due to small deviations in the computed location of the s_{ni} and values of R_{ni} for $\omega b/c > 30.0$ in the s plane.

The product expansion provides a rapid and accurate means of calculating the values of $1/a_n(s)$ in the complex frequency plane, whereas the Laplace inverse of the partial fraction expansion is useful and accurate in the time domain. These two representations provide the necessary tools to accomplish all required calculations for the loop antenna accurately and quickly.

One further question remains concerning the poles s_{ni} for the unloaded loop. It has been pointed out that the third category of poles, i.e., the ones paralleling the imaginary axis in the s plane, do not correspond to similar poles of either dipoles or spheres. Some speculation has been made that these poles are due to the thin wire approximations used to derive the transfer functions

$a_n(s)$. One should keep in mind, however, that such structures as dipoles, spheres, and prolate spheroids are topologically identical in that one structure can be continuously deformed into another and that as such, there must be a one-to-one correspondence of their poles. This correspondence is determined by noting which poles merge into those of a sphere, say, as an object is continuously deformed into a sphere. The loop, however is not topologically equivalent to a sphere, however, because a sphere without handles can never be deformed into a loop and its poles do not necessarily correspond to those of a sphere. To test this hypothesis, a method of moments solution for the n = 0 mode current induced in a toroidal antenna of Ω = 10 was implemented. The mathematical derivation of the integral equation together with the numerical considerations are contained in Appendix B. Basically, the loop is treated as a conducting toroid divided up into a large number of curvilinear patches. The wire circumference was divided into 24 segments with the current assumed to be uniform in each segment. Since in Wu's solution the function $1/a_0(s)$ is proportional to the total current for a uniformly excited wire, in the moment solution the current density on the wire was integrated to find the total current under the condition

of uniform excitation of the entire wire surface. The total current found this way corresponds to $1/a_0(s)$ and the contour plots of the current should yield the true poles of the loop (within moment method approximations).

It was found that in order to generate the required values for filling the matrix, more computer time was required than expected. Consequently, it was necessary to employ a minimum number of points in the contour generation scheme in order to keep the required computer time within reasonable limits. The resulting transfer admittance for mode 0, $\Omega = 10$ is shown in Figure 10. We will show in Chapter III that by comparing phase and magnitude values near the imaginary axis for the method of moments and the product expansion (Figure 11), one finds nearly the same pole structure. The poles s_{0i} of Type III are not only present, but are in approximately the same location as predicted. However, a set of zeros in the total current lies interspersed with the poles in a zigzag fashion running parallel to the imaginary axis. This set of zeros in the total current is caused by surface currents which flow in opposite directions on the inside and outside of the wire such that the total current is zero. In addition to the zeros, there is also a second layer of pole-zero pairs which parallels the first. While

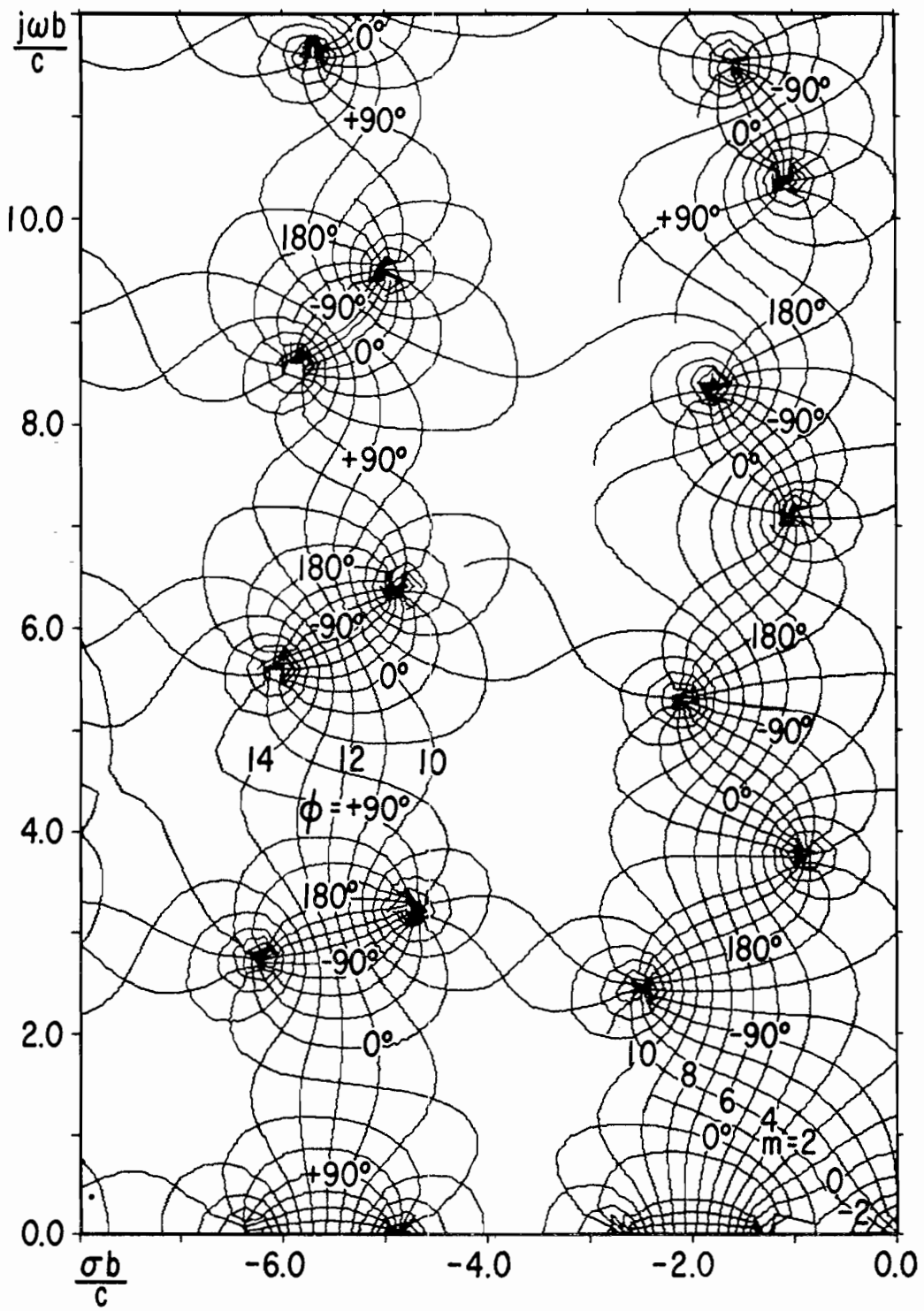

Figure 10. Impedance transfer function obtained by method of moments for n = 0, Ω = 10.0

this layer has such large damping constants that it has negligible contribution in the time and frequency domain, its appearance is interesting, nevertheless.

The matrix determinant, of course, would not have the zeros, but in order to plot the determinant, the density of points calculated would have had to be increased by 10 to 100 times. This is because the appearance of the zeros of the determinant were found to be extremely localized in the s plane.

No attempt was made to generalize the moment method program to investigate the Type III poles for modes other than n = 0, but it is expected that they, too, do indeed exist.

CHAPTER III

ANALYSIS OF THE UNIFORMLY LOADED LOOP ANTENNA

The analysis of an unloaded loop antenna has been presented in the previous chapter using the singularity expansion method. In the present chapter, the effects of uniformly loading a conducting loop are considered. From the point of view of the singularity expansion method, the loading merely shifts the location of the poles of the structure. It is shown that contour plots of the transfer impedance defined in Chapter II may be used to find the shifted pole positions and to determine what shifts are possible. Furthermore, it is shown that the effect of the loading can be interpreted as introducing a feedback loop into a block diagram representation of the impedance transfer function. This observation permits one to use the root-locus techniques well-known in the area of feedback controls to predict certain features of the pole trajectories as the loading is continuously varied. Finally, representative time domain calculations for the step response of a linear antenna are given for various values of purely resistive loading.

3.1 Derivation of the Admittance Transfer Function for the Loaded Loop

Consider uniformly loading the loop with an impedance $Z_L(s)$ total impedance around the loop or $Z_L(s)/2\pi b$ impedance per unit length. The boundary condition on the loop is that the tangential electric field equal the product of the total current and the impedance per unit length. Thus the integral equation (2.2) is replaced by

$$\left(\frac{1}{\rho}\frac{\partial \Phi}{\partial \phi} + sA_\phi\right) + \frac{Z_L(s)I(\phi)}{2\pi b} = \frac{V_o\delta(\phi)}{b} \qquad (3.1)$$

Expanding Φ, A_ϕ, and $I(\phi)$ as in section 2.1, we have

$$\frac{jn}{2}\sum_{n=\infty}^{\infty} a_n I_n e^{-jn\phi} + \frac{Z_L(s)}{2\pi b}\sum_n I_n e^{-jn\phi} = V_o^e\delta(\phi) \qquad (3.2)$$

which can be written as

$$\frac{jn}{2}\sum_{n=\to 0}^{\infty}\left[a_n - \frac{jZ_L}{\pi b n}\right] I_n e^{-jn\phi} = V_o^e\delta(\phi) \qquad (3.3)$$

a form which parallels (2.25). Hence corresponding to (2.27), we now have

$$I_n(s) = \frac{-j}{\eta\pi} \frac{V_o^e(s)}{a_n(s) - jZ_L(s)/\pi b\eta} \tag{3.4}$$

so that the admittance transfer function for the loaded loop is

$$\frac{-j}{\eta\pi} \frac{1}{a_n(s) - jZ_L(s)/\pi b\eta} \tag{3.5}$$

This transfer function has poles at frequencies $s = s'_{ni}$ such that

$$a_n(s'_{ni}) = jZ_L(s'_{ni})/\pi b\eta \tag{3.6}$$

or equivalently,

$$\left|a_n(s'_{ni})\right| = \left|Z_L(s'_{ni})\right|/\pi b\eta \tag{3.7}$$

$$\text{Arg}\left[a_n(s'_{ni})\right] = \text{Arg}\left[Z_L(s'_{ni})\right] + 90° \tag{3.8}$$

where the prime distinguishes quantities defined for the loaded loop from those defined for the unloaded loop. The argument given by Umashankar [8] for the expansion of the admittance transfer function applies here also and results in the partial fraction expansion

$$\frac{1}{a_n(s) - jZ_L(s)/\pi b} = \sum_i \frac{R'_{ni}}{s - s'_{ni}} \qquad (3.9)$$

The residues R'_{ni} in (3.9) above are easily found to be

$$R'_{ni} = \frac{1}{a'_n(s'_{ni}) - jZ'_L(s'_{ni})/\pi b n} \qquad (3.10)$$

where

$$a'_n(s'_{ni}) = \frac{d}{ds} a_n(s)\Big|_{s=s'_{ni}} \qquad (3.11)$$

$$Z'_L(s'_{ni}) = \frac{d}{ds} Z_L(s)\Big|_{s=s'_{ni}} \qquad (3.12)$$

The form of the partial fraction expansion in (3.9) above is identical to (2.28) but with primed quantities replacing unprimed quantities. Hence the discussion of the time and frequency domain current response in Chapter II applies to the loaded loop as well.

3.2 Use of Contour Plots to Represent Poles of the Loaded Loop

Equations (3.7) and (3.8) indicate that contour plots of the magnitude and phase of $a_n(s)$ in the complex frequency plane would simultaneously be plots of the magnitude and

phase (shifted by 90°) of the normalized impedance loading required at each point in the complex frequency domain in order to have a pole there. Using the product expansion formulas (2.49) and (2.50), and including all poles in the range

$$\left| \mathrm{Im}\left(s_{ni} b/c\right) \right| \leq 200 \qquad (3.13)$$

magnitude and phase contours of the $a_n(s)$ are plotted in Figures 11 through 21. These figures are for modes n = 0 through n = 20 for Ω = 10.0.

The magnitude lines m = constant in the figures determine the contours of constant magnitude of a_n and the normalized impedance loading according to

$$m = \frac{8}{\pi} \ln \left| a_n(s) \right| = \frac{8}{\pi} \ln \left| \frac{Z_L(s)}{\pi b \eta} \right| \qquad (3.14)$$

The phase ϕ in degrees is given for $Z_L(s)$ and is related to the phase of $a_n(s)$ by

$$\phi = \arg\left[Z_L(s)\right] = \arg\left[a_n(s)\right] - 90° \qquad (3.15)$$

A number of observations concerning the contour plots are appropriate. One notes, for instance, that only $a_0(s)$ has a pole at s = 0; for all other $a_n(s)$, s = 0 is the only

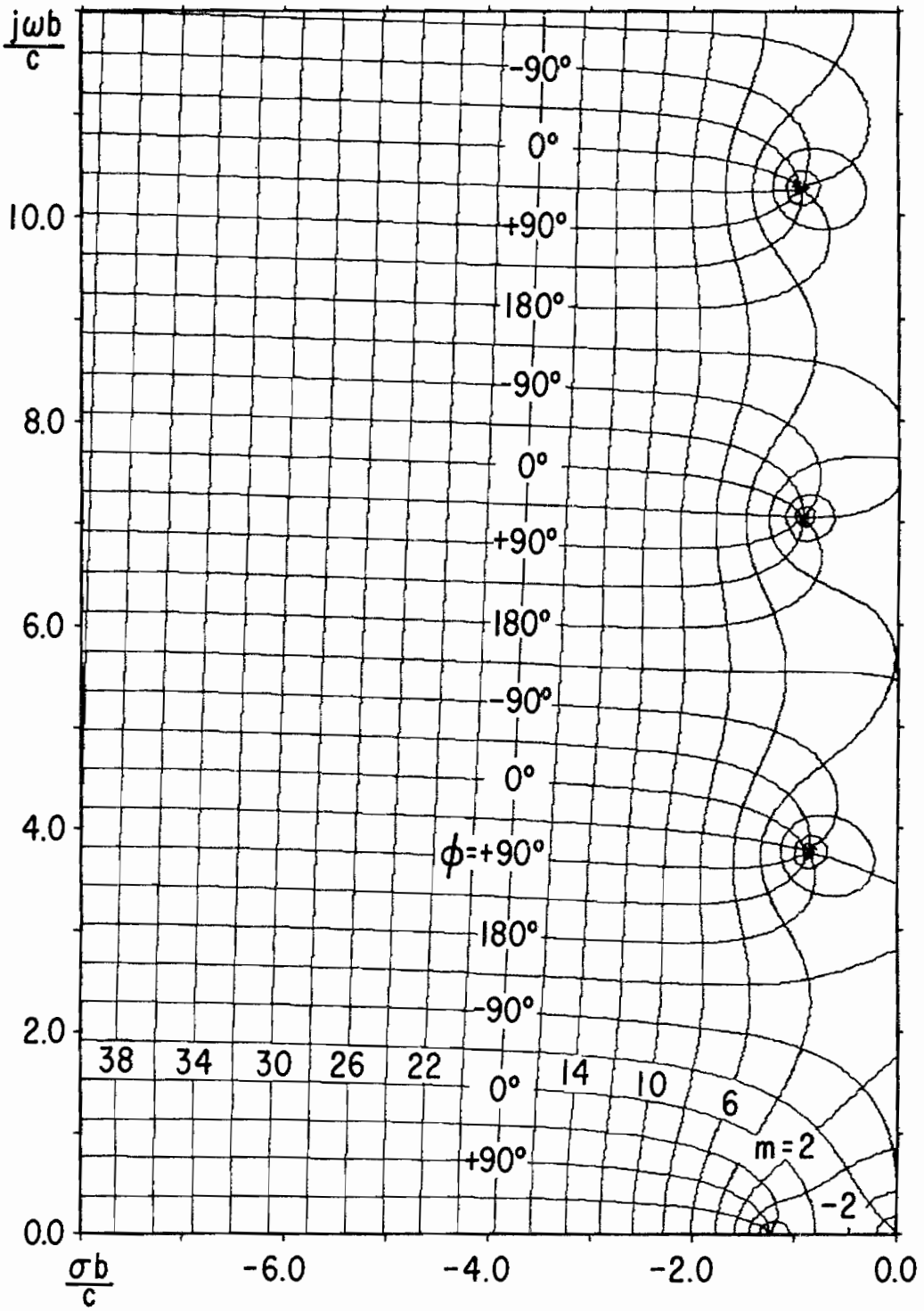

Figure 11. Phase and magnitude contour plot for a_0, Ω = 10.0

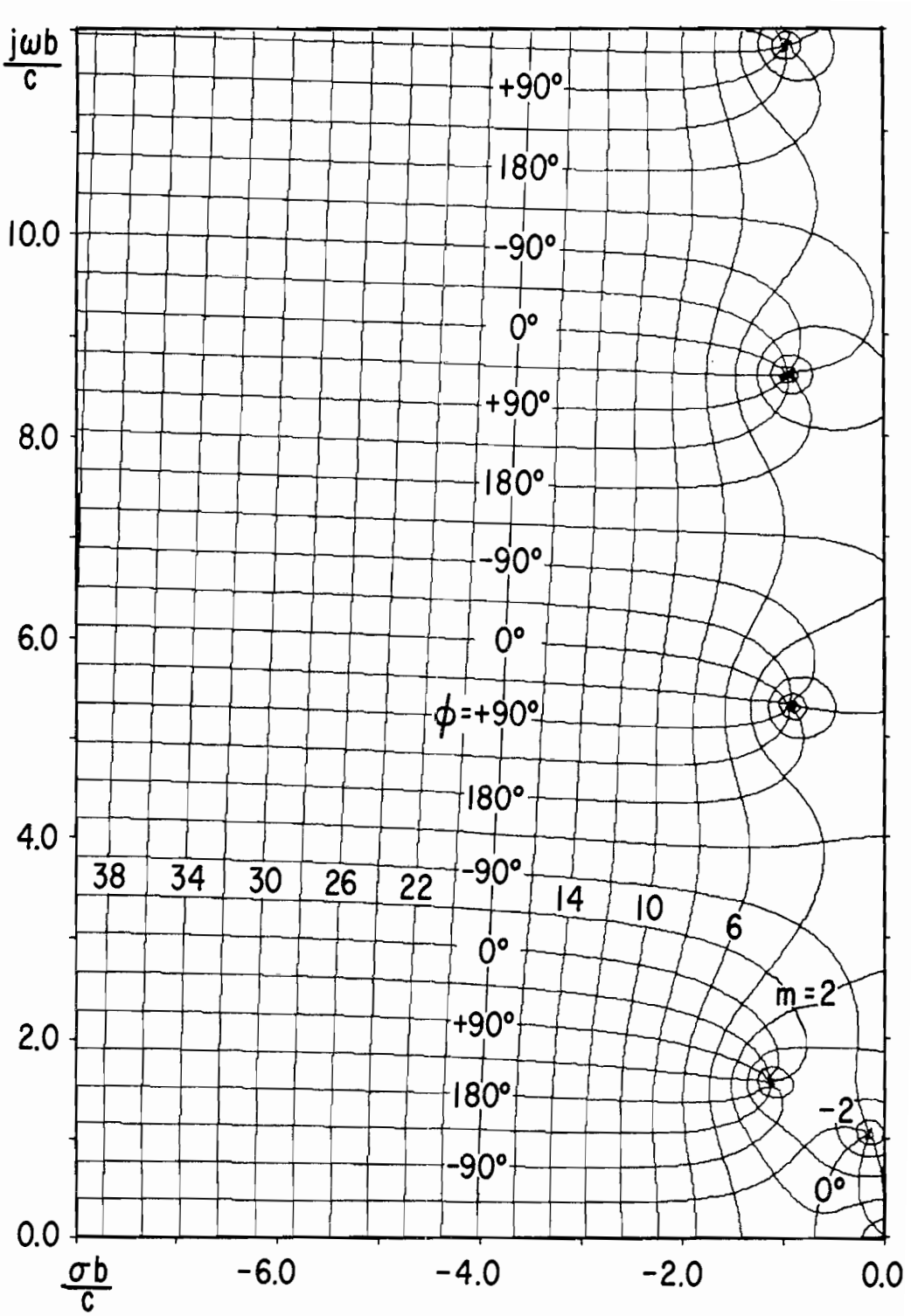

Figure 12. Phase and magnitude contour plot for a_1, Ω = 10.0

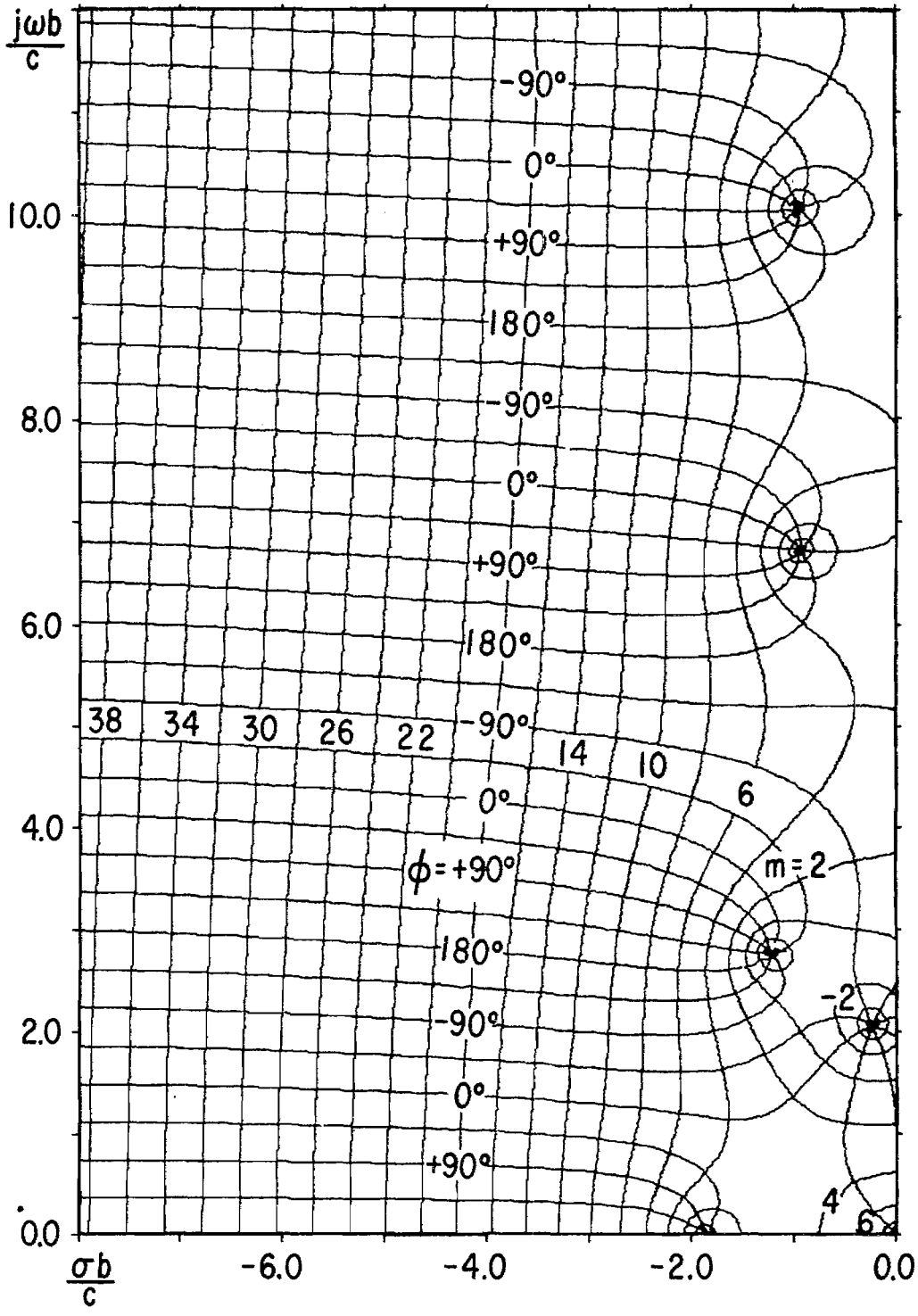

Figure 13. Phase and magnitude contour plot for a_2, Ω = 10.0

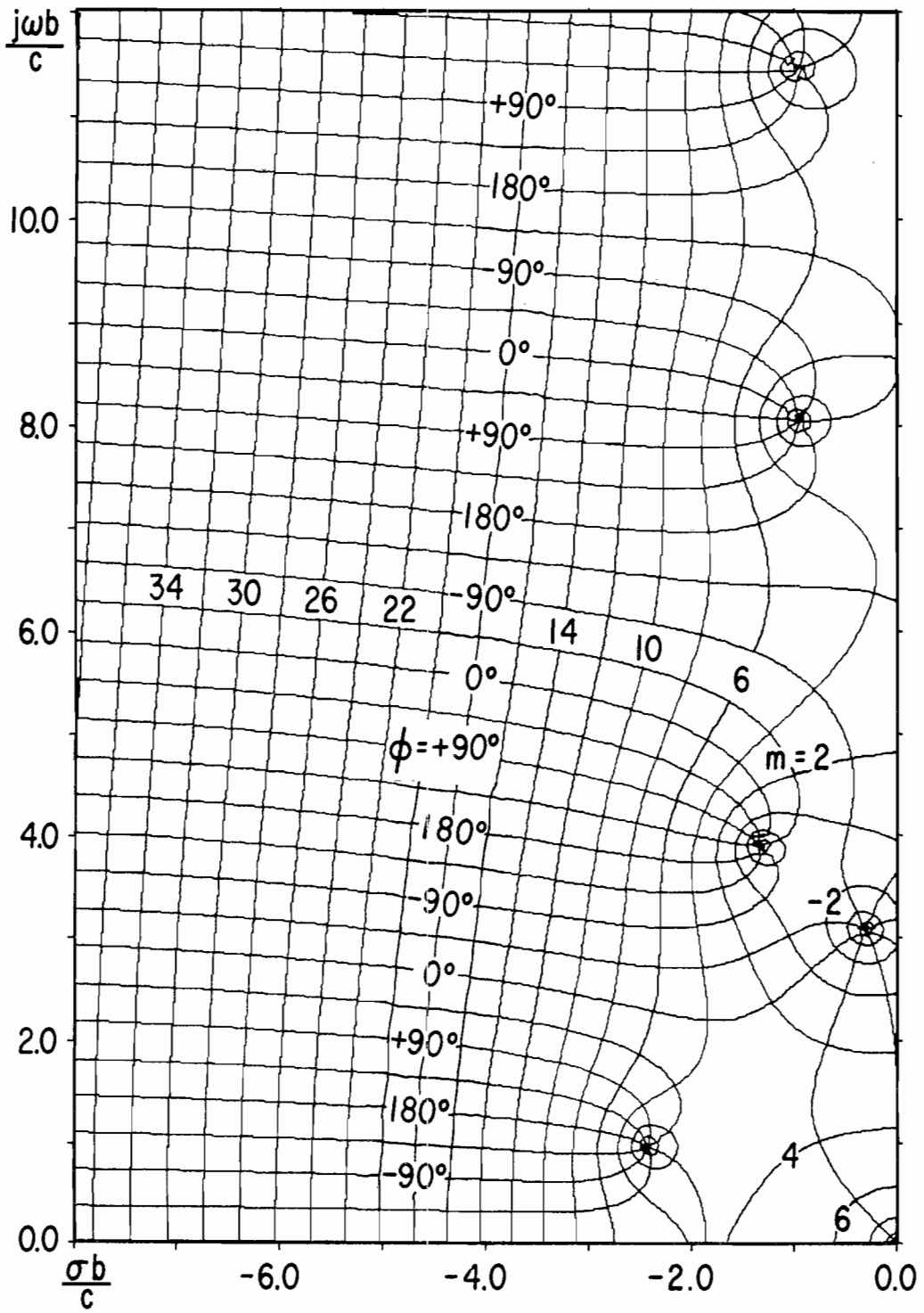

Figure 14. Phase and magnitude contour plot for a_3, $\Omega = 10.0$

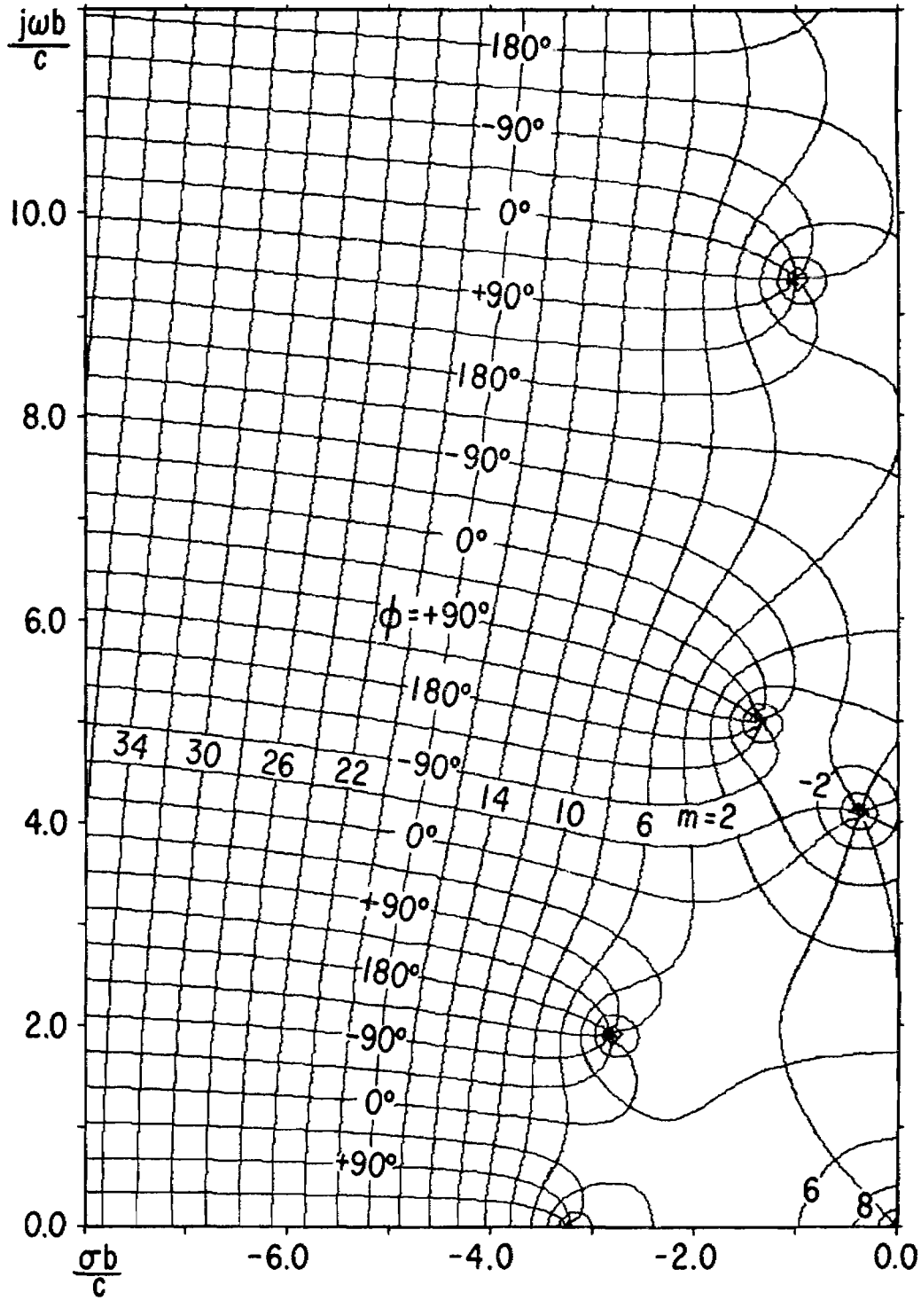

Figure 15. Phase and magnitude contour plot for a_4, $\Omega = 10.0$

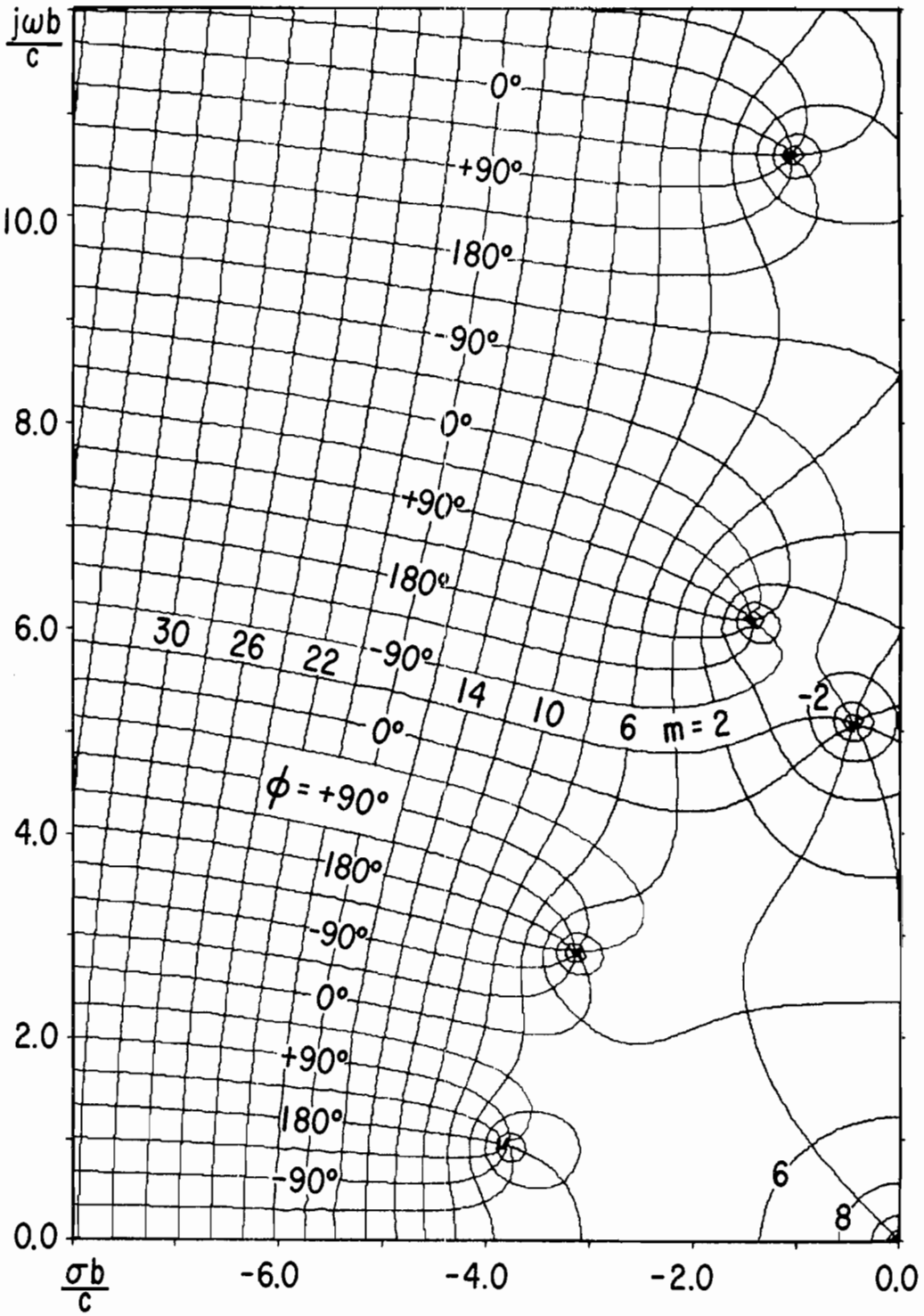

Figure 16. Phase and magnitude contour plot for a_5, Ω = 10.0

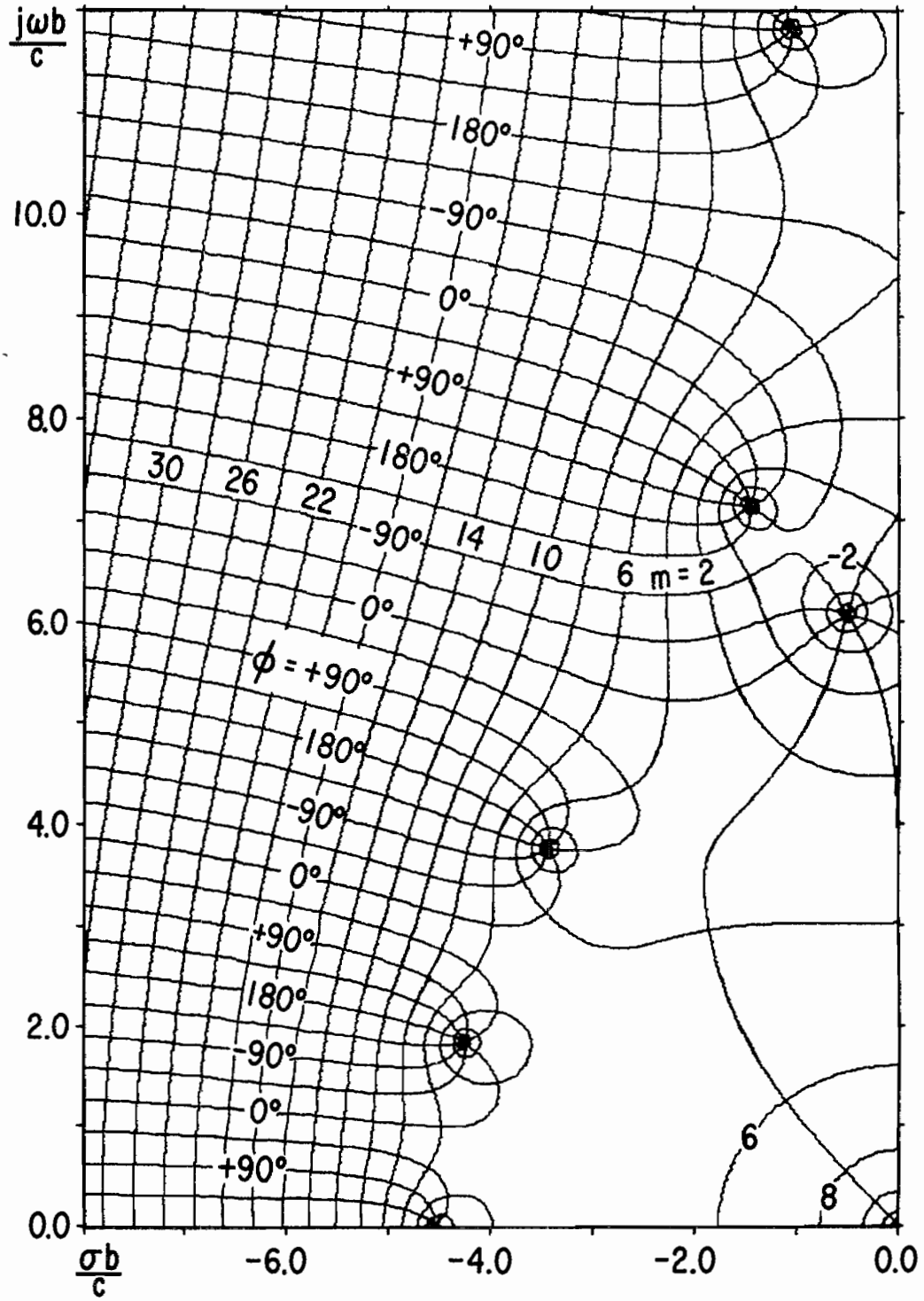

Figure 17. Phase and magnitude contour plot for a_6, $\Omega = 10.0$

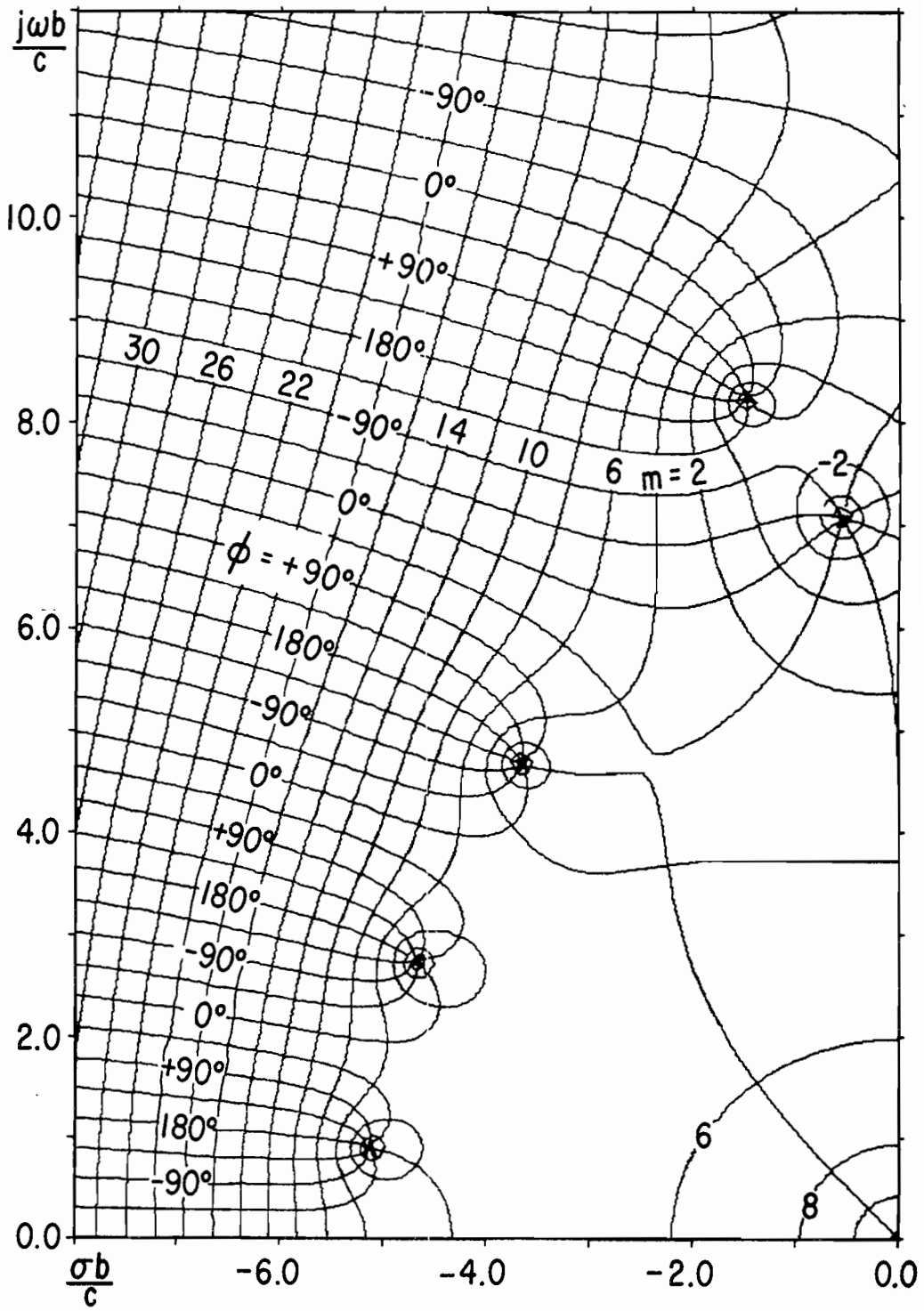

Figure 18. Phase and magnitude contour plot for a_7, $\Omega = 10.0$

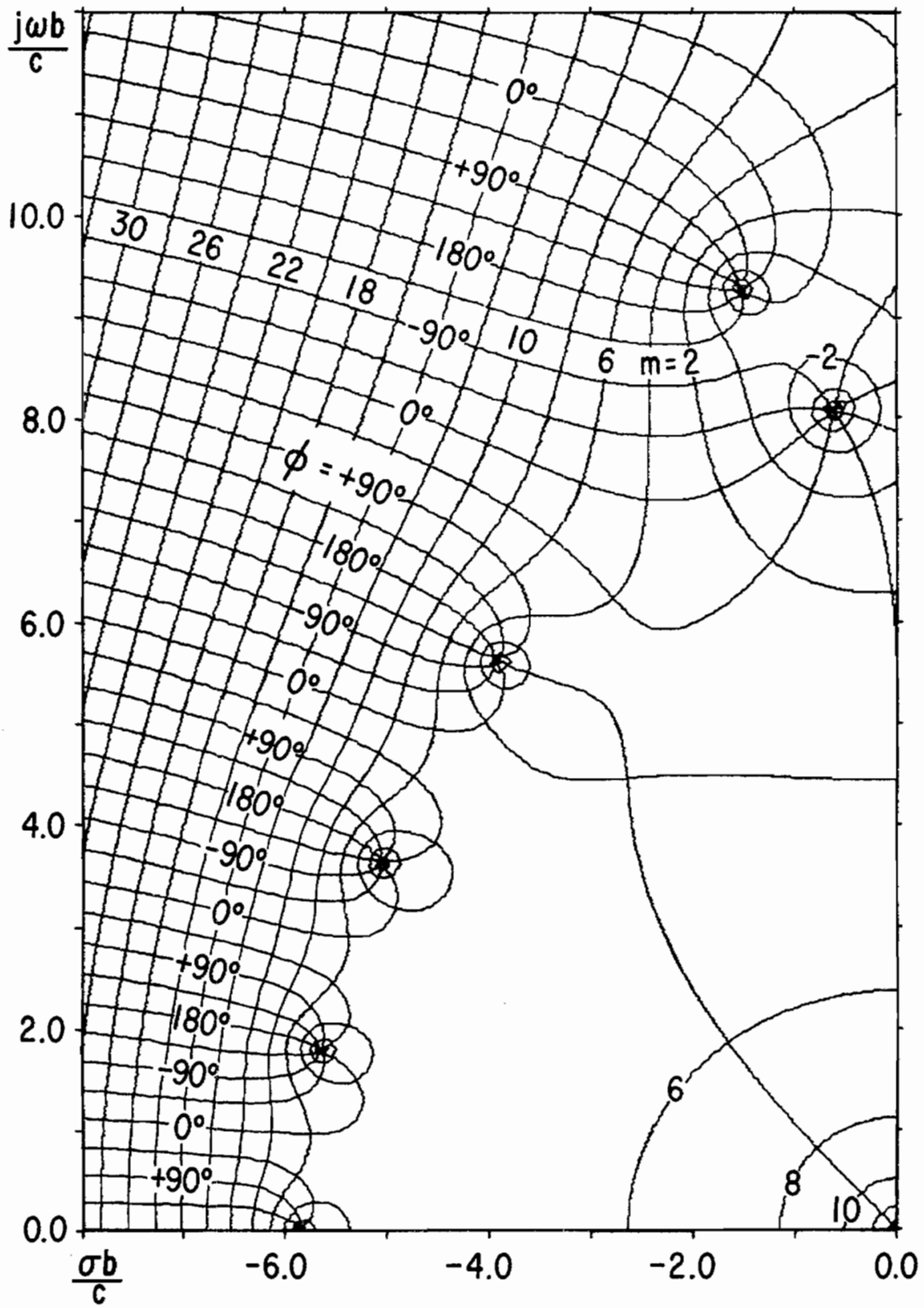

Figure 19. Phase and magnitude contour plot for a_8, Ω = 10.0

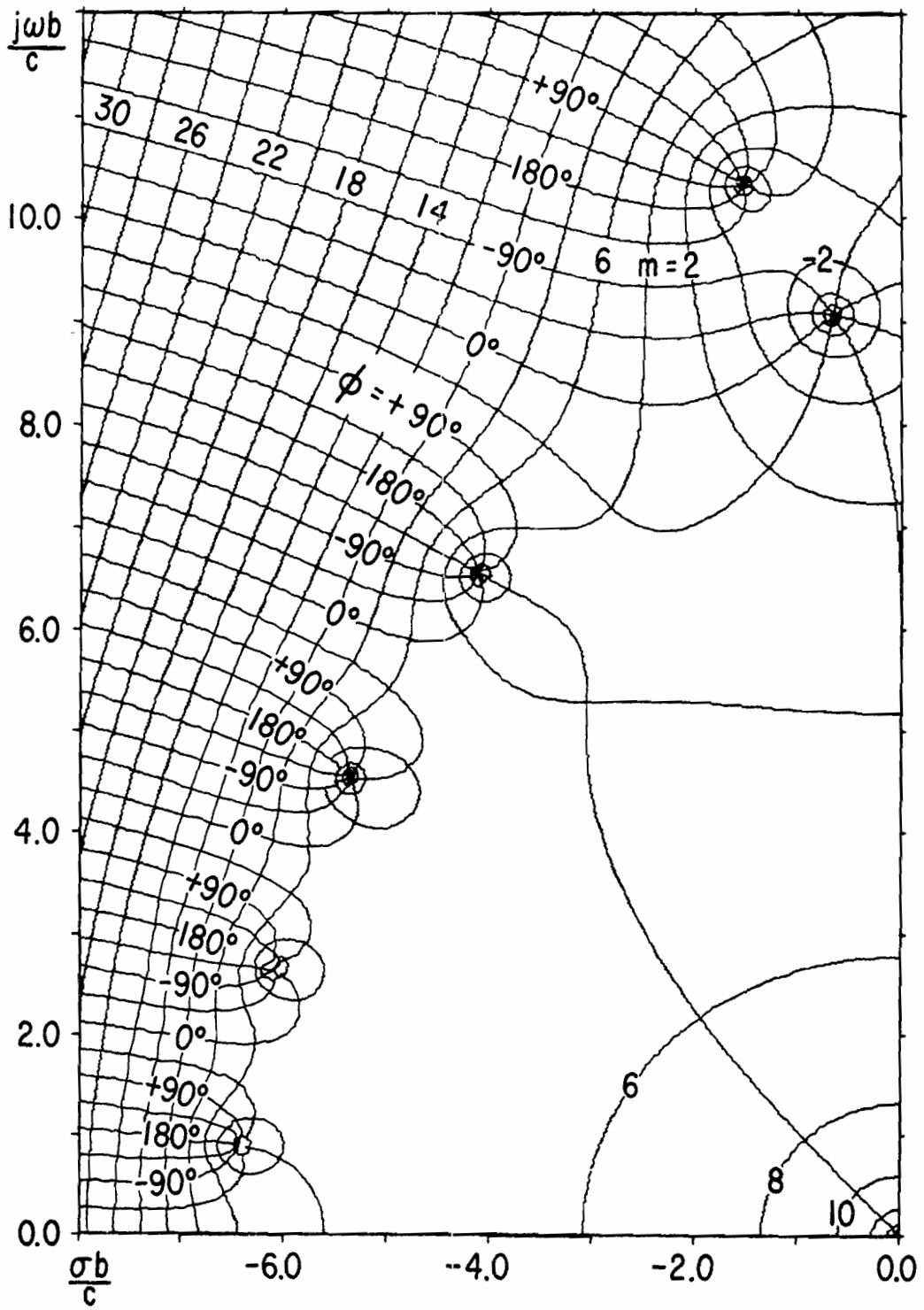

Figure 20. Phase and magnitude contour plot for a_9, $\Omega = 10.0$

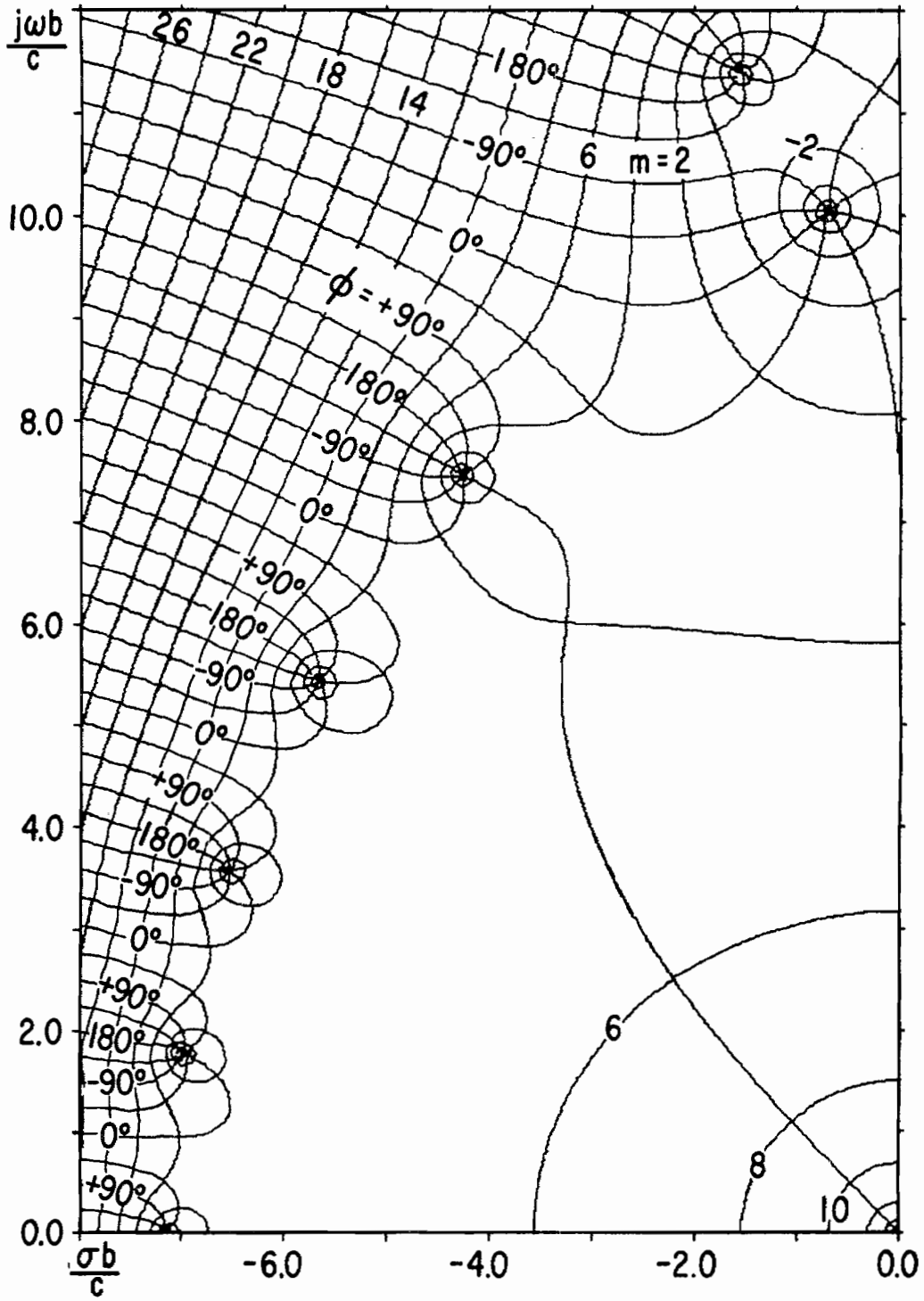

Figure 21. Phase and magnitude contour plot for a_{10}, Ω = 10.0

zero of the transfer impedance. Furthermore, one notes that at each point on the contour plot, we simply read off the magnitude and phase the impedance should have in order to have a pole at that point. This fact is very important and is exploited in the next chapter in synthesizing the loop response by choosing the pole locations. When the loading function $Z_L(s)$ is given (i.e., in the analysis problem), some additional effort is required to graphically find the pole locations. What is needed is a separate contour plot of $Z_L(s)$ using the same complex frequency, magnitude and phase scales. Then by overlaying the two plots, loci of common magnitudes and phases can be drawn. Their intersection will be the pole positions for the given loading function $Z_L(s)$. Note that this would have to be done for every mode, n = 0, 1, 2, . . ., because the loading affects all poles.

One notes that it is possible to shift poles into the right half plane, but this could only be done with active loading. However, generally speaking, Figures 11 through 21 indicate that the heavier the loading (that is, the larger the magnitude of $Z_L(s)$) the larger the damping constant becomes for the shifted pole. One should recall, however, that in Figure 10 in Chapter II, which was computed using moment methods with no thin wire assumptions,

one finds in actuality a layer of zeros just beyond the first layer of poles for mode n = 0 and that heavy loading shifts the poles toward these zeros rather than toward infinity. A similar situation will probably exist for higher order modes.

Finally, it is noted that the lines where the phase is zero on each plot correspond to purely resistive loading and that if the resistance is frequency independent, then the poles will all be on the same magnitude contour. Further, note that the Type I pole (at s = 0) and the Type II pole (on the negative real axis) for mode n = 0 approach each other with increased resistive loading, form a double pole on the negative real axis for a certain critical resistance, and then split into a complex conjugate pair with increased loading. The dominant Type I pole for mode n = 1 approaches the negative real axis with increased resistive loading, forms a double pole there with its conjugate pair, and then the two poles split apart and move away from each other along the negative real axis. These are the only two cases for which dominant (Type I) poles combine with other poles to form a double pole. At either of these loading conditions, one may call the antenna "critically damped." The trajectories of the dominant poles for modes n = 0 to n = 7 with resistive loading only are shown in Figure 22.

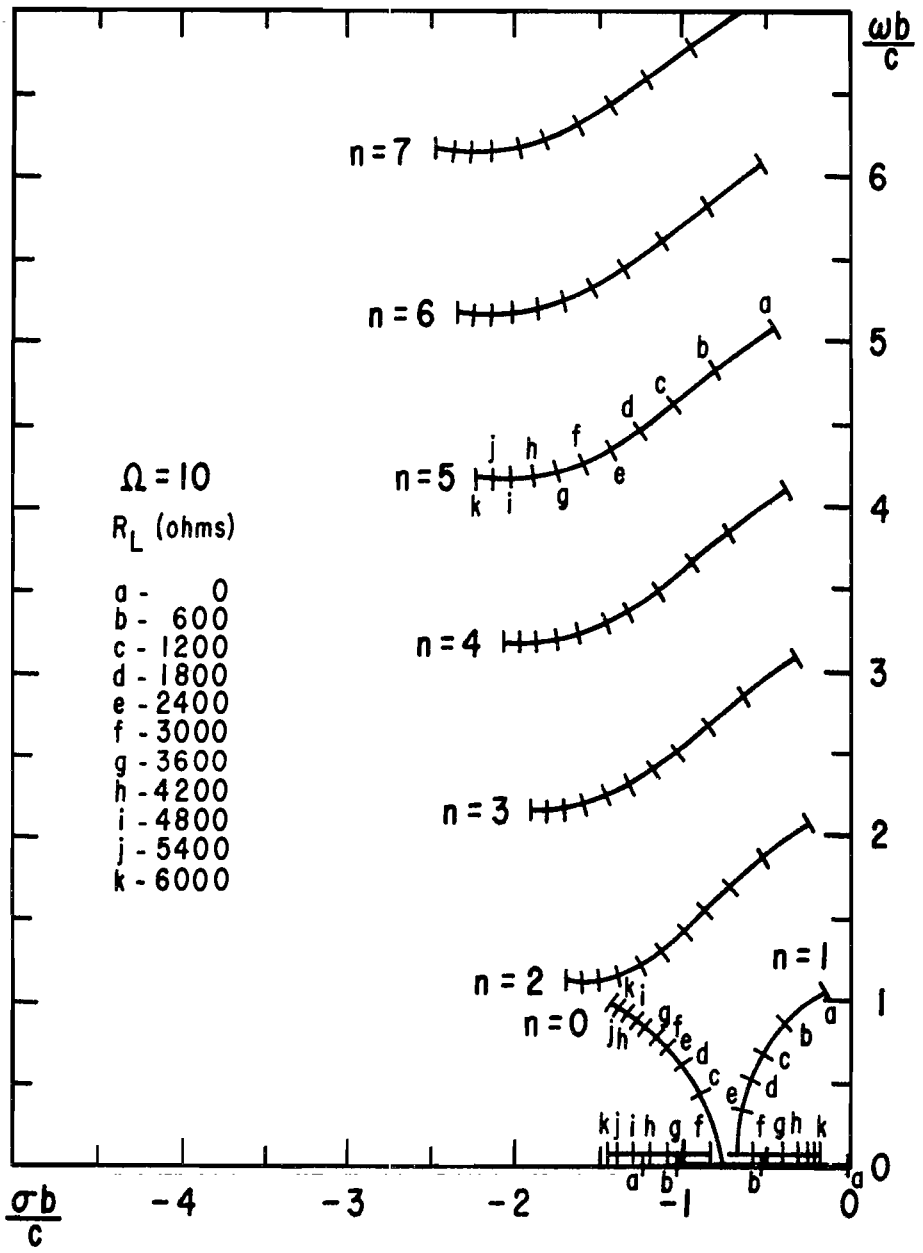

Figure 22. Trajectories of the primary poles of the loop antenna as a function of impedance loading

3.3 Feedback Interpretation of Impedance Loading and Root Locus Methods

The relation between the excitation and the Fourier components of current for the unloaded loop,

$$I_n(s) = \frac{-j}{n\pi} \frac{V_o^e(s)}{a_n(s)} \tag{3.16}$$

may be represented in block diagram form as in Figure 23. The corresponding relation for the loaded loop is

$$I_n(s) = \frac{-j}{n\pi} \frac{V_o^e(s)}{a_n(s) - jZ_L(s)/\pi bn} \tag{3.17}$$

$$= \left[\frac{1}{\left(\frac{n\pi a_n(s)}{-j} \right) + \frac{Z_L(s)}{b}} \right] V_o^e(s) \tag{3.18}$$

which can be represented in the block diagram of Figure 24. One sees that the effect of the loading is to add a feedback loop into the unloaded loop transfer function which shifts the poles of the original unloaded system. This interpretation of loading as adding a feedback path permits one to use the techniques of control system theory [13] to analyze, for example, the effect of feedback on the pole

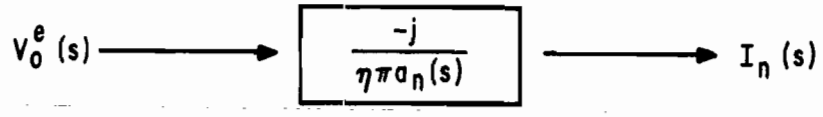

Figure 23. Block system diagram representation of the transfer function of the unloaded loop

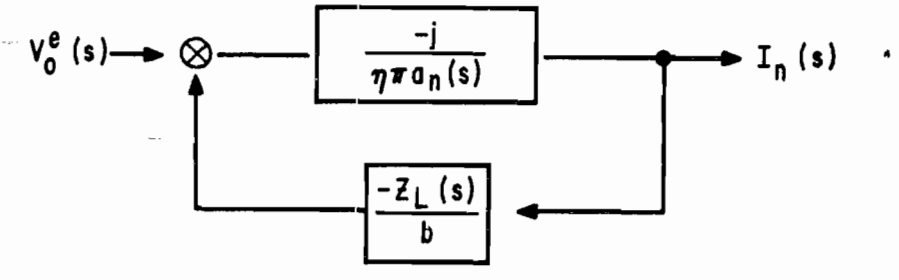

Figure 24. Block system diagram representation of the transfer function of the loaded loop

locations and their movement as the feedback (loading) changes. We discuss in the following the use of the root locus technique of control theory [14] as applied to the loaded loop.

In order to apply the root locus techniques, it is convenient to think of attaining a certain given uniform loading $Z_L(s)$ by loading the loop with a uniform impedance $\mathbf{K}Z_L(s)$ where the real constant $\mathbf{K}$ is varied from $\mathbf{K} = 0$ (corresponding to an unloaded loop) to $\mathbf{K} = 1$ (corresponding to loaded with the desired loading). To consider infinite loading, we merely let $\mathbf{K}$ tend to infinity. Thus the loop transfer function for a given loading $\mathbf{K}Z_L(s)$ is

$$I_n(s) = \left[\frac{1}{\left(jn\pi a_n(s)\right) + \mathbf{K}\,\dfrac{Z_L(s)}{b}} \right] V_o^e(s) \qquad (3.19)$$

The poles of the system are now those frequencies $s = s'_{ni}$ such that

$$\left(jn\pi a_n(s)\right) + \mathbf{K}\, Z_L(s)/b = 0 \qquad (3.20)$$

Ghausi and Kelly [14] have generalized the root locus techniques of control theory to handle characteristic equations of the form

$$F_1(s) + \mathbf{K}\ F_2(s) = 0 \qquad (3.21)$$

for distributed parameter systems where $F_1(s)$ and/or $F_2(s)$ can be written in an infinite product expansion. If one of the factors $F_1(s)$ or $F_2(s)$ cannot be written as an infinite product, then it must be a rational function. Equation (3.20) is of the form (3.21) and since $a_n(s)$ is expandable in an infinite product expansion, we only require that $Z_L(s)$ be a rational function (i.e., $Z_L(s)$ as a "lumped circuit") or have an infinite product expansion ($Z_L(s)$ in a distributed parameter system). The root locus rules given by Ghausi and Kelly as modified to apply to the present problem of a loaded loop are given below [15].

START AND TERMINATION

The loci start ($\mathbf{K} = 0$) at the zeros of $a_n(s)$ and terminate ($\mathbf{K} = \infty$) on the zeros of $Z_L(s)$ as $\mathbf{K}$ varies from zero to infinity.

NUMBER OF LOCI

Since $a_n(s)$ is a trancendental function, there are an infinite number of loci.

SYMMETRY

The loci are symmetrical about the real axis.

LOCI ON REAL AXIS

The loci include those sections of the real axis that lie to the left of an odd number of zeros of $a_n(s)$ and $Z_L(s)$ for $\mathbf{K}$ positive and to the left of an even number of

the zeros of the two functions for K negative.

When a portion of the real axis between two successive zeros of $a_n(s)$ or two successive zeros of $Z_L(s)$ is part of the root locus, there will be a particular value of K for which there will exist a second-order root on the real axis. This root is known as the breakaway point.

BREAKAWAY POINT

The points at which the loci break away from the real axis are found as solutions of the equation

$$a_n(s)Z_L'(s) = a_n'(s)Z_L(s) \tag{3.22}$$

ANGLES OF ARRIVAL AND DEPARTURE

If s_{ni} is a simple zero of $a_n(s)$, the angle of departure of the locus from s_{ni} is given by

$$\phi_d = \frac{\pi}{2} + \arg \frac{Z_L(s_{ni})}{a_n'(s_{ni})} \tag{3.23}$$

If s_j is a simple zero of $Z_L(s)$, the angle of arrival of the locus at s_j is given by

$$\phi_a = \frac{3\pi}{2} + \arg \frac{a_n(s_j)}{Z_L'(s_j)} \tag{3.24}$$

INTERSECTIONS WITH IMAGINARY AXIS

For $\mathbf{K} > 0$, the intersections of the loci with the imaginary axis occur at those values ω_c for which

$$\arg\left[\frac{Z_L(j\omega_c)}{a_n(j\omega_c)}\right] = -\pi/2 \pm 2n\pi \qquad n = 0, 1, 2, \ldots \quad (3.25)$$

and for $\mathbf{K} < 0$, the corresponding values of ω_c are found from

$$\arg\left[\frac{Z_L(j\omega_c)}{a_n(j\omega_c)}\right] = \pi/2 \pm 2n\pi \qquad n = 0, 1, 2, \ldots \quad (3.26)$$

ASYMPTOTIC BEHAVIOR

As $\mathbf{K}$ becomes infinite, the loci may become very complicated. In order to study the loci, we equate both real and imaginary parts of (3.20) to zero:

$$-n\pi\ \mathrm{Im}\left[a_n(s)\right] + \frac{\mathbf{K}}{b}\mathrm{Re}\left[Z_L(s)\right] = 0 \qquad (3.27)$$

$$n\pi\ \mathrm{Re}\left[a_n(s)\right] + \frac{\mathbf{K}}{b}\mathrm{Im}\left[Z_L(s)\right] = 0 \qquad (3.28)$$

Elimination of $\mathbf{K}$ between these two equations defines the root loci. Thus, we obtain for the loci the expression

$$\frac{\mathrm{Re}\left[a_n(s)\right]}{\mathrm{Im}\left[Z_L(s)\right]} = -\frac{\mathrm{Im}\left[a_n(s)\right]}{\mathrm{Re}\left[Z_L(s)\right]} \qquad (3.29)$$

When Equation (3.29) is used, care should be exercised regarding the sign of $\mathbf{K}$ that has been eliminated. As written, the equation defines the loci for both positive and negative values of $\mathbf{K}$.

3.4 Step Response of a Resistively Loaded Loop

Figure 25 shows the step response loop current computed by taking the Laplace inverse of (2.33) at $\phi = 120^{o}$ for a resistively loaded loop with $Z_L = R_L = 600$, 1800 and 5400 ohms. Figure 26 shows the pulse response at the same location with $Z_L = R_L = 600$ and 1800 ohms for a pulse width equal to 0.75 $ct/\pi b$. Noncausal oscillations can be seen in the time interval near $t = 0$ before the first signal arrives at the observation point. The frequency of the noncausal oscillations corresponds to the Type I pole of the first Fourier mode not included in the current representation, as expected. The various discontinuities in the response come from the first current pulse which arrives at the observation point, the current which travels around the longer path from the source to the observation point, the second trip around the loop, and so on. Note that for this loop, $\Omega = 15.0$, the value of $R_L = 5400$ corresponds to a "critically damped" loop.

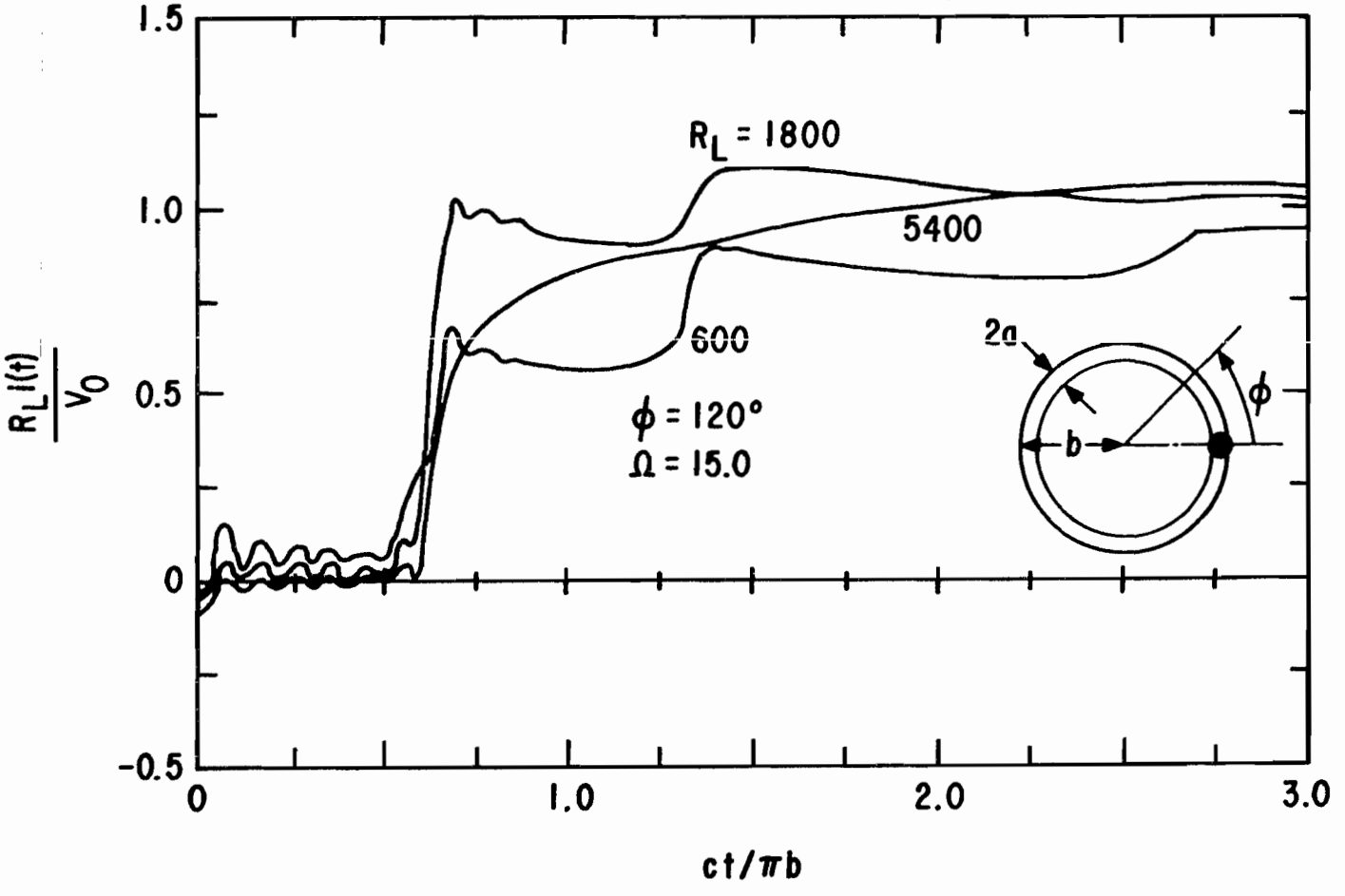

Figure 25. Step response current at ϕ = 120° for various values of resistive loading for a loop antenna

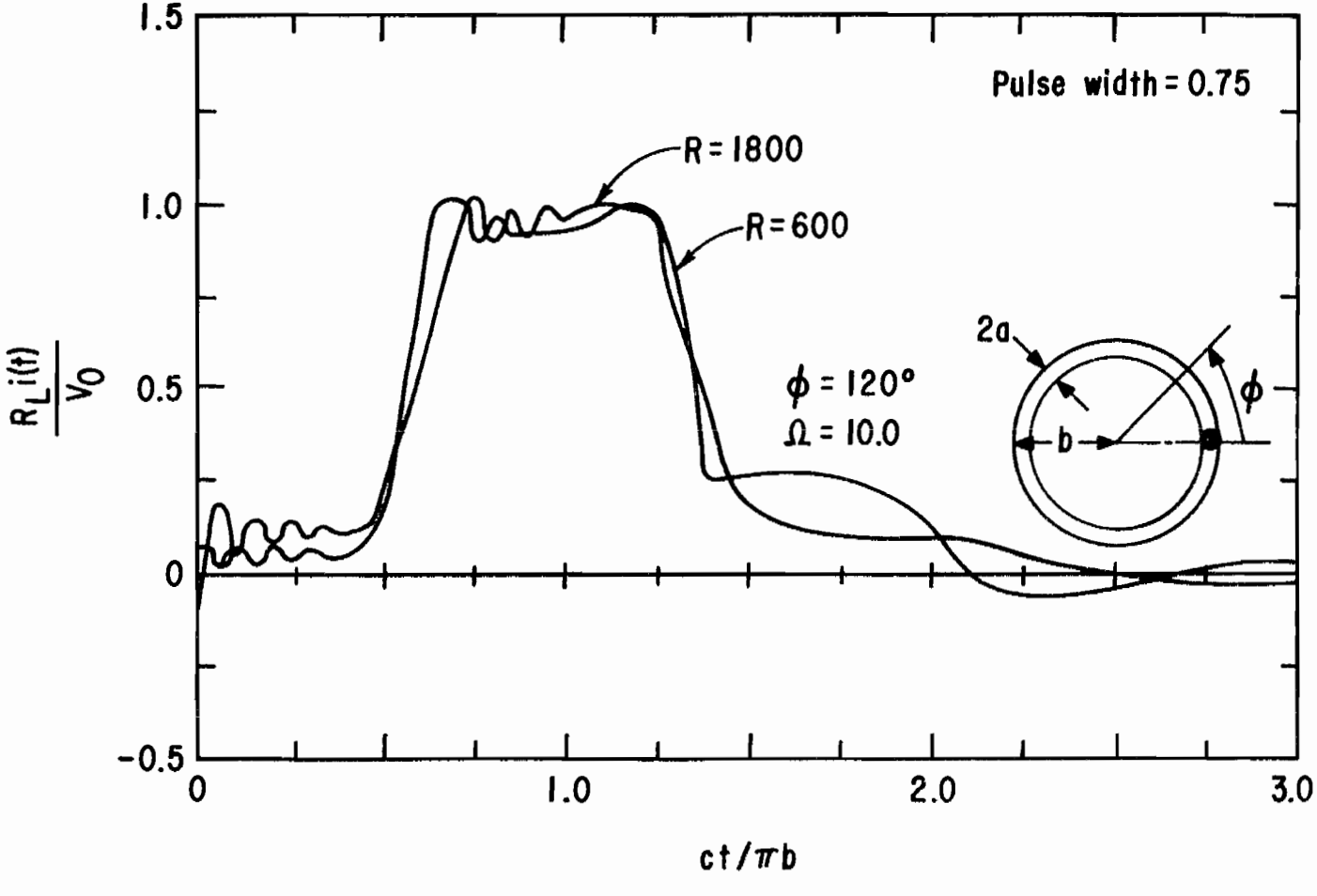

Figure 26. Pulse response current at ϕ=120° for various values of resistive loading for a loop antenna

CHAPTER IV

SYNTHESIS OF THE RESPONSE OF A LOOP ANTENNA

In the previous chapter, various techniques of analysis have been developed and analytical formulations governing the electromagnetic behavior of loop antennas have been derived. These techniques and results are, of course, essential in determining the response of a loop antenna for a given excitation and specified impedance loading. In the following, we demonstrate that some of the results can also be used to change the resonant frequencies such that for a proper excitation (or input), a desired response (i.e., current or radiated field) might be obtained. Thus we obtain, using the singularity expansion representation, a means of extending to an electromagnetic problem a capability that is well-developed in network theory--the ability to synthesize the desired response when the input or excitation waveform is given.

In this chapter the analytic properties of the admittance transfer functions discussed in the previous chapter are employed to formulate the synthesis problem. Some of the considerations and problems involved in elementary time-domain synthesis will be illustrated by using these fundamental synthesis techniques on some simple

example problems.

4.1 Formulation of the Synthesis Problem

Suppose that one is given the voltage transform at the gap, $V_o^e(s)$, and one wishes to find some response quantity such as the current at some point on the loop or the field at some point in space. Then for each Fourier component of the current, there will be a transfer function $T_n(s)$ relating that Fourier component to its contribution to the response at the observation point. The total observed response Y(s) is then just the sum

$$Y(s) = \sum_{n=-\infty}^{\infty} T_n(s)\ I_n(s) \qquad (4.1)$$

For example, if the current at a point ϕ is desired, $T_n(s) = e^{jn\phi}$, whereas for a field point, the transfer functions $T_n(s)$ can be obtained from Appendix C. Using (3.4) for the current, we obtain

$$Y(s) = \frac{-j}{\eta_o \pi} \sum_{n=-\infty}^{\infty} \frac{T_n(s)\ V_o^e(s)}{a_n(s) - jZ_L(s)/\pi b\eta} \qquad (4.2)$$

If we assume that the input $V_o^e(s)$ is given and hence fixed and that $T_n(s)$ depends only on the response quantity we wish to observe, the desired response may be obtained only by manipulating the admittance transfer function by

impedance loading. We may do this as in classical network theory by prescribing both the poles and the residues of the admittance transfer function. The relationship between the loading function and the poles and residues has already been described in the previous chapter. Namely, from (3.6), the condition for a pole at $s = s'_{ni}$ is

$$Z_L(s'_{ni}) = -j\pi b_n a_n(s'_{ni}) \qquad (4.3)$$

and from (3.10) the condition on the residue requires that

$$Z'_L(s'_{ni}) = -j\pi b_n \left[a'_n(s'_{ni}) - \frac{1}{R'_{ni}}\right] \qquad (4.4)$$

where R'_{ni} is the desired residue of the shifted pole. Thus the synthesis problem is that of requiring interpolation conditions on $Z_L(s)$ and its derivative at the desired pole positions. If the residue is not of particular interest, then the condition on the derivative can be relaxed.

One notes that this is not the usual condition required of the admittance transfer function in the circuit theory context. There, the poles and residues (or zeros) of the desired function are those of the response function. In the problem posed by (4.3) and (4.4), on the other hand, the poles and zeros of the function to be

synthesized, $Z_L(s)$, will not be those of the response function.

4.2 Construction of the Impedance Loading Function

We initially begin with the simplifying assumption that the impedance loading function is to be synthesized using only linear lumped circuit elements and devices. Since we are uniformly loading the loop, we may, for example, use many electrically small lumped circuits in series with and uniformly spaced around the loop so as to approximate continuous uniform loading. With the lumped circuit requirement, $Z_L(s)$ must be either a polynomial in s or a rational function; that is, a ratio of two polynomials in s. Since a polynomial is simpler, we consider it first.

Suppose we have N poles we wish to synthesize so that the condition on $Z_L(s)$ is of the form

$$Z_L(s_n) = Z_{Ln}, \quad n = 1, 2, \ldots, N \qquad (4.5)$$

where we assume that in the sequence of poles $s_1, s_2, \ldots, s_N$. If any pole is complex, its complex conjugate counterpart is included in the sequence. The polynomial of lowest order satisfying the interpolation condition (4.5) is constructed using the Lagrange polynomials [16]

$$Z_L(s) = \sum_{n=1}^{N} L_n(s)\, Z_{Ln} \qquad (4.6)$$

where

$$L_n = \frac{f_n(s)}{f_n(s_n)} \tag{4.7}$$

and where

$$f_n(s) \prod_{\substack{i=1 \\ i \neq n}}^{n} (s - s_i) \tag{4.8}$$

Thus $Z_L(s)$ will be a polynomial of degree N - 1.

If, in addition to the pole locations, one specifies the residues, we have, according to (4.4), additional constraints on the derivatives of the loading function:

$$Z'_L(s_n) = Z'_{Ln}, \quad n = 1, 2, \ldots, N \tag{4.9}$$

The problem of interpolating both a function and its first derivative at a set of points is solved by the Hermite or osculating polynomials [15]

$$Z_L(s) = \sum_{n=1}^{N} U_n(s)\, Z_{Ln} + \sum_{n=1}^{N} V_n(s)\, Z'_{Ln} \tag{4.10}$$

where the functions $U_n(s)$ and $V_n(s)$ are polynomials having properties similar to those of the Lagrange interpolation functions $L_n(s)$ of (4.7) and defined by

$$U_n(s) = \left[1 - 2L_n'(s_n)(s - s_n)\right]\left[L_n(s)\right]^2$$

$$V_n(s) = (s - s_n)\left[L_n(s)\right]^2 \qquad (4.11)$$

In this case $Z_L(s)$ will be of degree 2N - 1.

If the degree of the polynomial representing $Z_L(s)$ is greater than one, it is not possible to synthesize $Z_L(s)$ using only passive circuit elements. Since in many applications it may not be economically or technically feasible to use active devices, we examine some further conditions on $Z_L(s)$ which restrict it to be a "positive-real" function of s.

The driving-point admittance or impedance functions of passive networks (that is, networks consisting only of lumped resistors, capacitors, and inductors) are positive-real functions. That is, our impedance loading function must be a positive-real function to be physically realizable as a driving-point impedance. A number of analytical properties of a positive-real function can be derived from its definition. The most basic and significant ones are summarized in Table 9 for convenience. Note that (4) in Table 9 restricts the degree of the polynomial that can be used to represent $Z_L(s)$ to no

Table 9. Properties of Positive Real Functions

1. For lumped networks, the driving-point immittance (admittance or impedance) function W(s) is rational.
2. The coefficients of the numerator and denominator polynomials in W(s) = P(s)/Q(s) are real and positive. As a consequence of this,
   a. Complex poles and zeros of W(s) occur in conjugate pairs.
   b. W(s) is real when s is real.
   c. The scale factor $W(0) = a_0/b_0$ is real and positive.
3. The poles and zeros of W(s) have nonpositive real parts.
4. The degrees of the numerator and denominator polynomials in W(s) differ at most by unity.
5. Poles of W(s) on the jw axis must be simple with real positive residue.
6. The exponent of the lowest power of s in the numerator and denominator polynomial of W(s) can differ at most by unity.
7. At real frequencies (s = jw) the real part of W(s) is an even function of w and the imaginary part is an odd function of w.

greater than first degree. However, $Z_L(s)$ may be a rational function of s,

$$Z_L(s) = \frac{P(s)}{Q(s)} = \frac{a_p s^p + a_{p-1} s^{p-1} + \ldots + a_o}{b_q s^q + b_{q-1} s^{q-1} + \ldots + b_o} \quad (4.12)$$

where $p + q + 2 = N$ if $Z_L(s)$ is required only to satisfy (4.3) and $p + q + 2 = 2N$ if it also satisfies (4.4). In either case, if $Z_L(s)$ is to be positive-real, $|p - q| \leq 1$. The coefficients $a_o, a_1, \ldots, a_p$ and $b_o, b_1, \ldots, b_q$ may be found by substituting (4.12) into (4.3) and (4.4) and solving the resulting system of linear equations for the coefficients.

A <u>necessary</u> condition on the values Z_{Ln} that can be interpolated by positive-real functions has been devised by Youla and Saito [17] based on energy considerations. The condition is that the "Nevalinna-Pick" N x N Hermitian matrix (the asterisk denotes complex conjugate),

$$A = \left[A_{ij}\right] = \left[\frac{Z_i^* + Z_j}{s_i^* + s_j}\right] \quad (4.13)$$

must be nonnegative definite, that is,

$$x^T A x \geq 0 \quad (4.14)$$

for all vectors x. They further show that this condition is sufficient if the s_n are distinct and in the right half plane, i.e., Re $s_n > 0$, $n = 1, 2, \ldots, N$. This would imply, however, that the loop transfer admittance function contains active sources, which is impossible. Unfortunately, necessary and sufficient conditions for the existence of a positive real interpolating function, both with and without the derivative condition, do not appear to be available at this time. The development of a criterion for the loading function to exist and to be positive real is a challenging problem for further research.

4.3 Time Domain Synthesis Applied to the Design of a Pulse Simulator

One application of loaded loop antennas designed to radiate a specified waveform is in the simulation of the electromagnetic pulse (EMP) generated by a high-altitude nuclear detonation. The pulse shape required can be approximated as the difference of two damped exponential functions, one having a very short time constant which determines the rise time of the pulse and another having a long time constant which determines the rate of decay of the pulse. A typical EMP waveform [18] can be expressed as

$$E = E_0\left[e^{\alpha t} - e^{\beta t}\right] \qquad (4.15)$$

where

$$\alpha \approx -2.0 \times 10^6$$

$$\beta \approx -2.6 \times 10^8$$

The value of E_o is a constant, and for the purpose of calculations has been set to unity.

First, we wish to specify the generator output V_o^e. For the pulse generators in common use, it has been found that generator output can be accurately represented by a step function with a finite rise time. The generator rise time and that of the waveform to be synthesized are chosen to have the same rise time so that in the Laplace domain

$$V_o^e(s) = \mathcal{L}\left\{1 - e^{\beta t}\right\} = \frac{-\beta}{s(s-\beta)} \qquad (4.16)$$

where $\beta = -2.6 \times 10^8$.

In the far field there exist only two components of electric field, E_θ and E_ϕ (cf. Figure 27). The area of primary interest for obtaining the desired transient waveform is near the axis of the loop within a cone angle of about 30° from the axis. The ranges of angles θ considered are therefore

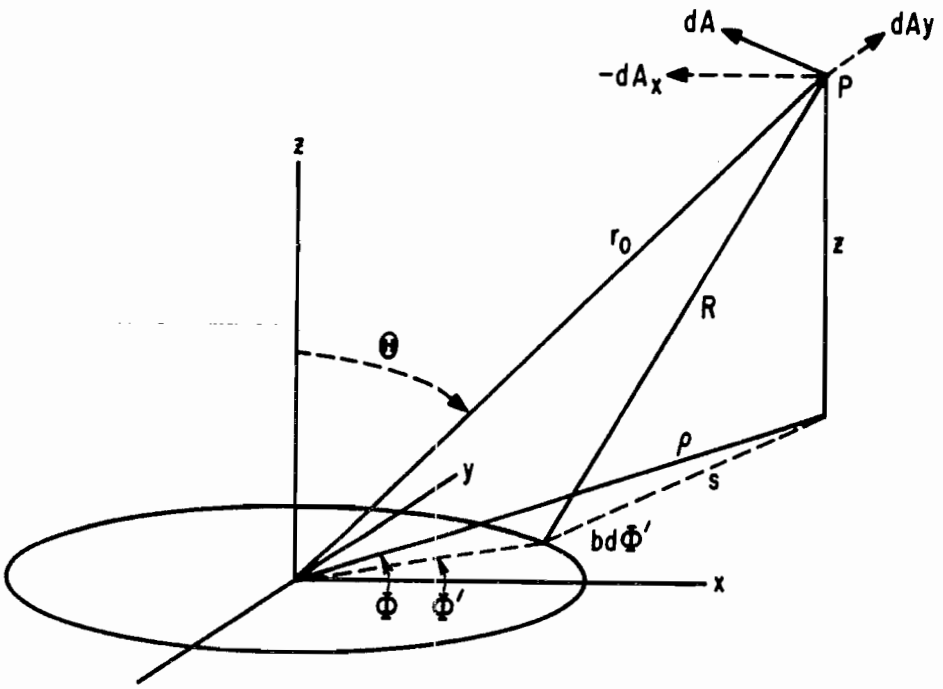

Figure 27. Vector potential at an arbitrary point due to current element $I(\phi')\ bd\phi'$

$$0 \leq \theta \leq 30°$$

and

$$150° \leq \theta \leq 180° \qquad (4.17)$$

On the loop axis only the n = 1 mode contributes to the currents and for the narrow range of angles considered, one may make the simplifying assumption that the field components are coupled to only the n = 1 Fourier mode of current on the loop. That is, we assume that other modes of current on the loop do not contribute significantly to the far fields radiated on and near the axis of the loop antenna.

We wish to find the electric and magnetic fields generated by a prescribed source function (generator) and the resulting induced currents on the loop. These field components are easily obtained with the help of the magnetic vector potential, which is (cf. Figure 27)

$$\bar{A} = \frac{\mu_o}{4\pi} \int_0^{2\pi} (2\pi a)\, \bar{J}(\phi') \frac{e^{-jkR}}{R}\, b d\phi' \qquad (4.18)$$

The complete solution for the field components is obtained by using vector differential operators with (4.18). An expansion for the vector potential in spherical harmonics is derived in Appendix C for an arbitrary observation point in space. This solution is in no way restricted,

and near as well as far fields can be obtained. However, for the case being considered, considerable simplification is possible with no loss in generality if one considers observation points to be in the far field.

The electric field components in the far field are given in [5] for several modes, and specifically for mode n = 1,

$$E_\theta = \frac{-4\pi\, Qs}{a_1 - jZ_L/\pi bn} \frac{J_1(-jsb/c \sin\theta)}{-jsb/c \sin\theta} \cos\theta \sin\phi \tag{4.19}$$

$$E_\phi = \frac{-4\pi\, Qs}{a_1 - jZ_L/\pi bn} J_1'(-jsb/c \sin\theta) \cos\phi \tag{4.20}$$

where

$$Q = \frac{-jV_o^e \mu b}{4\pi^2 \eta_o} \frac{e^{sr/c}}{r} \tag{4.21}$$

For the range of θ near the loop axis at $\theta = 0$, (4.19) and (4.20) reduce to

$$E_\theta = \frac{+jsb \sin\phi}{2\pi c} \frac{V_o^e}{a_1 - jZ_L/\pi bn} \frac{e^{sr/c}}{r} \tag{4.22}$$

$$E_\theta = \frac{+jsb \cos\phi}{2\pi c} \frac{V_o^e}{a_1 - jZ_L/\pi bn} \frac{e^{sr/c}}{r} \tag{4.23}$$

For convenience we will set $\phi = 0$, factor out the time delay $e^{sr/c}$, and drop all other unnecessary constants, exhibiting only the remaining dependence of E_θ on s:

$$E_\theta \propto \frac{jsV_o^e(s)}{a_1(s) - jZ_L(s)/\pi b\eta} \tag{4.24}$$

Equation (4.24) shows that the radiated field is proportional to the time derivative of the current. For mode $n = 1$, the partial fraction expansion of the admittance transfer function is

$$\frac{1}{a_1 - jZ_L/\pi b\eta} = \sum_i \frac{R_i'}{s - s_i'} \tag{4.25}$$

Substituting (4.25) into (4.24), we have

$$E_\theta \propto js\ V_o^e(s) \sum_i \frac{R_i'}{s - s_i'} \tag{4.26}$$

where the s_i' correspond only to mode $n = 1$. Thus, it is seen that the effect of space is to differentiate the current since the far field transform is just proportional to the current transform multiplied by s.

The functional relationship between the above quantities is described below:

$$\text{Output} = \begin{matrix}\text{Admittance}\\ \text{Transfer}\\ \text{Function}\end{matrix} \times \begin{matrix}\text{Space}\\ \text{Transfer}\\ \text{Function}\end{matrix} \times \begin{matrix}\text{Generator}\\ \text{Function}\end{matrix}$$

Using the results of (4.26) and (4.16),

$$E_\theta \propto \sum_i \left(\frac{R_i'}{s - s_i'}\right) \quad \frac{-\beta}{(s - \beta)} \tag{4.27}$$

$$= \sum_i \frac{-\beta R_i'/\left(\beta - s_i'\right)}{(s - \beta)} + \frac{-\beta R_i'/\left(s_i' - \beta\right)}{s - s_i'} \tag{4.28}$$

$$= \frac{-\beta}{a_1(\beta) - jZ_L(\beta)\pi bn} \frac{1}{(s-\beta)} + \sum_i \frac{-\beta R_i'/\left(s_i' - \beta\right)}{s - s_i'} \tag{4.29}$$

When the impedance loading function is restricted to be of the one- or two-element kind, considerable simplification results in the synthesis. In the following, attention is focused on uniformly distributed resistive and RC networks. This choice is made for simplicity and because resistive and RC networks are frequently encountered in high-frequency circuits. Since the complexities involved in general RLC synthesis are much greater, we limit ourselves to a few basic, simple, and useful techniques.

The radiated fields of the unloaded loop antenna do not appear similar to those of an EMP waveform due to the marked oscillations in time. One way to modify the radiated fields is to add resistive loading along the structure so as to reduce the effects which cause the oscillations.

If the structure is resistively loaded so that $Z_L(s) = R_L$, then as the loading is increased the poles in the first layer (see Figure 12) move generally in the $-\sigma b/c$ direction, indicating that their contributions in time attenuate more rapidly. The behavior of the unloaded Type I pole for mode n = 1, located where $\omega b/c \approx 1$ close to the $\omega b/c$ axis, deserves special attention. As the loading is increased, this pole moves on a curved arc down to the $-\sigma b/c$ axis, at which point a double pole is formed with its conjugate pole. As the loading is further increased, this double pole splits, one pole moving to $-\infty$, and the other toward zero along the $\sigma b/c$ axis. This behavior is completely analogous to that observed as the resistance is increased in a series resonant RLC circuit. At the point where the double pole first is formed, we refer to the loaded antenna as being critically damped.

In the following, we examine several possible approaches toward the synthesis of a double exponential waveform (4.15). The problem might be considered as representative of the general synthesis problem. In particular, we encounter certain limitations and considerations which should be common to any synthesis problem involving the loop antenna.

The approach taken here is to force the Type I pole to be the synthesized pole. Since it will have a long damping constant and since the loading generally forces the other poles to have shorter damping constants this pole should dominate the late time response. With the observation point along the loop axis, we consider only the n = 1 mode and observe it in the far field. Finally we restrict our consideration to simple loading functions involving only resistors and capacitors.

We begin by attempting to specify both the pole and its residue. In (4.15) the values of the residues are equal, and the requirement exists to specify only one remaining pole in the sum (4.29) which we call s_1'. Let s_1' be equal to the coefficient α in (4.15), i.e., the pulse decay constant, $s_1' = -2.0 \times 10^6$. The remaining task then is to equate residues. From (4.29) this requirement is met if we let

$$\frac{\beta R_1'}{\beta - s_1'} = \frac{\beta}{a_1(\beta) - jZ_L(\beta)/\pi b\eta} \qquad (4.30)$$

where the impedance loading function $Z_L(\beta)$ is to be determined.

Note that for the required zero of the transfer impedance function, it is also true that

$$a_1(s_1') - jZ_L(s_1')/\pi b\eta = 0 \quad . \tag{4.31}$$

Solving equation (4.30) for $Z_L(\beta)$ we obtain

$$Z_L(\beta) = j\pi b\eta \left(\frac{(\beta - s_1')}{R_1'} - a_1(\beta) \right) \tag{4.32}$$

where R_1' is the value of the residue of the admittance transfer function. If we specify a series RC network, then

$$Z_L(s) = R + \frac{1}{Cs} \tag{4.33}$$

From the residue condition,

$$R_1' = \frac{1}{a_1'(s_1') - \frac{1}{Cs_1'^2}} \tag{4.34}$$

Substituting (4.34) into (4.32) and equating to (4.33)

$$R + \frac{1}{C\beta} = j\pi b\eta \left[\left(a_1'(s_1') - \frac{1}{Cs_1'^2} \right)(\beta - s_1') - a_1(\beta) \right] \tag{4.35}$$

Similarly, substituting (4.33) into (4.31) yields

$$\frac{j}{\pi b \eta}\left(R + \frac{1}{Cs_1'}\right) = a_1(s_1') \tag{4.36}$$

Thus we have two equations with two unknowns, which can be solved for R and C.

Solving the system of equations (4.35) and (4.36) gives

$$C = \frac{\frac{1}{\beta} + \frac{\beta}{s_1'^2} - \frac{2}{s_1'}}{j\pi b\eta\left[(\beta - s_1')a'(s_1') + a(s_1') - a(\beta)\right]} \tag{4.37}$$

and

$$R = -j\pi b\eta a_1(s_i) - \frac{1}{Cs_1'} \tag{4.38}$$

The solution expressed by (4.37) and (4.38) is theoretically correct; in practice it is not realizable with passive elements since the denominator of C is negative, whereas the numerator is positive. Thus specifying <u>both</u> the pole and its residue yields an unphysical solution.

One sees that the requirement that the residues be equal arises from (4.15) because the response at t = 0 should be zero. Since the short time constant exponential is provided by the source and the longer time constant comes from the

antenna "ringing down," and the waveform shape during the transition between the rise and decay is not critical, one should be able to obtain roughly the desired response without specifying the residue of the pole. Accordingly, three additional cases were selected where the pole location was specified to yield a decay constant equal to the value of α specified in (4.15). The first case used a purely resistive load of 4944 Ω; in the second case, 3000 Ω and 66 μf capacitance were used; and, in the third case, a 1000 Ω resistance and 399 μf capacitance were used. These combinations were chosen by requiring $Z_L(s_1') = 4944 + j0$ which puts the pole at the desired position. The time domain response for each case is plotted in Figure 28. In the figure, the shape in each case is almost identical, as expected. However, the decay time is much shorter than the desired value. To see that this effect is independent of both the generator excitation pulse shape and the loading, the step function response was computed and is shown in Figure 29. The similarity of the response in each case leads one to the conclusion that it is a zero of the loop transfer admittance at $s = 0$ which causes the difficulty. Recall that the unloaded loop transfer impedance function has a pole at $s = 0$ which translates to a zero in the loop admittance for both the loaded and the unloaded case. This transmission zero tends to cancel the synthesized pole at $s = s_1'$

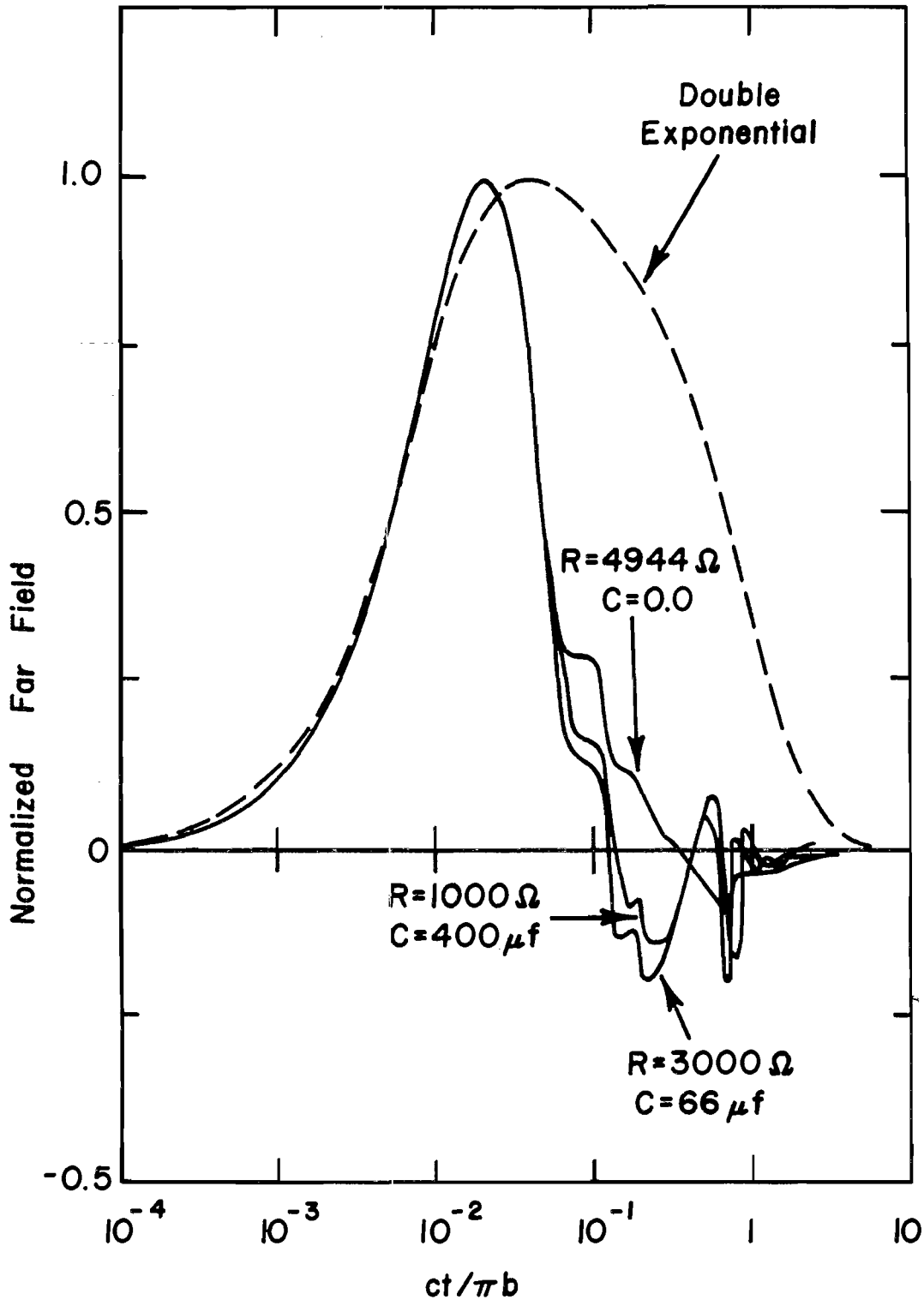

Figure 28. Radiated far field waveform for a modified step input for various values of impedance loading.

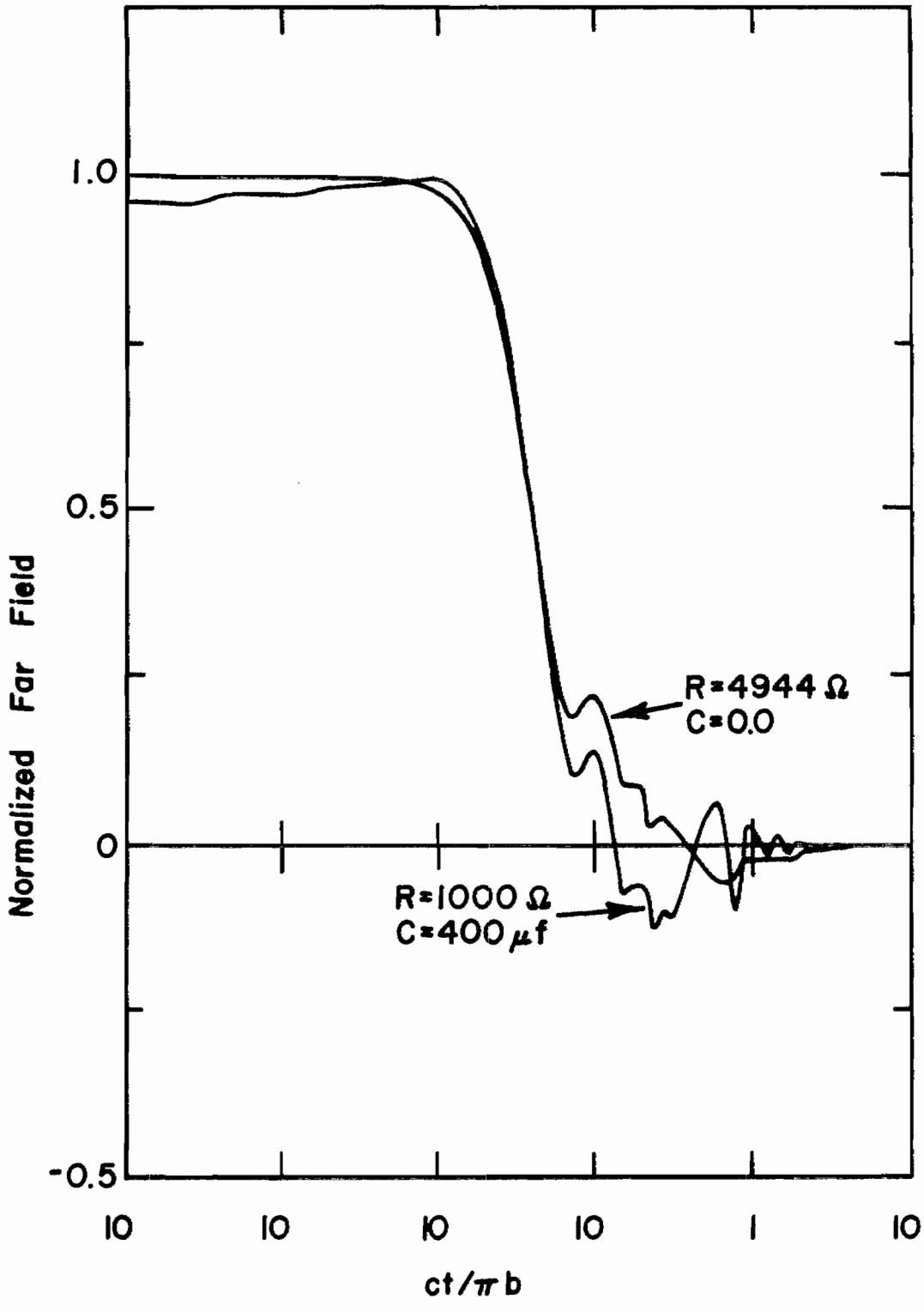

Figure 29. Radiated far field waveform for a step input for various values of impedance loading.

which is close to the origin resulting in a very decreased late time response.

This zero arises, of course, from the combined effect of the remaining poles of the loop which have been unconstrained. Hence, their effect in the late time response is not negligible as was originally assumed.

Since $a_1(s)$ has a pole at $s = 0$ then for low frequencies the loop transfer impedance is capacitive. Since the unloaded loop is passive, this equivalent circuit element must be positive. In order for loading to be chosen so as to cancel the pole of $a_1(s)$ (i.e., the zero of the admittance transfer function), $Z_L(s)$ would have to cancel the low frequency behavior of $a_n(s)$, which would require a non-physical negative capacitance. Hence, it is not possible to cancel the zero in the admittance transfer function by using passive loading.

To test the validity of this explanation for the poor late time behavior, a numerical experiment was conducted to determine if it was possible to eliminate the zero in the admittance transfer function. Accordingly the generator output waveform was modified to the time integral of the original excitation, which introduced another factor of $1/s$ in the transform domain so as to cancel the zero in the transfer admittance at $s = 0$.

This, of course, introduces a ramp in the time domain output of the generator but fulfills our requirement for an additional pole in the denominator of (4.27). The resulting time domain response is plotted in Figure 30. The similarity of the late time response to the desired double exponential confirmed the conclusion that the zero in the admittance transfer function caused the previous difficulty in achieving good late time response. The integration, however, further degrades the early time response.

Since good early time response was obtained with a generator frequency dependence given by

$$V_o^e(s) = \frac{-\beta}{s(s-\beta)} \qquad (4.39)$$

while good late time domain behavior was obtained with the frequency dependence

$$V_o^e(s) = \frac{-\beta}{s^2(s-\beta)} \qquad (4.40)$$

one might speculate that perhaps a good overall approximation to the desired response might be obtained by the excitation

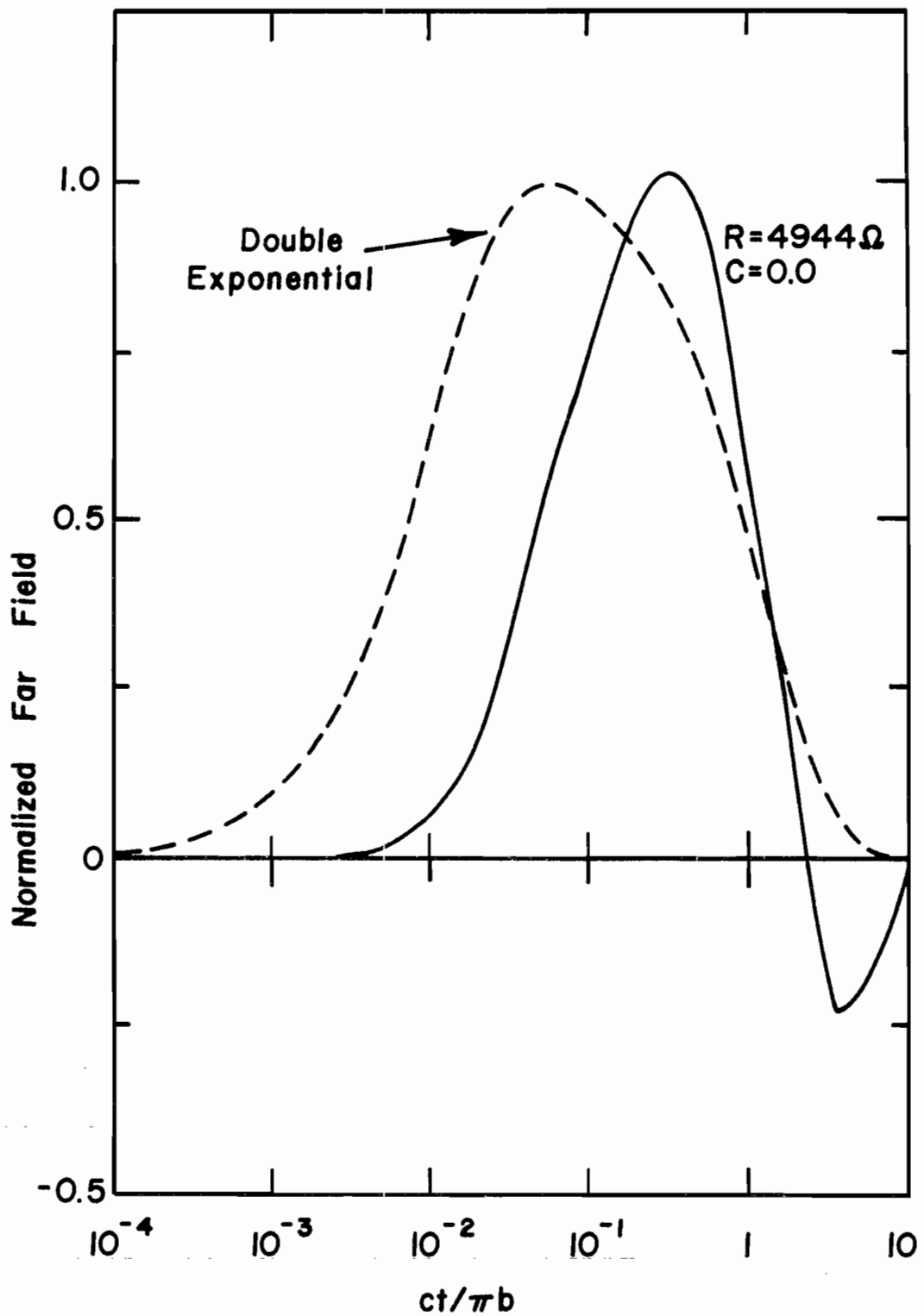

Figure 30. Radiated far field waveform for a modified ramp input for various values of impedance loading.

$$V_o^e(s) = \frac{-\beta(s+1)}{s^2(s-\beta)} \qquad (4.41)$$

which has the desired high frequency (early time) behavior of (4.39) and the desired low frequency (late time) behavior of (4.40). That this is indeed the case is seen by noting that the response of (4.41) is obtained by superposition of the responses due to (4.39) (Figure 28) and (4.40) (Figure 30). However, this approach (i.e., modifying the generator waveform to produce the desired response) runs counter to the objective of synthesizing the desired response by loading the loop. It appears, then, that although we may be able to synthesize the pole pattern of the loop for a finite number of the poles, we may require a more elaborate treatment to guarantee that the positioning of a finite number of the poles by impedance loading does indeed lead to the desired time domain waveform.

The complexities introduced by the infinite number of poles and the apparent late time differentiation of the decaying waveform due to a zero in the admittance transfer function pose a unique and difficult set of constraints. This is a problem outside the scope of this study but offers interesting possibilities for future research.

CHAPTER V

CONCLUSIONS

The objective of this research has been to develop some fundamental techniques for the analysis and synthesis of the response of a loaded loop antenna. In the past, the time domain response for such a problem would be determined either by time harmonic analysis coupled with Fourier inversion, or by direct time domain solution. With the addition of impedance loading, considerable effort would then be spent recalculating the entire response of the loop antenna without making use of any of the information about the response of the unloaded antenna. Use of the singularity expansion method (SEM), however, permits one to systematically examine the effects of loading using the solution for the unloaded loop antenna.

The observation that the solutions of electromagnetic problems are analytic functions of the complex frequency s except at singularities forms the basis of the SEM and permits one to use the many powerful theorems of complex variables to more efficiently represent the solution. The resulting time domain response representation is a superposition of damped exponentials whose complex frequencies correspond to s-plane poles of the admittance transfer function. These

poles are determined from the impedance loading and the unloaded admittance transfer function. Thus, the advantage of the singularity expansion technique is that one can separate and characterize basic attributes of the structure only once, and the time domain response for various loadings and excitations can then be easily determined from the structure's characteristic behavior.

In Chapter III, it is shown that s-plane contour plots of the magnitude and phase of the unloaded impedance transfer function of the loop permit one to readily determine the trajectories of the poles as loading is added to the structure. Furthermore, the observation that the loading can be interpreted as adding a feedback path to the admittance transfer function permits one to use the root locus techniques of control systems to further aid in the determination of the pole movements with increased loading. Since we are dealing with an antenna that is a distributed parameter system, the conventional root locus technique was generalized so as to be applicable to a system with a countably infinite number of singularities. The generalized root-locus technique provides a valuable tool for studying the effect of varying the impedance loading over a wide range.

The synthesis of time domain waveforms by impedance loading has been considered in Chapter IV. It was found that

the required condition on the impedance loading to locate a pole at any point in the complex s-plane is that it interpolate the impedance transfer function at the desired pole frequency. If the residue at the pole is also to be specified, the derivative of the impedance function also satisfies an interpolatory constraint. These conditions may be satisfied by Lagrange or Hermite interpolating polynomials, respectively. However, if one is restricted to passive loading, the loading function must be a rational function of s. A necessary condition on the interpolation constraints is given for the realization of passive loading. A sufficiency condition for realization with passive elements is apparently lacking at this time however. Some simple attempts in Chapter IV to synthesize a radiated waveform consisting of the sum of two exponential functions were only partially successful. The difficulties seemed to arise from attempting to control an infinite number of poles by loading and from the presence of zeros in the output response due to the admittance transfer function and the free space transfer function.

In summary, this research was directed towards simplifying the understanding of impedance loaded loop antennas using the singularity expansion solution technique. On the basis of the results of this study, several recommendations concerning future research are suggested. Further study

is needed to determine what constraints exist on the realizability of passive loads. Also needed is an approximate theory for treating the infinite number of poles of Type III. Possibly a transmission line model would enable one to factor these poles out of the admittance transfer function enabling one to work with a few poles in partial fraction form, the rest being absorbed into a transcendental function representing the transmission line approximation. Hopefully, such an approach might lead to a better understanding of the constraints on the realizability of time domain waveforms imposed by the structure. Another approach to synthesis might involve optimization techniques to choose the loading so as to minimize the error between the desired response and that actually obtained from the antenna. Here the shifted poles would not be specified but would enter the calculations only as a means to compute the time domain response. Finally, an interesting area for future research is in developing efficient ways to handle non-uniform and point loading. In the case of the loop, such loading unfortunately couples all the modes together.

APPENDIX A

DERIVATION OF THE INFINITE PRODUCT REPRESENTATION

Weierstrass' Theorem for infinite products [19] requires derivatives with respect to s. In the following, it is notationally convenient to use both the wavenumber k = -js/c and the Laplace transform variable s simultaneously. Thus, for example,

$$\frac{da_n(s)}{ds} = \frac{da_n}{dk}\,\frac{dk}{ds} = \frac{-j}{c}\,\frac{da_n}{dk} \qquad \text{(A-1)}$$

Except for n = 0, $a_n(s)$ has a pole at s = 0 which we wish to eliminate. Hence we consider the intermediate function

$$f_n(s) = sa_n(s),\ n = \pm 1,\ \pm 2,\ \ldots \qquad \text{(A-2)}$$

which has only zeros in the finite complex plane and hence is an entire function.

We now consider the logarithmic derivative

$$\frac{f_n'(s)}{f_n(s)} = \frac{a_n(s) + sa_n'(s)}{sa_n(s)} \qquad \text{(A-3)}$$

which is meromorphic. If this function is bounded on a set of contours C_n enclosing the poles, then an infinite product

representation exists [20].

Recall that

$$a_n = \frac{kb}{2}\left[K_{n+1} + K_{n-1}\right] - \frac{n^2}{kb} K_n \qquad \text{(A-4)}$$

where the K_n are defined as

$$K_o = \frac{1}{\pi} \ln \frac{8b}{a} - F_o(kb) \qquad \text{(A-5)}$$

and

$$K_n = K_{-n} = \frac{1}{\pi}\left[K_o\left(\frac{na}{b}\right) I_o\left(\frac{na}{b}\right) + C_n\right] - F_{2n}(kb) \qquad \text{(A-6)}$$

The function $F_n(z)$ is defined as

$$F_n(z) = \frac{j}{2}\int_0^{2z} \left[J_n(z) - j\Omega_n(z)\right] dz \qquad \text{(A-7)}$$

and the constant C_n is

$$C_n = \ln 4_n + \gamma - 2\sum_{m=o}^{n-1} \frac{1}{(2m+1)} \qquad \text{(A-8)}$$

In (A-6), K_o and I_o are modified Bessel functions, γ is Euler's constant, and $z = \frac{-jbs}{c}$.

The function in (A-7) $F_n(z)$ can also be written in integral form as [21]

$$F_n(z) = \frac{j}{2\pi}\int_o^{2z}\int_o^{\pi} e^{-j\,(z\,\sin\theta - n\theta)} d\theta\, dz \qquad \text{(A-9)}$$

Next we derive a recursion formula for the derivative of

$F_n(z)$. From (A-9), we have

$$F_{n-1}(z) - F_{n+1}(z) = \frac{j}{2\pi}\int_0^{2z}\int_0^{\pi}\left[e^{-j[z\sin\theta - (n-1)\theta]}\right.$$

$$\left. - e^{-j(z\sin\theta-(n+1)\theta}\right] d\theta\, dz \qquad \text{(A-10)}$$

$$= \frac{j}{2\pi}\int_0^{2z}\int_0^{\pi} e^{-j(z\sin\theta-n\theta)}\left[e^{-j\theta} - e^{j\theta}\right] d\theta\, dz \qquad \text{(A-11)}$$

$$= \frac{1}{\pi}\int_0^{2z}\int_0^{\pi} e^{-j(z\sin\theta-n\theta)}\sin\theta\, d\theta\, dz \qquad \text{(A-12)}$$

$$= \frac{1}{\pi}\int_0^{2z}\left[\frac{d}{dz}\int_0^{\pi} e^{-j(z\sin\theta-n\theta)} d\theta\right] dz \qquad \text{(A-13)}$$

$$= \frac{j}{\pi}\left[\int_0^{2z} e^{-j(z\sin\theta-n\theta)} d\theta\right]_{z=0}^{2z} \qquad \text{(A-14)}$$

$$= \frac{j}{\pi}\int_0^{\pi}\left[e^{-j(z\sin\theta - n\theta)} - e^{jn\theta}\right] d\theta \qquad \text{(A-15)}$$

Integrating the second term yields finally

$$F_{n-1}(z) - F_{n+1}(z) = \frac{j}{\pi}\int_0^{\pi} e^{-j(z\sin\theta - n\theta)}\,d\theta + \frac{1-(-1)^n}{n\pi} \qquad \text{(A-16)}$$

Differentiating (A-9) with respect to z, we have

$$F_n'(z) = \frac{j}{\pi}\int_0^{\pi} e^{-j(z\sin\theta - n\theta)}\,d\theta \qquad \text{(A-17)}$$

which upon comparison with (A-16) yields the desired recussion formula,

$$F_{n-1}(z) - F_{n+1}(z) = F_n'(z) + \frac{1-(-1)^n}{n\pi} \qquad \text{(A-18)}$$

Using the Fundamental Theorem of Calculus with (A-7) we can alternatively write

$$F_{n-1}(z) - F_{n+1}(z) = \Omega_n(z) + jJ_n(z) + \frac{1-(-1)^n}{\pi n} \qquad \text{(A-19)}$$

We may now return to (A-3) which we write as

$$\frac{f_n'(s)}{f_n(s)} = \frac{1}{s} + \frac{a_n'(s)}{a_n(s)} \qquad \text{(A-20)}$$

Differentiating (A-4) with respect to s we have

$$a_n'(s) = \frac{-j}{c}\left[\frac{b}{2}\left[K_{n+1} + K_{n-1}\right] + \frac{kb}{2}\left[K'_{n+1} + K'_{n-1}\right] + \frac{n^2}{k^2 b} K_n - \frac{n^2}{kb} K'_n\right] \qquad \text{(A-21)}$$

where

$$K'_{n+1}(s) + K'_{n-1}(s) = -b\left[F'_{2n+2}(kb) + F'_{2n-2}(kb)\right] \qquad \text{(A-22)}$$

$$= -b\left[F_{2n+1}(kb) - F_{2n+3}(kb) + F_{2n-3}(kb) - F_{2n-1}(kb)\right] \qquad \text{(A-23)}$$

where (A-18) has been used in (A-23).

Using the asymptotic expansion obtained by Umashankar [8],

$$\lim_{kb\to\infty}\left[K'_{n+1}(s) + K'_{n-1}(s)\right] = \frac{b}{2\sqrt{\pi kb}}\, e^{-j(2kb - \pi/4)} \left[e^{j\left(\frac{2n+1}{2}\right)\pi} - e^{-j\left(\frac{2n+3}{2}\right)\pi} + e^{j\left(\frac{2n-3}{2}\right)\pi} - e^{-j\left(\frac{2n-1}{2}\right)\pi} \right] \tag{A-24}$$

so that finally, we have

$$\lim_{kb\to\infty}\left[K'_{n+1}(s) + K'_{n-1}(s)\right] = \frac{2j(-1)^n b}{\sqrt{\pi kb}}\, e^{-j(2kb-\pi/4)} \tag{A-25}$$

From (A-6), we have

$$K'_n(s) = -b\, F'_{2n}(kb) \tag{A-26}$$

$$= -b\left[F_{2n-1}(kb) - F_{2n+1}(kb)\right] \tag{A-27}$$

From [8], for large values of kb,

$$\lim_{kb\to\infty}\left[K_n'(s)\right] = \frac{b}{2\sqrt{\pi kb}}\, e^{-j(2kb - \pi/4)}$$

$$\left[e^{j\left(\frac{2n-1}{2}\right)\pi} - e^{-j\left(\frac{2n-1}{2}\right)\pi}\right] \qquad \text{(A-28)}$$

$$= \frac{-j\, b\, (-1)^n}{\sqrt{\pi kb}}\, e^{-j(2kb - \pi/4)} \qquad \text{(A-29)}$$

Therefore $a_n'(s)$ can be directly evaluated from (A-21) for large kb as

$$\lim_{kb\to\infty} a_n'(s) = \frac{-j}{c}\left\{\frac{b}{2}\left[\frac{-2}{\pi}\ln kb + \frac{(-1)^{n+1}}{\sqrt{\pi kb}}\right.\right.$$

$$\left.e^{-j(2kb - \pi/4)}\right] + \frac{kb}{2}\left[\frac{2j(-1)^n b}{\sqrt{\pi kb}}\, e^{-j(2kb - \pi/4)}\right]$$

$$+ \frac{n^2}{k^2 b}\left[\frac{-\ln kb}{\pi} + \frac{(-1)^n}{2\sqrt{nkb}}\, e^{-j(2kb - \pi/4)}\right] -$$

$$\left.\frac{n^2}{kb}\left[\frac{-j(-1)^n b}{\sqrt{\pi kb}}\, e^{-j(2kb - \pi/4)}\right]\right\} \qquad \text{(A-30)}$$

Keeping only the dominant terms in (A-30), we have

$$\lim_{kb\to\infty} a_n'(s) = \frac{-jb}{c}\left[-\frac{\ln(kb)}{\pi} + j(-1)^n\sqrt{\frac{kb}{\pi}}\; e^{-j(2kb - \pi/4)}\right] \qquad \text{(A-31)}$$

Therefore (A-3) reduces to

$$\lim_{kb\to\infty} \frac{f_n'(s)}{f_n(s)} = \frac{1}{jkc} + \frac{b}{jc}\left[\frac{-1/\pi \ln kb + j(-1)^n\sqrt{\frac{kb}{2}}\; e^{-j(2kb - \pi/4)}}{-\frac{kb}{\pi}\ln kb + \frac{(-1)^{n+1}}{2}\sqrt{\frac{kb}{\pi}}\; e^{-j(2kb - \pi/4)}}\right] \qquad \text{(A-32)}$$

This function is bounded in both the left and right s-plane as $s\to\infty$ and also on a circular contour which passes between the poles of $f_n(s)$ which are the zeros of $a_n(s)$.
Thus, the product expansion of $f_n(s)$ is given by [20]

$$f_n(s) = f_n(0)e^{\left[f_n'(0)/f_n(0)\right]s}\prod_i (1-s/s_{ni})e^{s/s_{ni}} \qquad \text{(A-33)}$$

where

$$\frac{f_n'(0)}{f_n(0)} = \lim_{kb\to 0}\left\{ \frac{1}{jck} - \frac{j}{c}\left[\frac{b}{2}(kb)\left(K_{n+1} + K_{n-1}\right) + \frac{k^2b^2}{2}\right.\right.$$

$$\left.\left.\left(K'_{n+1} + K'_{n-1}\right) + \frac{n^2b}{kb}K_n - n^2K'_n\right]\right\}$$

$$\left\{\frac{k^2b^2}{2}\left(K_{n+1} + K_{n-1}\right) - n^2K_n\right\}^{-1} \qquad \text{(A-34)}$$

$$= \lim_{kb\to 0}\left[\frac{1}{jck} + \frac{-\frac{j}{c}\left(\frac{n2b}{kb}K_n - n^2K'_n\right)}{-n^2K_n}\right] = \frac{j}{c}\frac{K'_n(0)}{K_n(0)} \qquad \text{(A-35)}$$

However, from (A-6),

$$K_n(0) = 1/\pi\left[K_o\left(\frac{na}{b}\right)I_o\left(\frac{na}{b}\right) + C_n\right] \qquad \text{(A-36)}$$

and

$$K'_n(0) = -b\,F'_{2n}(0) \qquad \text{(A-37)}$$

$$= -b \left[F_{2n-1}(0) - F_{2n+1}(0) \right] = 0 \qquad \text{(A-38)}$$

Finally, we have that

$$f_n(0) = \frac{-jn^2C}{b} \quad K_n(0) = \frac{-jn^2c}{\pi b} \left[K_o\left(\frac{na}{b}\right) I_o\left(\frac{na}{b}\right) + C_n \right]$$

(A-39)

so that combining (A-33) - (A-39), we have

$$f_n(s) = sa_n(s) = \frac{-jn^2c}{\pi b} \left[K_o\left(\frac{na}{b}\right) I_o\left(\frac{na}{b}\right) + C_n \right]$$

$$\prod_i \left(1 - \frac{s}{s_{ni}}\right) e^{s/s_{ni}} \quad n \neq 0 \quad \text{(A-40)}$$

Thus, the infinite product representation for $a_n(s)$ is

$$\frac{1}{a_n(s)} = \frac{j\pi \left(\frac{bs}{c}\right)}{n^2 \left[K_o\left(\frac{na}{b}\right) I_o\left(\frac{na}{b}\right) + C_n \right] \prod_i \left(1 - s/s_{ni}\right) e^{s/s_{ni}}}$$

(A-41)

Turning to the representation of $a_0(s)$, we note that $a_0(s)$ has a zero at $s = 0$, so we consider the function

$$f_o(s) = \frac{a_o(s)}{s} \tag{A-42}$$

The logarithmic derivative is

$$\frac{f_o'}{f_o} = \frac{sa_o'(s) - sa_o(s)}{sa_o(s)} \tag{A-43}$$

$$= \frac{a_o'(s)}{a_o(s)} - \frac{1}{s} \tag{A-44}$$

From (A-4), we note that

$$a_o(s) = kb\ K_1 \tag{A-45}$$

where

$$K_1 = 1/\pi\left[K_o\left(\frac{a}{b}\right) I_o\left(\frac{a}{b}\right) + C_1\right] - F_2(kb) \tag{A-46}$$

Differentiating (A-45), we have

$$a_o'(s) = -\frac{j}{c}\left[b\ K_1 + kb\ K_1'\right] \tag{A-47}$$

where

$$K_1' = -b\, F_2'(kb) \tag{A-48}$$

$$= -b\left[F_1(kb) - F_3(kb)\right] \tag{A-49}$$

The asymptotic formulas from [8], yield

$$\lim_{kb\to\infty} a_o(s) = kb\left[\frac{-\ln(kb)}{\pi} - \frac{1}{2\sqrt{\pi kb}}\, e^{-j(2kb-\pi/4)}\right] \tag{A-50}$$

$$= \frac{-kb}{\pi} \ln(kb) - \frac{1}{2}\sqrt{\frac{kb}{\pi}}\, e^{-j(2kb-\pi/4)} \tag{A-51}$$

and for the derivative

$$a_o'(s) = \frac{-j}{c}\left[b\left(\frac{-\ln kb}{\pi} - \frac{1}{2\sqrt{\pi kb}}\, e^{-j(2kb-\pi/4)}\right)\right.$$

$$-kb^2\left[\frac{-1}{2\sqrt{\pi kb}}\,e^{-j(2kb-\pi/4)}\left(e^{j\,\pi/2}-e^{+3\pi/2}\right)\right]\Bigg] \tag{A-52}$$

$$= \frac{-j}{c}\left[\frac{-b\ \ln\ kb}{\pi} + \frac{b}{2\sqrt{\pi kb}}\,e^{-j(2kb-\pi/4)}(2jkb-1)\right] \tag{A-53}$$

On keeping only only the dominant terms, we have

$$\lim_{kb\to\infty} a_o'(s) = \frac{-jb}{c}\left[\frac{-\ln\ kb}{\pi} + j\sqrt{\frac{kb}{\pi}}\,e^{-j(2kb-\pi/4)}\right] \tag{A-54}$$

Therefore

$$\lim_{kb\to\infty} \frac{a_o'(s)}{a_\theta(s)} = \left\{\frac{-jb}{c}\left[\frac{-\ln\ kb}{\pi} + j\sqrt{\frac{kb}{\pi}}\,e^{-j(2kb-\pi/4)}\right]\right\}\left\{kb\left[\frac{-\ln\ kb}{\pi} - \frac{1}{\sqrt{\pi kb}}\,e^{-j(2kb-\pi/4)}\right]\right\}^{-1} \tag{A-55}$$

This function is bounded on a circle of radius R attached at the origin and passing between poles in the asymptotic layer.

Hence $\frac{f_o'(s)}{f_o(s)}$ is bounded on a sequence of such circles R_p, enclosing p poles. We now need the value of

$$\frac{f_o'(0)}{f_o(0)} = \lim_{s\to o} \left(\frac{a_o'(s)}{a_o(s)} - \frac{1}{s} \right) \qquad \text{(A-56)}$$

From (A-55), we have

$$\frac{f_o'(0)}{f_o(0)} = \lim_{k\to 0} \left[\frac{-\frac{j}{c}\,(bK_1 + kb\,K_1')}{kb\,K_1} - \frac{1}{jkc} \right] \qquad \text{(A-57)}$$

$$= \frac{-j}{c} \frac{K_1'(0)}{K_1(0)} \qquad \text{(A-58)}$$

But

$$K_1(0) = 1/\pi \left[K_o\left(\frac{a}{b}\right) I_o\left(\frac{a}{b}\right) + C_1 \right] \qquad \text{(A-59)}$$

and

$$K_1'(0) = -b\left[F_1(0) - F_3(0) \right] = 0 \qquad \text{(A-60)}$$

so that

$$\frac{f_o'(0)}{f_o(0)} = 0 \qquad \text{(A-61)}$$

and we have finally,

$$f_o(s) = f_o(0) \prod_i \left(1 - \frac{s}{s_{oi}} \right) e^{s/s_{oi}} \qquad \text{(A-62)}$$

where the produce is over all the zeros of $a_n(s)$ except s=0. Since

$$f_o(0) = \lim_{kb \to 0} \frac{a_o(s)}{jkc} = \lim_{kb \to 0} \frac{kbK_1}{jkc} \qquad \text{(A-63)}$$

$$= -j \frac{b}{c} K_1(0) \qquad \text{(A-64)}$$

$$= -j\frac{b}{c\pi} \left[K_o\left(\frac{a}{b}\right) I_o\left(\frac{a}{b}\right) + C_1 \right] \qquad \text{(A-65)}$$

we have finally,

$$\frac{a_o(s)}{s} = \frac{-jb}{c\pi}\left[K_o\left(\frac{a}{b}\right) I_o\left(\frac{a}{b}\right) + C_1\right] \prod_i \left(1 - \frac{s}{s_{oi}}\right) e^{s/s_{oi}} \tag{A-66}$$

In summary, the infinite product representations are

$$\frac{1}{a_n(s)} = \frac{j\left(\frac{sb}{c}\right)}{n^2 K_n(0) \prod_i \left(1-\frac{s}{s_{ni}}\right) e^{s/s_{ni}}}, \quad n \neq 0 \tag{A-67}$$

and

$$\frac{1}{a_o(s)} = \frac{j}{\left(\frac{sb}{c}\right) K_1(0) \prod_i \left(1-\frac{s}{s_{oi}}\right) e^{s/s_{oi}}} \tag{A-68}$$

where

$$K_n(0) = 1/\pi\left[K_o\left(\frac{na}{b}\right) I_o\left(\frac{na}{b}\right) + C_n\right] \tag{A-69}$$

APPENDIX B

CALCULATION OF THE NATURAL FREQUENCIES BY THE METHOD OF MOMENTS FOR THE n = 0 MODE

The method of moments solution for mode = 0 requires only a J_ϕ component of surface current which is ϕ independent. By symmetry, there exists only a ϕ component of magnetic vector potential which is also ϕ independent. The scattered electric field is given by

$$\bar{E}^s = \frac{1}{j\omega\mu_o\varepsilon} (k^2 + \nabla\nabla \cdot) \bar{A} \qquad \text{(B-1)}$$

Because of the ϕ independence, the ϕ component of the scattered electric field is

$$E_\phi = \frac{k^2}{j\omega\mu\varepsilon} A_\phi \qquad \text{(B-2)}$$

where the magnetic vector potential is given by

$$A_\phi = \frac{\mu_o}{4\pi} \int_0^{2\pi} \int_0^{2\pi} J_\phi(\psi') \frac{\cos \phi' \; e^{-jkR}}{R} \rho' d\phi' a d\psi' \qquad \text{(B-3)}$$

and where

$$R^2 = |\bar{r} - \bar{r}'|^2 = 2a^2(1 - \sin\psi \sin\psi' - \cos\psi \cos\psi' \cos\phi')$$

$$+ 2b^2(1 - \cos\phi')$$

$$+ 2ab(1 - \cos\phi')(\cos\psi + \cos\psi') \qquad (B\text{-}4)$$

and

$$\rho' = b + a \cos\psi'$$

The coordinates ϕ', ψ, and ψ' are defined in Figure 1. Since the fields are ϕ independent, ϕ has been set equal to zero in (B-3) and (B-4). The singularity occurring in (B-3) when $\psi = \psi'$ and $\phi' = 0$ (i.e., $R = 0$) is difficult to handle in a numerical solution. Accordingly, we extract the singular part of the integrand analytically in the following.

Considering the integration on ϕ' first, we write the distance from the source point to the field point as

$$R = (B - C \cos\phi')^{1/2} \qquad (B\text{-}5)$$

where

$$B = 2a^2 - 2a^2 \sin\psi \sin\psi' + 2b^2 + 2ab(\cos\psi + \cos\psi')$$

$$C = 2a^2 \cos\psi \cos\psi' + 2b^2 + 2ab(\cos\psi + \cos\psi') \qquad (B\text{-}6)$$

so that (B-3) becomes

$$A_\phi = \frac{\mu_o}{2\pi} \int_0^{2\pi} J_\phi(\psi')(b + a \cos \psi')\, a$$

$$\left\{ \int_0^{\pi} \cos \phi' \, \frac{e^{-jk(B-C \cos \phi')^{1/2}}}{(B - C \cos \phi')^{1/2}} \, d\phi' \right\} d\psi' \qquad \text{(B-7)}$$

Consider the integral in the brackets. We isolate the singularity by adding and subtracting a term having the same singularity as the integrand but which is integrable;

$$\int_0^{\pi} \cos (\phi') \left[\frac{e^{-jk(B - C \cos \phi')^{1/2}}}{(B - C \cos \phi')^{1/2}} \right] d\phi'$$

$$= \int_0^{\pi} \cos (\phi') \left[\frac{e^{-jk(B-C \cos \phi')^{1/2}} - 1}{(B - C \cos \phi')^{1/2}} \right] d\phi'$$

$$+ \int_0^{\pi} \frac{\cos (\phi')\, d\phi'}{(B - C \cos \phi')^{1/2}} \qquad \text{(B-8)}$$

The first integral on the right-hand side is nonsingular

and is hence amenable to numerical integration. The second integral, which we now proceed to evaluate, contains the singularity.

With the substitution $\cos \phi' = (2\cos^2 \phi'/2 - 1)$ and the change of variables $\phi' = \pi - 2\xi$, the second integral becomes

$$\int_0^{\pi} \frac{\cos \phi' \, d\phi'}{(B - C \cos \phi')^{1/2}}$$

$$= \frac{2}{(B + C)^{1/2}} \int_0^{\pi/2} \frac{(1 - m \sin^2 \xi) + (m/2 - 1)}{-m/2 \, (1 - m \sin^2 \xi)^{1/2}} \, d\xi$$

$$= \frac{-4}{m(B + C)^{1/2}} E(m) - \frac{2(1 - 2/m)}{(B + C)^{1/2}} K(m) \qquad \text{(B-9)}$$

where $m = 2C/B+C$ and $K(m)$ and $E(m)$ are elliptic integrals of the first and second kind, respectively [22]. Thus, with (B-8) and (B-9), (B-7) becomes

$$A_\phi = \frac{\mu_o}{2\pi} \int_0^{2\pi} J_\phi(\psi')(b + a \cos \psi') \, a$$

$$\left\{ \int_0^{\pi} \cos \phi' \left[\frac{e^{-jk(B-C \cos \phi')^{1/2}} - 1}{(B - C \cos \phi')^{1/2}} \right] d\phi' \right.$$

$$- \frac{4E(m)}{m(B + C)^{1/2}} - \frac{2(1 - 2/m)\, K(m)}{(B + C)^{1/2}} \Bigg\} d\psi' \qquad \text{(B-10)}$$

The term involving $K(m)$ is still singular since as ψ approaches ψ', m tends to unity. Using (B-6), we rewrite m to exhibit its dependence on ψ' explicitly;

$$m = \frac{D + E \cos \psi'}{F + G \cos \psi' - H \sin \psi'} \qquad \text{(B-11)}$$

where

$$D = 4b^2 + 4ab \cos \psi$$

$$E = 4a^2 \cos \psi + 4ab$$

$$F = 2a^2 + 4b^2 + 4ab \cos \psi$$

$$G = 2a^2 \cos \psi + 4ab$$

$$H = 2a^2 \sin \psi \qquad \text{(B-12)}$$

The singular integral of interest is

$$\frac{\mu_o}{2\pi} \int_0^{2\pi} J_\phi(\psi')(b + a \cos \psi')\, a \left[\frac{-2(1 - 2/m)}{(B + C)^{1/2}}\right] K(m)\, d\psi' \qquad \text{(B-13)}$$

The order of the singularity may be determined by evaluating the limit of the terms in the integrand as ψ approaches ψ' or, equivalently, as m approaches 1. Thus we have

$$\lim_{\psi \to \psi'} (B + C)^{1/2} = 2(b + a \cos \psi)$$

and

$$\lim_{m \to 1} K(m) = \ln \frac{16}{1 - m}$$

$$= \ln(16) - \ln \left[\frac{2a^2 - 2a^2 \cos\psi\cos\psi' - 2a^2 \sin\psi\sin\psi'}{F + G \cos \psi' - H \sin \psi'} \right]$$

$$= \ln(16) - \ln \left\{ \frac{2a^2 [1 - \cos (\psi - \psi')]}{F + G \cos \psi' - H \sin \psi'} \right\} \qquad \text{(B-14)}$$

from (B-11) and (B-12). Expanding $\cos (\psi - \psi')$ in a power series and keeping only the dominant singular term from (B-14), we have

$$K(m) \approx -2 \ln \left(|\psi - \psi'| \right) \qquad \text{(B-15)}$$

Hence,

$$\lim_{\psi' \to \psi} \frac{\mu_o}{2\pi} J_\phi(\psi')(b + a \cos \psi') \frac{(-2a)(1 - 2/m) K(m)}{(B + C)^{1/2}}$$

$$= \frac{\mu_o}{2\pi} a J_\phi(\psi') \left(-2 \ln|\psi - \psi'|\right) \qquad \text{(B-16)}$$

We now consider dividing the cross section of the loop into N subsections of angular extent

$$\Delta\psi = \frac{2\pi}{N} \qquad \text{(B-17)}$$

and define midpoints and end points of each interval as

$$\psi_n = (n - 1)\,\Delta\psi$$

$$\psi_{n+} = (n - 1/2)\,\Delta\psi$$

$$\psi_{n-} = (n - 3/2)\,\Delta\psi \qquad n = 1, 2, \ldots, N$$

(B-18)

The current is expanded in pulse functions

$$J_\phi(\psi) = \sum_{n=1}^{N} I_n\, p_n(\psi) \qquad \text{(B-19)}$$

where

$$p_n(\psi) = \begin{cases} 1, & \psi_{n-} < \psi \leq \psi_{n+} \\ 0, & \text{otherwise} \end{cases} \qquad \text{(B-20)}$$

and substituted into the vector potential. Since by (B-2), vector potential is proportional to the electric field, at a natural resonant frequency, the vector potential due to the current along the surface is zero. If this condition is enforced at the points ψ_p, p = 1, 2, . . . , N, a matrix results whose determinant is zero at the pole frequency. That is,

$$\det |Z(s)| = 0 \qquad \text{(B-21)}$$

when s is a natural resonant frequency. The matrix Z(s) is defined by

$$Z_{pn} = \frac{\mu_o a}{2\pi} \int_{\psi_{n-}}^{\psi_{n+}} W(\psi') \left[\int_0^{\pi} \cos \phi' \, \frac{e^{-jk(B-C \cos \phi')^{1/2}}}{(B - C \cos \phi')^{1/2}} \, d\phi' \right]$$

$$d\psi' \Big|_{\psi=\psi_p}, \qquad p \neq n$$

$$\frac{\mu_o a}{2\pi} \int_{\psi_{n-}}^{\psi_{n+}} \left[W(\psi') \int_0^{\pi} \cos \phi' \left[\frac{e^{-jk(B-C\cos\phi')^{1/2}} - 1}{(B - C\cos\phi')^{1/2}} \right] d\phi' \right.$$

$$- \frac{4W(\psi')\,E(m)}{m(B + C)^{1/2}}$$

$$- \frac{2W(\psi')(1 - 2/m)\,K(m)}{(B + C)^{1/2}}$$

$$\left. + 2 \ln \left(|\psi_p - \psi'| \right) \right] d\psi'$$

$$- 2\Delta\psi \left(\ln \frac{\Delta\psi}{2} - 1 \right) \Bigg|_{\psi=\psi_p}, \quad p=n$$

(B-22)

where $W(\psi') = b + a \cos \psi'$ in the above expressions. Note that the singular term (B-16) has been extracted from the integrand and its integral is added outside the integral in (B-22) for p = n.

The Fourier expansion of the voltage across a uniform gap is

$$V = \begin{bmatrix} 1 \\ 1 \\ \cdot \\ \cdot \\ \cdot \\ 1 \end{bmatrix} \qquad \text{(B-23)}$$

Using (B-22), we can write a function dependence for the total current where

$$\frac{k^2}{j\omega\mu\epsilon} Z I = V \qquad \text{(B-24)}$$

It is pointed out that the total current is equal to the sum of individual current. That is,

$$\sum I_n \cong C \frac{1}{a_0(s)} \qquad \text{(B-25)}$$

where $C = -\mu V/\pi\eta_0$ and the sum is the quantity plotted in Chapter II, Figure 10.

APPENDIX C

DERIVATION OF THE NEAR FIELD EXPRESSIONS

The electromagnetic field of a circular loop antenna with a current distribution given by (2.37)

$$I(\phi) = \frac{-jV_o^e(s)}{\eta_o \pi}\left[\frac{1}{a_o(s)} + 2\sum_{1}^{n}\frac{\cos n\phi}{a_n(s)}\right] \qquad (C\text{-}1)$$

may be determined from the vector potential for any arbitrary point.

The element of vector potential $d\bar{A}$ at a point r_o, θ, ϕ or X, Y, Z, Figure 27, has two components

$$dA_x = -dA \sin \phi'$$

$$dA_y = dA \cos \phi' \qquad (C\text{-}2)$$

These may be expressed as

$$dA_x = \frac{-\mu_o}{4\pi} I(\phi') \frac{e^{-jkR}}{R} \sin \phi' \, bd\phi'$$

$$dA_y = \frac{\mu_o}{4\pi} I(\phi') \frac{e^{-jkR}}{R} \cos \phi' \, bd\phi' \qquad (C\text{-}3)$$

We may write

$$I(\phi') = \sum_{n} I_n e^{-jn\phi'} \qquad (C\text{-}4)$$

where comparing with (C-1), we have

$$I_n = -j \frac{V_o^e(s)}{\eta_o \pi a_{|n|}(s)} \qquad \text{(C-5)}$$

Furthermore, noting that

$$\frac{e^{-jkR}}{R} = -jkh_o^{(2)}(kR) \qquad \text{(C-6)}$$

where $h_o^{(2)}$ is the spherical Hankel function of order zero, second kind, we may employ the addition theorem [23] to write

$$h_o^2(kR) = \sum_{\ell=0}^{\infty} (2\ell+1)\, h_\ell^{(2)}(kb)\, J_\ell(kr_o)\, P_\ell(\cos\xi), \quad r_o < b$$

$$\sum_{\ell=0}^{\infty} (2\ell+1)\, h_\ell^{(2)}(kr_o)\, J_\ell(kb)\, P_\ell(\cos\xi), \quad r_o > b \qquad \text{(C-7)}$$

The Legendre functions can further be expanded as [23]

$$P_\ell(\cos\xi) = \sum_{m=0}^{\ell} \varepsilon_m \frac{(\ell-m)!}{(\ell+m)!} P_\ell^m(\cos\theta)$$

$$P_\ell^m(\cos\theta') \cos m(\phi-\phi') \qquad \text{(C-8)}$$

where $\varepsilon_m = 1$ for $m = 0$ and $\varepsilon_m = 2$ for $m > 0$. This may also be written as

$$P_\ell(\cos \xi) = \sum_{m=-\ell}^{\ell} \frac{(\ell-|m|)!}{(\ell+|m|)!} P_\ell^{|m|}(\cos \theta) \, P_\ell^{|m|}(\cos \theta') \, e^{-jm(\phi-\phi')} \quad \text{(C-9)}$$

Hence, for $r_o > b'$, we have

$$dA_x = \frac{-\mu_o}{4\pi} \sum_n I_n \, e^{-jn\phi'}(-jk) \sum_{\ell=0}^{\infty} (2\ell+1) \, h_\ell^2(kr_o) \, J_\ell(kb) \, P_\ell(\cos \xi) \sin \phi' \, b d\phi', \quad r_o > b \quad \text{(C-10)}$$

Substituting (C-9) into (C-10), we may rearrange the order of the summation to obtain

$$dA_x = \frac{-\mu_o}{4\pi} \sum_n I_n \, e^{-jn\phi'}(-jk) \sum_{m=-\infty}^{\infty} \sum_{\ell=|m|}^{\infty} (2\ell+1) \left[h_\ell^2(kr_o)\right] J_\ell(kb) \, \frac{(\ell-|m|)!}{(\ell+|m|)!}$$

$$P_\ell^{|m|}(\cos\theta)\, P_\ell^{|m|}(\cos\theta')$$

$$e^{-jm(\phi-\phi')}\left(\frac{e^{j\phi'}-e^{-j\phi'}}{2j}\right)b\,d\phi' \qquad \text{(C-11)}$$

Let the inner summation be represented by an indexed term

$$C_m = \sum_{\ell=|m|}^{\infty} (2\ell+1)\left[h_\ell^2(kr_o)\right]\, J_\ell(kb)\, \frac{(\ell-|m|)!}{(\ell+|m|)!}$$

$$P_\ell^{|m|}(\cos\theta)\, P_\ell^{|m|}(\cos\theta') \qquad \text{(C-12)}$$

so that the vector potential can be written as

$$dA_x = \frac{\mu_o k}{8\pi} \sum_n I_n\left[e^{-j\phi'(n-1)} - e^{-j\phi'(n+1)}\right]$$

$$\sum_{m=-\infty}^{\infty} C_m\, e^{-jm(\phi-\phi')}\, b\,d\phi' \qquad \text{(C-13)}$$

Integrating over all ϕ' and using the orthogonality of the function $\exp(jm\phi')$, we obtain finally,

$$A_x = \frac{\mu_o kb}{4} \sum I_n\left[e_{n-1}\, e^{-j(n-1)\phi} - C_{n+1}\, e^{-j(n+1)\phi}\right] \qquad \text{(C-14)}$$

Similarly, A_y is found to be

$$A_y = \frac{\mu_o kb}{4j} \sum_n I_n \left[C_{n-1} e^{-j(n-1)\phi} + C_{n+1} e^{-j(n+1)\phi} \right] \tag{C-15}$$

If the vector potentials are required for $r_o < b$, then C_m in (C-12) is replaced by

$$C_m = \sum_{\ell=|m|}^{\infty} (2_\ell+1) \left[h_\ell^2(kb) \right] J_\ell(kr_o) \frac{(\ell-|m|)!}{(\ell+|m|)!}$$

$$P_\ell^{|m|}(\cos\theta) \; P_\ell^{|m|}(\cos\theta') \tag{C-16}$$

This completes the derivation of the rectangular components of vector potential. It is pointed out that the vector potential equations (C-14) and (C-15) are valid for near and far fields. The electric and magnetic field quantities may be derived from

$$\bar{B} = \nabla \times \bar{A} \tag{C-17}$$

$$\bar{E} = -j\omega \left[\bar{A} + \frac{1}{k^2} \nabla\nabla \cdot \bar{A} \right] \tag{C-18}$$

for periodic time dependence where $k = \omega/c$. In the Laplace transform domain, we have simply $s = jkc$.

REFERENCES

[1] Baum, C. E., URSI Meeting, Washington, DC, Spring 1972.

[2] Hallen, E., "Transmitting and Receiving Qualities of Antennae," Nova Acts Upsaliensic, Ser. IV, Vol 11, pp 1-43, 1938.

[3] Storer, J. E., "Impedance of Thin Wire Loop Antennas," Am. Inst. Elect. Engrs., Vol 75, pt 1, No. 27, pp 606-19, November 1956.

[4] Wu, T. T., J. Math. Phys., Vol 3, pp 1301-04, November-December 1962.

[5] King, R. W., and C. W. Harrison, Antennas and Waves: A Modern Approach, The MIT Press, Cambridge, Chapters 9 and 10, 1969.

[6] King, R. W. P., "The Loop Antenna for Transmission and Reception," Chapter 11 of Antenna Theory (R. E. Collin and F. J. Tucker, eds.), Part 1, McGraw-Hill Book Company, New York, 1969.

[7] Otto, Brune, "Synthesis of a finite two-terminal network whose driving-point impedance is a prescribed function of frequency," J. Math. Phys, 10, pp 191-236, 1931.

[8] Umashankar, K. R. and D. R. Wilton, Transient Characterization of Circular Loop Using Singularity Expansion Method, Interaction Notes, Note 259, August 1974.

[9] Kron, Gabriel, "Equivalent Circuit of the Field Equations of Maxwell, IRE Proc. 32, pp 289-299, May 1944.

[10] Baum, C. E., H. Chang, and J. P. Martinez, Analytical Approximations and Numerical Techniques for the Integral of the Anger-Weber Function, Air Force Weapons Laboratory Mathematics Note Series, Note 25, August 1972.

[11] Korn, G. A., and Korn, T. M., Mathematical Handbook for Scientists and Engineers, McGraw-Hill, New York, 1968, pp. 722-723.

[12] Tesche, F. M., On the Singularity Expansion Method as to Applied to Electromagnetic Scattering from Thin-Wires, Interaction Notes, Note 102, Apr 72.

[13] Thaler and Brown, Analysis and Design of Feedback Control Systems, pp -18.

[14] Kuo, B. C., Automatic Control Systems, Prentice-Hall, New Jersey, pp 329-362, 1967.

[15] Ghausi, M. S., and J. J. Kelly, Introduction to Distributed-Parameter Networks, Holt-Rinehart Winston, pp 91-186, 1968.

[16] Prenter, P. M, Splines and Variational Methods, Wiley, New York 1975.

[17] Youla, D. C., and M. Saito, Interpolation With Positive-Real Functions, Technical Report No. RADC-TR-67-70, Rome Air Development Center, New York (Polytechnic Institute of Brooklyn), April 1967.

[18] Barnes, P. R., and D. B. Nelson. Transient Response of Low Frequency Vertical Antennas to High Altitude Nuclear Electromagnetic Pulse (EMP), Interaction Notes, Note 160, March 1974

[19] Knopp, Theory of Functions, Part II, p. 18.

[20] Morse, P. M., and H. Feshback, Methods of Theoretical Physics, Part I, McGraw-Hill Book Co., 1953.

[21] Jahnke, Eugene, and Fritz Emde, Table of Functions, Dover, 1945.

[22] Handbook of Mathematical Functions, edited by Milton Milton Abramowitz and Irene A. Stegun (Dover Publications, Inc., NY) 1968.

[23] Harrington, Roger F., Time Harmonic Electromagnetic Fields (McGraw-Hill, N. Y.) 1961.